Committee I.2: Loads

Jungyong Wang[1](✉), Arash Abbasnia[2], Louis Diebold[3], Andre Fujarra[4], Tomaso Gaggero[5], Spyros Hirdaris[6], Sangyeob Kim[7], Dimitrios Konispoliatis[8], Masayoshi Oka[9], Jose Miguel Rodrigues[10], Mahmud Sazidy[11], Florian Sprenger[12], Peter Wellens[13], and Guiyong Zhang[14]

[1] St. John's, Canada
Jungyong.Wang@nrc-cnrc.gc.ca
[2] Instituto Superior Técnico (University of Lisbon), Lisbon, Portugal
[3] Bureau Veritas, Paris, France
[4] Federal University of Santa Catarina, Florianópolis, Brazil
[5] University of Genoa, Genova, Italy
[6] Athens, Greece
[7] Pusan, South Korea
[8] National Technical University of Athens, Athens, Greece
[9] National Maritime Research Institute, Tokyo, Japan
[10] SINTEF Ocean, Trondheim, Norway
[11] Defence Research and Development Canada, Ottawa, Canada
[12] University of Rostock, Rostock, Germany
[13] Delft University of Technology, Delft, the Netherlands
[14] Dalian University of Technology, Dalian, China

Committee Mandate. Concern for the environmental and operational loads from waves, wind, current, ice, slamming, sloshing, green water, weight distribution, and other operational factors. Consideration shall be given to deterministic and statistical load predictions based on model experiments, full-scale measurements and theoretical methods. Uncertainties in load estimations shall be highlighted. The committee is encouraged to cooperate with the corresponding ITTC committee.

Keywords: Wave loads · Current loads · Wind loads · Ice loads · Wave-current interaction · Airgap · Slamming · Sloshing · Wave-in-deck · Uncertainty · Potential theory · CFD · Field methods · Model tests · Full-scale measurements · Data-Driven methods · Ships · Offshore structures · Wind turbines · Mooring systems · Benchmark

1 Introduction

This report comprehensively reviews the types of loads acting on ships and offshore structures over the past three years (2021–2024), highlighting key research trends and emerging methodologies. By addressing hydrodynamic forces, wind and current loads, ice loads, and associated uncertainties, the report serves as a valuable resource for understanding the forces influencing the design, analysis, and operation of ships and offshore structures.

W. Wu and J. Ding (Eds.): ISSC 2025, LNME, pp. 133–252, 2026.
https://doi.org/10.1007/978-981-95-2668-0_2

Wave loads, discussed in Sect. 2, represent one of this field's most extensively studied areas. Sections 2.1 and 2.2 focus on wave loads acting on ships and offshore structures, respectively. For both sections, common attention has been given to potential theory methods and field methods. For ships (Sect. 2.1), full-scale measurement, sloshing, and slamming research were addressed. For offshore structures (Sect. 2.2), wave-current interactions, airgap and wave-in-deck loads, and mooring systems were reviewed. These loads are also examined through model tests and data-driven methods, reflecting the growing use of machine learning and artificial intelligence in marine engineering.

Current and wind loads, covered in Sect. 3, are essential considerations in marine operations, as they often overlap with wave loads to create combined environmental forces. The section explores current loads in Sect. 3.1 and wind loads in Sect. 3.2, with dedicated subsections addressing the unique challenges posed to ships and offshore structures.

Ice loads, discussed in Sect. 4, are particularly relevant for Arctic and sub-Arctic operations. This section is divided into sections addressing ice loads on ships (Sect. 4.1) and offshore structures (Sect. 4.2). Most recent research in this domain involves numerical approaches, with studies introducing advanced methods to simulate ice failure behaviour, including ice fracture. Given the increasing demand for wind turbines in ice-covered waters, an ice-induced vibration section has been included, offering a detailed review. Generally, the scarcity of full-scale data remains challenging for validating these studies.

Section 5 addresses the discussion of uncertainty for both experimental and numerical approaches. An overview of uncertainty analysis methods is provided to illustrate the different approaches. Section 6 provides a summary as well as key findings for each section.

This committee also performed benchmark tests for numerical prediction of slamming experiments. Four different numerical approaches were used, and the results are discussed in Appendix A.

2 Wave Loads

2.1 Wave Loads on Ships

Wave loads are critical in ship design and operation, influencing structural integrity and performance. This section provides an overview of the recent developments and research results contributing to this field's progress. The survey covers numerical, experimental, and data-driven approaches and highlights phenomena such as slamming and sloshing. Linear and non-linear potential flow methods can model fluid-structure interaction in ideal fluids at low computational cost. Typical application examples encompass pressure-induced loads, wave-induced motions and added resistance. Field methods complement this approach by capturing viscous effects, turbulence, and flow separation, with continuous developments that allow for increasingly high-fidelity simulations of wave-structure interaction. Lately, data-driven methods are rapidly evolving, utilizing machine learning and large datasets to improve predictions of wave loads and structural responses, offering the potential for enhanced efficiency and accuracy.

Nevertheless, experimental methods, particularly model tests with segmented and elastic hulls, are crucial to validate theoretical predictions and investigate hydroelasticity, whipping, and springing. Advances in instrumentation have improved the accuracy of these tests in controlled laboratory environments. To verify both numerical and experimental observations and to gain knowledge with respect to fatigue assessment and operational safety, full-scale measurements using onboard monitoring are required. Techniques like indirect load estimation and machine learning extract valuable insights from this data. One of the particular phenomena that are addressed in this section is slamming. This highly localized and nonlinear load, caused by impulsive wave impacts, is explored using advanced simulations and experiments to address its effects on structural safety and fatigue. Another phenomenon that has been the focus of investigation over the recent years is sloshing, causing challenges, particularly for liquid cargo ships, due to internal fluid dynamics affecting stability and loads. Besides the effects caused by sloshing, mitigation strategies through numerical and experimental methods are discussed. This section integrates these phenomena and approaches, providing a comprehensive view of the latest research work on wave loads to provide guidance.

2.1.1 Potential Theory Method

Potential flow methods are commonly used to model physical processes where viscous effects, turbulence or flow separation are not essential or play only a minor role. Typical applications where such methods can be applied to determine wave loads on ships include added resistance, wave excitation forces, pressure distribution, and slamming loads. Solving the interaction between the waves and advancing floating bodies requires formulating the motion of fluid particles oscillating randomly in reality. Therefore, the superposition attribute of potential flow has been deployed to develop computational methodologies for implicitly solving the equations of motion for fluid particles and advancing floating bodies. Thus, potential flow solvers are faster and computationally cheaper than the viscous models, whilst the range of fidelity of the potential flow solutions extends over a vast domain of applications.

Potential flow theory can be used to calculate the wave interaction with advancing or stationary floating bodies (such as ships) using the boundary integral equation. Hence, the Laplace equation governs the flow field and the boundary conditions are required to yield a unique solution. The computational boundary encompasses the free surface boundary, body boundary, sea-bottom and lateral walls such as waterways or channels. Hence, various analytical and numerical approaches have been developed to treat the complexities of the moving boundaries (the free surface and the body). The frequency domain solution has been developed by taking advantage of the superposition of the velocity potential function to determine the exciting loads on ships advancing in irregular waves in arbitrary heading angles. The frequency domain solution has been classified as linear/weakly nonlinear potential flow solutions due to simplifying the boundary conditions, such as the linearised free surface boundary conditions. By using the Fast Fourier Transform (FFT) and the impulse function, the frequency-domain solution can be converted to the time domain. Moreover, fully nonlinear potential flow models have been developed since a couple of decades ago, wherein the time-domain solution is obtained from the exact boundary conditions. The computational cost for the fully nonlinear models is remarkably higher than the frequency-domain solution.

Linear and Weakly Nonlinear Potential Flow Theory

Strip theory has been known as the fastest potential solver and is widely used to determine the dynamic of slender bodies advancing in a range of wave frequencies. Therefore, the strip theory has been appreciated in comparative studies on ship manoeuvring (Waskito et al., 2022) and the added resistance of advancing ships in different heading angles (Lee et al., 2021b). To implement the far-field method to approximate the added resistance, the strip theory was modified by Amini-Afshar & Bingham (2021) to calculate high-frequency solutions. Moreover, a modification was made by Duan et al. (2022) to approximate the dynamic of ships in shallow water and beam sea encountering angle. (Nielsen et al., 2021) used the strip theory to tune the transfer function for wave interaction with ships in different heading angles. Since the longitudinal component of the body normal vector is neglected in the slender body assumption, the two-dimensional boundary integral equation based on the second Green's identity has been implemented to obtain the hydrodynamic coefficients of the ship section. To elevate the accuracy of the body boundary condition, the three-dimensional boundary integral equation has been employed to take the exact normal vector components into account. Thus, three-dimensional Green's functions, which stand for the velocity potential of a source pulsating underneath the free surface to satisfy the linearised free surface boundary conditions, and the image method has been employed to impose the constant water depth and lateral walls. Submergence of the singular points leads to neglecting the instantaneous body boundary condition in the linear potential theory. The quadrilateral flat panel method was developed by Abbasnia et al. (2024) in which Fredholm's boundary integral equation was employed to obtain the strength of pulsating source in uniform currents, and the calculated hydrodynamic coefficients were inserted into the equation motion of rigid bodies in six degrees of freedom over a range of frequencies. Analogously, Yang et al. (2023, 2022) used the curvilinear quadratic element to calculate the response of advancing ships in the head sea. A hybrid three-dimensional linear potential flow model was developed by Dong et al. (2024) to approximate the near-field and the far-field fluid flow induced by advancing ships in head seas. The near-field solution was used to compute the ship's response, and the far-field solution was used to approximate the added resistance, which is equivalent to the steady drift force. However, the developed model was verified for a monohull, and Yao et al. (2023) extended the application to a trimaran.

Fully Nonlinear Potential Flow Theory

Fully nonlinear free surface boundary conditions and the instantaneous body boundary condition can be imposed into the solution of the boundary value problem using the Mixed Eulerian-Lagrangian (MEL) method. Three-dimensional, fully nonlinear wave tanks have been developed based on the different approaches of the MEL method, and various implicit approaches have been outlined to calculate the time derivative of the velocity potential. A development was made by Tian et al. (2024) for the instantaneous wave interaction with a real ship hull over a range of frequencies. The cumulative chord cubic parameter spline method was deployed to enhance the mesh re-generation and the time marching. Sustainability and the convergence of the numerical solution drastically depend on the accuracy of the intersection between the exact free surface and the instant wetted surface. The response of an advancing real ship form in irregular waves using a fully nonlinear wave tank was determined by Tang et al. (2021). Further development was carried out by Tang et al. (2023) and Sun et al. (2021) to calculate the bending moment and shear force along advancing flexible ships in nonlinear waves. Additionally, Wang et al. (2024) performed further development, in which the torsion of the ship structure was investigated using the solution of a fully nonlinear potential model.

Since there is a massive cost of computation for the fully nonlinear potential model, only few attempts at deploying parallel computation to tackle bottlenecks such as those by Dombre et al. (2019) and Abbasnia & Guedes Soares (2020) have been made.

2.1.2 Field Methods

This section is about assessing wave loads on ships using field methods. Field methods can be used to determine ship slamming in waves, but that topic already has its own section and is therefore avoided here as much as possible. Another topic often encountered in the literature in the context of field methods is hydro-elasticity; however, hydro-elasticity also already has its own section and is therefore not discussed here. The emphasis is also on ships as offshore structures are discussed in the next section.

Sometimes, field methods are used without it being clear what the advantages of the method are compared to (nonlinear) potential flow methods. For instance, Chen et al. (2022e) verified field method results against a strip theory potential flow code and a comparison between two ships in waves that could have been performed with a weakly nonlinear panel method. Such applications, however, demonstrate the applicability of field methods for loads and motions in waves, even when their application is not strictly necessary. This is also exemplified by the results of Mandru et al. (2024), who compared experimental data to a field method and analyzed field method results at model-scale and full-scale. The results in terms of motions in waves and the wave-added resistance showed little difference. According to the authors, differences between model-scale and full-scale were observed in the velocity distribution of velocities in the propeller plane due to viscous effects.

The advantages of field methods for ships in waves over potential flow methods, that have a longer tradition, are twofold: 1. viscous effects are addressed, and 2. large deformations of the free surface, such as those involved in wave breaking, are modelled. Note that field methods typically specialize in one of the aforementioned advantages and not both. Viscous effects for ships in waves are highly relevant when roll (and the notorious roll-damping) is considered. This reporting period has seen a number of articles in this category, so they deserve to be discussed as a group.

Large deformations of the free surface are encountered by ships, for instance, when loaded by green water or when undergoing slamming events. During green water loading, a significant relative wave height at the ship's bow, or sometimes along the sides or at the stern, develops into a flow on deck that can interact with structures on deck and cause damage. During slamming in waves, the ship itself causes large free surface deformations along the hull when a large (but negative) relative wave height initially brings part of the ship out of the water. The way free surface development takes place along the ship hull upon slamming defines how the load on the ship develops.

In any categorization, there is the risk of omitting relevant accounts of field methods for wave loads on ships. For this reason, a number of articles will be presented before moving on to the final part of this section, in which new field methods with potential future applications for ships are discussed. ‘New’ indicates novel techniques for dealing with the free surface or with more physics than incompressible one-phase or two-phase flows commonly used in current ship studies.

Roll Damping of Ships in Waves

The challenge with roll damping is that it is dominated by flow features that are several orders of magnitude smaller than a typical measure of the size of the ship. The ship requires a fairly large computational domain, whereas the flow features that induce damping need a very fine grid size. These requirements combined lead to a number of unknowns that are too large to solve within a reasonable time span during the engineering of a ship. At present, simulations provide comparatively good results for roll amplitudes (and hence roll damping) when compared to model test results. Note that this does not necessarily imply that simulation results are also good predictors of full-scale roll motions because the Reynolds numbers differ significantly at model-scale and full-scale.

Ghamari et al. (2022) overcame the challenge of roll damping in field methods by proposing a hybrid strategy for a ship cross-section with a keel (which induces flow features) and rounded bilges (which are typically more challenging because the location of flow separation is part of the solution itself). A field method, validated effectively using experiments presented in the article, was applied to find the linear and quadratic damping coefficients from roll decay simulations with the ship. The coefficients were then incorporated in the ship motion solver of a potential flow method for wave interaction with structures. When exposed to regular waves, the roll motion amplitudes of the ship in the potential flow solver with the additional damping coefficients were within 10% of the roll motion amplitudes from an experiment.

For a ship with a moonpool, Duan et al. (2023) proposed a strategy to obtain improved damping coefficients that include the effect of the moonpool on roll motions from more highly resolved decay tests so that they could be incorporated in simulations of the ship in waves at lower resolutions. Response Amplitude Operators (RAO) of lateral accelerations for a range of wave frequencies were determined from the simulations and compared with measurements from experiments. Differences between the two were not larger than around 5%. Although the authors’ main intention was to exclude waves from their evaluation of a ship’s roll motion at forward speed, the procedure proposed by Sumislawski & Abdel-Maksoud (2023) can be used to find the roll damping coefficients that are necessary to assess the correct roll motion behaviour of a ship at forward speed in waves. Harmonic Excitation of Roll Motion (HERM) uses an actuator to induce roll motions of the ship. For their study, a system based on the gyroscopic effect of rotating disks was developed to make the HERM procedure more efficient. The system was used to evaluate the effect of the rudder on roll damping, to determine the added resistance of the ship due to the roll motion, and to investigate parametric rolling. The latter was performed through a field method so that the omission of waves allowed for shorter simulations and, therefore, a more efficient evaluation of the ship’s performance.

Parametric roll was also investigated using a field method described by Liu et al. (2024). The final roll motion amplitude of the ship in head waves at several forward velocities of the ship from the simulations was compared to measurements from an experiment, and both were found to be within 10% of each other. The parametric roll was then investigated with different orientations of the ship's course with respect to the direction of the waves. The final investigation evaluated roll motion mitigation in the form of bilge keels, showing that bilge keels reduced the roll motions under the study's conditions by between 25 and 45%.

Green Water on Ships

Representing green water loading in field methods is challenging because the free surface near the ship undergoes abrupt changes, with the wave that exceeds the deck level developing in a bore-type flow that can cause impacts with deck structures. After impact, a vertical jet of water can form, and the free surface development is decisive for how the load on the deck structure develops. The aforementioned processes need to be resolved with high resolution in both space and time to lead to results that can be trusted. Green water loading can be deemed so challenging that authors go to lengths to try to avoid it. For instance, Islam & Guedes Soares (2022) artificially increased their deck level when assessing the sea margin and the added resistance in waves using a field method. The simulation results typically overpredict added resistance compared to the experiment, but only by a small margin so that they can be used to formulate the conclusion. The conclusion was that the rule of thumb for a sea margin of 25% is not sufficient in moderately steep waves, and the authors advise revisiting this rule.

Green water was the specific subject of study for Sun et al. (2023a). The authors used a field method to evaluate a Tublehome vessel with a wave baffle on deck in regular waves with four different steepness values. First, the suitability of the software for representing green water loading was established by comparing the simulation results to measurements of the water level on the deck and pressure from experiments. Then systematic simulations were performed, leading to the following findings: steeper waves did not lead to a longer duration of green water, but the steepness significantly affected the water level on deck. When plunging-type events occurred on deck, they led to more water being accumulated on deck behind the baffle. The conclusions state that the reported setup was suitable for investigating green water but that more work is necessary to investigate the effect of wave length, baffle shape and baffle inclination.

Notable Applications of Field Methods for Wave Loads

The following articles do not demonstrate the advantages of field methods mentioned above but show methods or applications that can be beneficial when using field methods to their advantage. Jeon et al. (2022) developed a wave maker for circular (or partial circular) domains that can be used to create directionally focused waves for emulating 'rogue' waves. The article shows ship motions due to the focused wave loads. However, it would be interesting to see if the directional wave focusing technique can be used to study green water loading in extreme waves.

In Gong et al. (2022), a field method was used to study broaching of a trimaran. Broaching in waves can lead to highly aperiodic motion of the ship and instability (more commonly for monohulls than for trimarans naturally). From their systematic set of simulations, the authors found that steep waves and a wave phase velocity close to the ship's forward velocity were necessary conditions broaching to occur.

New Field Methods for Wave Loads on Ships

Field methods typically solve for two-phase flow with the free surface as an interface between phases. In heavy seas, however, breaking and overturning waves entrain air in water, where it remains for several wave periods. The mixture of gas bubbles and water can be referred to as aerated water. With the typical percentages of 1 to 2% air by volume in water, the mixture is more compressible than air itself. The compressibility can significantly affect the pressure during wave impacts, green water impacts, or slamming events. van der Eijk & Wellens (2024) investigated a novel formulation incorporating aerated water as a third phase in a field method. The field method was compared to a purpose-built experiment involving wedges impacting the free surface of homogeneously aerated water. Their findings showed that increasing the percentage of aeration reduces the maximum impact pressure during slamming; 1% by volume of air in water reduces the pressure peak during slamming by 15% compared to the pressure in water without air. The pressure peaks of the field method simulations compared well with the pressure peaks in the experiment. Pressure variations after the impact could be attributed to density waves propagating through the aerated medium in both the experiments and simulations, and the simulations could be used to visualize the density waves. With aeration, simulations of slamming of ships in waves can be modelled more realistically in future.

2.1.3 Model Tests

Introduction

Model testing is a crucial component of the design process of ships. While the standard testing program usually addresses the determination of required power in calm water conditions, the standard structural ship design process follows class regulations and usually does not require experimental campaigns. However, model tests to measure the structural response of a ship in waves are essential for validating numerical models and ensuring the structural integrity and safety of ships, particularly for growing hull sizes and extreme environmental and operating conditions. Large ships with high elasticity and low natural frequencies can experience significant dynamic responses, such as whipping from impulsive wave loads and springing from short-period waves, potentially leading to severe ultimate loads and fatigue damage. Model tests with segmented hull models offer a more robust approach for analyzing ship hydroelasticity compared to traditional seakeeping tests. Yet, the impact of certain parameters on hydroelastic responses remains unclear. Several recent studies have looked into this field, and their findings are summarized in the following section: *Model and experiment design.* Several researchers have been investigating particular aspects of structural responses in waves by performing test campaigns. In recent notable efforts, the focus was mainly on large container ships. The work summarized in the section *Experimental studies* addressed nonlinearities related to wave steepness variation, the impact of forward speed and loading conditions and extreme wave heights.

Model and Experiment Design

Models used in hydroelastic experiments need to accurately reflect both the hull geometry and elastic characteristics of the prototype. Typically, two types of models are used: segmented (further distinguished in flexible joint and flexible backbone models) and fully elastic hulls. Grammatikopoulos (2023) reviewed the development of ship models used in hydroelastic experiments. The study highlights the importance of flexible models for investigating dynamic responses in slender ships and high-speed craft, discussing the advantages and limitations of the different model types in replicating ship stiffness and dynamic responses. The challenges of scaling and modelling in hydroelastic experiments are pointed out, including the difficulties in achieving full similarity between the model and full-scale ship due to physical constraints. The author also examined the application of these models in studying nonlinear responses such as springing, whipping, and antisymmetric vibrations, emphasizing the importance of correct scaling for accurate predictions. Looking ahead, further development of fully elastic models, improvements in measurement techniques like strain field measurement, and better calibration methods to enhance the accuracy of hydroelastic experiments are required.

Segmented models are the most used approach for estimating wave-induced loads, especially for new designs where established design load estimates are not yet available. Ibrahim et al. (2022) detailed their efforts to design, construct, and test a 6-foot segmented model of a medium-sized semi-displacement vessel. Their model was equipped with a backbone beam to replicate the structural stiffness characteristics of the full-scale ship. The instrumentation of the model includes strain gauges placed on the beam, local pressure sensors, and advanced Fiber Bragg Grating (FBG) strain and pressure sensors.

In order to investigate the effects of the number of segments, propulsion mode, and backbone configuration on ship hydroelastic behaviour, Chen et al. (2022b) developed a three-dimensional nonlinear time-domain hydroelastic method to account for the nonlinearity of the instantaneous wetted surface and slamming forces. From an analysis of natural frequencies and vertical bending moments (VBM), the authors conclude that self-propelled hull models with variable cross-section backbones representing the full-scale cross-sections' characteristics are more effective and reliable for studying nonlinear hydroelastic behaviour.

The design and fabrication of segmented ship models significantly impact wave-induced loads. Si et al. (2024) investigate three different segmented models of a 20,000 TEU ultra-large container ship, each with distinct support frames and backbones. Models A and B share similar fabrication methods but differ in backbone type and scale, while Model C employs steel framing validated by finite element methods and connected via welding. These models' dry and wet modes were measured and compared, revealing that design and fabrication methods notably influence ship model modes and wave-induced loads. Model A's lower natural frequencies were attributed to its lower frame stiffness (C_F), stiffness of the support crossbeams (C_{SCB}), and stiffness of the connections among the various members (C_C), impacting the transmission of wave-induced loads. Adequate values for CF, CSCB, and CC are crucial for effective load transmission and achieving similarity in vertical stiffness. FE analyses indicated that natural frequencies converge when segment numbers exceed ten, providing sufficient crossbeam stiffness. Additional uncertainty analysis highlighted significant variances in test uncertainties, stressing the need for precise control over repeated tests, moment of inertia, calibration coefficients, and wave height in future experiments.

While most studies focus on scaling for vertical bending modes, container ships also experience significant torsional moments due to large deck openings. Chen et al.

(2024) introduced a fully elastic ship-shaped model designed to replicate the vertical bending, horizontal bending, and torsional vibration modes of the S175 container ship. The model, equipped with strain gauges, enabled the measurement of critical hydroelastic responses, including vertical bending moments, vertical shear forces, and torsional moments. Comprehensive testing under different wave conditions and forward speeds showed that the model's structural responses align well with numerical simulations. The results show the benefits of this approach, noting that while the model produced reasonable bending and torsional modes, some fabrication limitations affected the final plate thickness. Future improvements in fabrication methods could enhance model accuracy. Overall, the authors demonstrated the model's effectiveness in capturing linear and non-linear responses, including slamming-induced whipping and springing effects in vertical bending and torsional modes, thus providing valuable insights into container ship behaviour under varied wave conditions.

Besides the hull and backbone properties, pressure sensors play a crucial role in the experiments. Commonly, strain gauges are used in ship model tests to measure elastic deformation, while the application of Fiber Bragg Grating sensors (FBG) is still relatively new in this field. FBG sense pressure based on the detection of changes in the wavelength of light reflected from a periodic variation in the refractive index of the fiber core, which shifts in response to external physical parameters such as strain or temperature. The advantages of FBG lie in their accuracy and sensitivity, but also in their small size which allows for distributed measurements with minimum intrusion. While their receptiveness to strain is beneficial in hydroelastic ship model testing, temperature sensitivity is somewhat problematic. Xu et al. (2022) developed a (FBG) pressure sensor to measure multi-point loads on ship hulls during wave experiments. The sensor detects changes in optical fiber responses due to hydraulic pressure and incorporates a steel diamond structure for effective temperature self-compensation using a single FBG. The authors showed that the sensor achieves suitable sensitivity and precision with a low-temperature sensitivity. Initial model tests in static and dynamic conditions with 15 sensor units installed on a ship model hull demonstrate the applicability to measure and monitor pressure distributions.

Given the stochastic nature of waves, it is crucial to determine how long and how many test realizations (seeds) are needed to obtain reliable extreme values for design purposes. Recent research by Scharnke et al. (2023) covered long-duration experiments with a ferry hull (see Fig. 1) to understand the convergence of most probable maximum (MPM) values and the number of seeds required for accurate statistics. Their work reveals that for convergence of wave crest MPM values, around 5–14 seeds with a 3-h duration or 8–22 seeds with a 1-h duration are needed. For example, the convergence requirements for green water impact forces on a ferry, which have a higher impact frequency, differ from those for wave-in-deck impacts on a stationary deck box with a lower impact frequency. The analysis shows that using only 1 or 2 seeds results in substantial inaccuracies, with root mean square errors (RMSE) of approximately 11% of significant wave height for wave crests and 5%–24% for green water forces. The study also evaluated the impact of fitting and extrapolation on convergence, finding that fitting introduces minor biases but does not significantly affect the number of seeds required.

The results provide practical guidelines for determining the number of seeds required to achieve reliable extreme value estimates in wave load experiments.

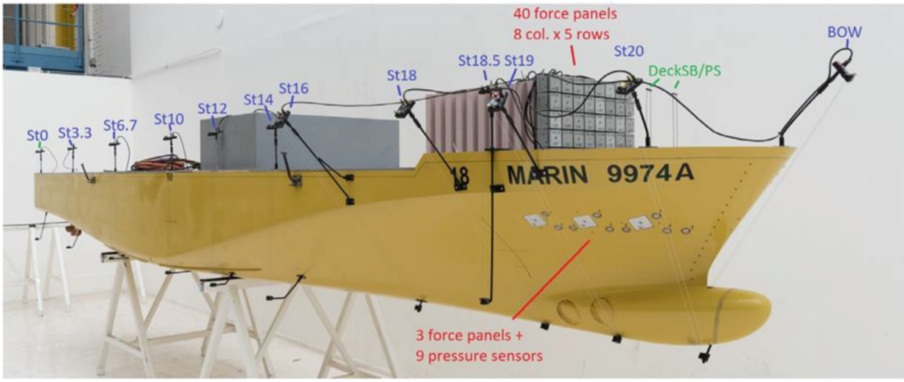

Fig. 1. Ferry model hull with relative wave elevation probes, force panels on the accommodation and force panels and local pressure sensors in the bow flare (Scharnke et al., 2023)

Experimental Studies

As the steepness of the waves that a ship encounters influences the motion and structural responses, experimental studies are required to investigate nonlinearities in both waves and responses systematically. A study by Kim et al. (2023b) investigated wave-induced motions and loads on a container ship model in 120° oblique regular waves, focusing on the influence of wave steepness. The experiments utilized a model at a scale of 1:65 with nine segments and a mooring system consisting of four horizontally arranged spring lines to maintain the model's heading angle. The authors aimed to understand how wave steepness affects nonlinear responses, including vertical bending moments (VBM) and horizontal bending moments (HBM) near amidships and six-degree-of-freedom motions at the centre of gravity. Various wave series with different steepness levels were tested, revealing that steeper waves increase higher-order harmonic components and slamming events in bending moments, deviating significantly from linear responses. The mooring system's impact on asymmetric HBM and average yaw motion was analyzed, showing that the system's restoring moments correlated with these responses. The findings indicate that nonlinear effects such as slamming significantly alter VBM and HBM responses in steep wave conditions, with differences in mooring line tensions influencing yaw motion. The results suggest that while the rigid model assumption is validated in head waves, further investigations are required for oblique wave conditions due to stronger slamming and structural vibrations. Further experiments were carried out by Kim et al. (2024) with a rigid container vessel in irregular waves. Long-duration tests, totalling approximately 25 h of data per sea state, were carried out across five different sea states (H_s from 6 m to 17 m) to calculate statistically significant extreme values of hogging and sagging. It was found that the ratio between linear and non-linear VBM, known as the non-linear factor, can be modelled as a function of the linear value alone, regardless of the sea state. This finding is significant as it facilitates the development of efficient design assessment methodologies using increased design sea states or design waves. Detailed investigations revealed that the non-linear factor depends mainly on the linear VBM value at a given return period, validating the approach of using increased design sea-states for experimental data. Although the conclusions are based on a single vessel, which limits their general applicability, they support previous studies and suggest that the non-linear factor remains consistent across different sea states.

An experimental campaign with a 10,000 TEU container ship has been performed by Zhang et al. (2022i). The authors designed a segmented ship model with adjustable cross-sections to ensure similarity in vertical, horizontal, and torsional stiffness along its length. The study included tests with both head and oblique waves. Frequency spectrum analysis revealed significant high-frequency wave loads affecting springing phenomena, with oblique waves exhibiting higher proportions of these loads. Non-linear wave-induced sag and hog ratios in vertical bending moments were attributed to high-frequency components. Bow flare slamming was predominant in a fully loaded condition, while stern and stem slamming became more pronounced as the draft decreased. Although stiffness has minimal effect on the frequency of slamming, it was found that reduced stiffness results in increased severity of mean slamming pressures and loads.

Ship forward speed relative to the incoming waves affects the impact of wave loads and the structural responses of ships. Zou et al. (2024) investigated bow flare slamming loads and whipping responses of a ship using a segmented model in regular waves. The model was designed to replicate the hull's vertical and horizontal bending stiffnesses. Temporal variations in harmonic components were analyzed using continuous wavelet transform. Key findings include that higher sailing speeds significantly impact the magnitude and distribution of bow flare slamming pressures, causing increased asymmetry in slamming loads under oblique waves. At higher speeds, the distribution of pressures on the bow flare became more uneven, with more significant impact on the waveward side. The whipping responses lead to noticeable periodic changes in harmonic strengths around the model's natural wet frequency, intensifying vertical bending moment asymmetry at midship. Repeated tests confirmed the experimental stability but highlighted significant variability in bow-slamming loads affecting higher-order harmonics.

Ship sizes have been increasing over the last years, with associated challenges for structural integrity under extreme environmental conditions. A study by Tang et al. (2022c) investigated the nonlinear bending moments of an ultra-large container ship in severe wave conditions. An experimental campaign with a 1:65 scaled model with a variable cross-section backbone beam was performed, focusing on the analysis of vertical bending moments (VBM, with strain gauges used for measurements) at various Froude numbers, wave headings, and wave heights. Key aspects investigated include resonance frequencies, high-order harmonic components, and the asymmetry of hogging and sagging moments. The backbone beam's design and calibration were crucial for accurate results. The model's natural frequencies were compared with theoretical predictions, showing satisfactory agreement. The authors also investigated the effects of wave height on VBM asymmetry, particularly in extreme waves (H_s up to 25 m) where high-frequency nonlinear loads become significant. Results indicate that sagging moments can be up to three times larger than hogging moments in severe conditions. Finally, the study highlights the variation in phase differences between wave-frequency and high-order harmonics, which differ significantly from moderate sea conditions.

By measuring ship responses in waves, it is also possible to draw conclusions on the wave parameters and subsequently derive further responses that may not have been measured. This approach might be of particular interest in real ship operation. However, establishing such a method under controlled laboratory conditions is favourable. Komoriyama et al. (2023) proposed a Kalman filter (KF) technique for identifying wave profiles encountered by a stationary ship from measured responses. The method was applied to tank test data with an acrylic resin ship model, measuring wave elevation, six degrees of freedom of ship motions, and hull strains using FBG sensors in long-crested irregular waves. The KF technique was validated by comparing identified wave profiles with reference measurements. Accuracy improved by selecting appropriate inputs and combining multiple signals. The method also estimated non-measured ship responses and predicted future wave profiles a few cycles ahead. Accuracy was affected by frequencies with low transfer function (TF) amplitudes. Combining multiple measurement signals enhanced accuracy, especially in low TF regions (see Fig. 2).

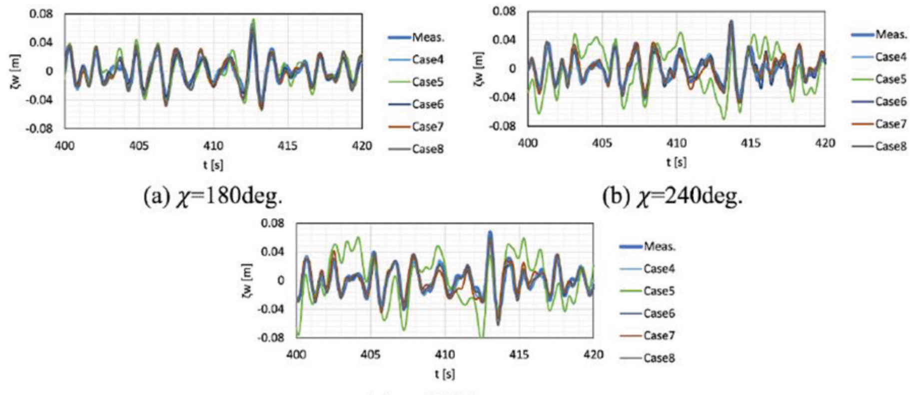

(a) χ=180deg. (b) χ=240deg.

(c) χ=300deg.

Fig. 2. Comparison of measured wave profiles with wave profiles that have been derived from different combinations of other measured signals (Komoriyama et al., 2023)

2.1.4 Full-Scale Measurement

Full-scale measurements, namely onboard monitoring, are an effective technology that contributes to a ship's health evaluation and design improvement, and research and development have progressed. As the technology has already reached the stage of practical application, the number of research papers has decreased compared to previous years. The main research topics in this field include the development of methods for estimating unmeasured responses and environmental conditions such as waves and ship conditions through data assimilation; the development of methods for evaluating designs and design criteria based on the data; and the formulation of standards and regulations based on the evaluation results.

As it is not always feasible to measure all parameters and responses that are relevant directly on board a ship, indirect estimation approaches can be used. Gebrezgabir et al. (2023) proposed a method to indirectly estimate slam and wave load responses using measurement data of strains, accelerations and angular velocities. It was applied to full-scale sea trial data of the 98 m high-speed catamaran HSV 2 Swift. The responses were reconstructed for different ship headings, speeds and sea conditions. Tested using only the transmissibility matrix without knowledge of sea conditions, excellent agreement was achieved, particularly for more significant loading events. This technique, in combination with finite element analysis (FEA), reduces the number of sensors, reduces data noise, improves data quality by recovering missing data, and improves data quality by reducing the number of sensors, reducing data noise, and recovering missing data. This makes it possible to estimate stress at any point. Chen et al. (2021b) proposed a method to estimate ocean wave spectra using stress and motion components measured by onboard monitoring. A method was proposed to estimate wave spectra of arbitrary shapes using nonlinear programming, one of the mathematical programming methods for solving optimization problems. The wave spectrum was estimated based on monitoring data of a 14000 TEU container ship. The results were compared for 1) using vertical bending stress and horizontal bending stress, 2) using vertical bending stress, horizontal bending stress, and double bottom bending stress. The selection of an appropriate combination of accuracy and response was discussed by comparing with Hindcast and radar data. Takami et al. (2024) proposed an approach to identify stability parameters based on onboard response measurements, namely linear and nonlinear roll damping coefficients, in conjunction with the natural roll frequency. Response measurements (heave, pitch, sway, etc.) from waves other than roll were used to estimate the encounter wave profile. Then, stability parameters that best reproduce the measured roll motion were identified through optimization. Good results were obtained for both long- and short-crested irregular waves.

Contributing to evaluating methods for fatigue design of hull structures, Warren et al. (2022) assessed the applicability of classification society rules for high-speed catamarans. A comparison was made of the long-term distribution of stresses measured on a 111-m-long wave-piercing catamaran ferry during operation in the Canary Islands with the load spectrum estimated using the method recognized by the Classification Society DNV GL (DNV-GL, 2015). In addition, an improved distribution fitting method for fatigue analysis was proposed based on the conversion of the stress history measured in the time domain into a suitable stress spectrum and a Weibull fitting method for cyclic stress in the low-stress and high-stress regions due to slamming. The results showed that the classification society method is very conservative regarding fatigue estimation compared to fatigue results based on measured data. Engelbrecht & Bekker (2023) investigated how to set the threshold for discomfort caused by vibrations due to slamming impacts based on onboard monitoring. Data were collected from two slamming-prone vessels. Vertical acceleration measurements were conducted near the ship's working and living areas. Human responses were collected from passengers using a daily survey. Observers on the bridge performed momentary slamming vibration comfort ratings during a series of intentionally induced slamming events. As a result, the limit value based on the RMS value converged to the same value (0.03 m/s^2) regardless of the cumulative time. This value is higher than the ISO and Classification Society standard value (0.01 m/s^2) and allows vibration.

2.1.5 Slamming

When a ship operates in rough seas, its bow may lift and then slap on waves because of the relative motions between the hull and the wave surface. Due to high vertical velocities during the re-entry of the ship hull in water, impulsive loads associated with the high hydrodynamic pressure peaks occur. This phenomenon is called ‘slamming’, and it is strongly nonlinear. When the global hull girder vibrations occur because of an impulsive wave loading, such as a wave slam at the bow (bow-slamming) or stern (stern-slamming), the phenomenon is denoted by the term whipping. Whipping is a transient phenomenon due to excessive impulsive loading in the bow or stern of the vessel. According to classical ship theory, the 2-node natural frequency dominates the dynamic response resonant mode during whipping, leading to hull girder stress variations (see Fig. 3).

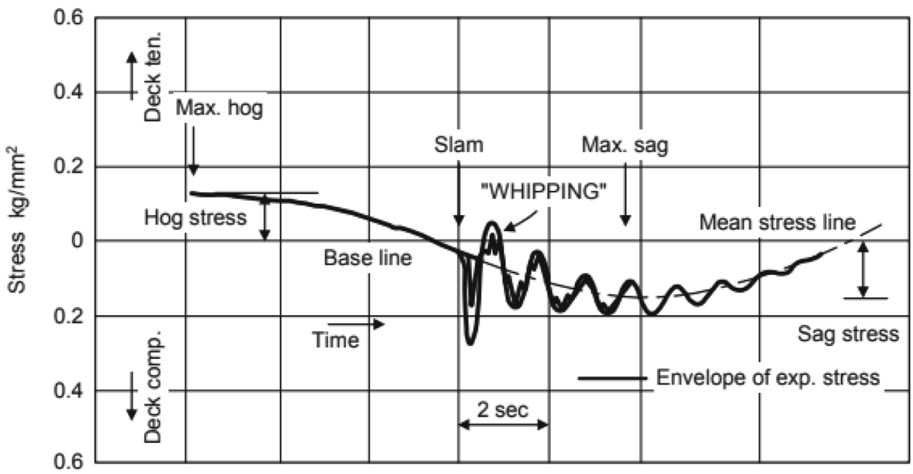

Fig. 3. Whipping stress due to slamming (ABS, 2024).

From a practical perspective, springing and whipping events manifest simultaneously in confused seas. Since associated wave-induced resonances are superimposed on wave frequency loading, they may contribute to fatigue damage accumulation (Hirdaris et al., 2023). Slamming tends to occur with waves in the ship’s bow sections, in which case the shape of the bow is of paramount importance, although there are ship forms that may be equally prone to bow and stern slamming. Research challenges relate to (a) accurate use and validation of advanced numerical methods for the prediction of local hydrodynamic pressures, especially in both symmetric and asymmetric planes, (b) methods for the prediction of global whipping responses and their impact on fatigue strength, and (c) understanding the influence of symmetric and antisymmetric higher vibration modes on global response. As applicable, this section reviews lessons from accidents, key advances of relevance local (bow and stern induced), and global slamming loads. Results from experiments and full-scale measurements (FSM) are also included.

Learning from Accidents

Accident records and FSM present the pathways for research and design updates, especially for the case of novel ship designs for which empirical methods may not be valid and computational tools may have limitations. Despite genuine attempts from both ISSC (2018) and ITTC (2021) communities, the experience based on FSM is not systematically developed and remains relatively scarce, particularly for ships operating in extreme conditions. This is because FSM data processing requires a large number of human resources and know-how for the rapid and meaningful processing of big data streams. Within the reporting period of this committee, practical results of relevance to slamming and whipping are limited to experiments (wedge drop tests for local slamming and segmented model tests for whipping) as discussed in relevant parts of the report (Chen et al., 2019; Hosseinzadeh et al., 2023b, 2023a; Li et al., 2022a; Lu et al., 2023; Zou et al., 2024).

The confidential nature of the vast majority of available data records also prohibits the transparent use and implementation of lessons learned. In relatively recent years, increased stresses have been recognized as relevant for the loss of ultra-large container ships MSC Napoli and MOL Comfort (see Fig. 4). The former was a United Kingdom-flagged ship that developed a hull breach due to rough seas and slamming in the English Channel on January 18, 2007. An investigation conducted by the UK Marine Accident Investigation Branch (MAIB), Det Norske Veritas (DNV) and Bureau Veritas (BV) demonstrated that she broke due to inadequate frame strengthening in the engine room area. The investigation recognized that wave loads were amplified by 30% during the accident, possibly due to whipping (MAIB, 2008). The adverse effects of an extreme slamming case also influenced the M/S Estonia accident in 1994. During her last journey in the Baltic Sea, due to slamming, the ship lost her bow visor JAIC (Joint Accident Investigation Commission) (1997). The damage to her watertight front door led to her capsize and the loss of 852 lives.

Fig. 4. Recent Container ship accidents (a) MSc Napoli – © gcaptain.com (b) MOL Comfort - © ship engineer worldpress.com.

The MOL Comfort experienced a fracture of the midship part while in the Indian Ocean on June 17, 2013. The ship was split into two halves and sank. The accident report suggested that the ship's structural strength could be exceeded because of wave loads (ClassNK, 2014; MJB, 2015). The analysis accounted for uncertainties associated with lateral load effects on hull girder strength, yield stress deviations, welding-induced residual stress, weather, operational conditions, whipping effects and cargo loads, etc. It was recommended that future rule requirements should account for the effects of lateral and whipping loads to evaluate ship structural strength. These investigations led to the revision of IACS longitudinal strength requirements and the selective introduction of Classification Society notations. The new longitudinal strength standard for container ships URS 11 A (IACS, 2015) introduced a partial safety factor that accounts for the influence of increased stresses along the double bottom of container ships. This new standard may be considered important especially in the hogging condition when a double-bottom topology may be exposed to high compressive stresses that can exceed the buckling capacity of shell structures or double-bottom plating and consequently trigger the progressive collapse of the hull. The same standard introduced a nonlinear correction factor to update the vertical wave-induced bending moment.

Forensic analysis demonstrated that the influence of whipping-induced loads on hull girder strength is still a matter of research, and Classification Society procedures still differ. Although whipping is included in the functional requirements for large container vessels, because of the uncertainties influencing design factors, it is left up to the individual assurance body to consider its relevance. For example, DNV (2015) classification guidelines introduced a partial safety factor of 0.9, reducing the effectiveness of whipping during collapse. BV does not use that reduction, claiming that there is no evidence for a factor of 0.9 (Derbanne et al., 2016). This could be attributed to uncertainties associated with (1) existing computational tools and hydroelastic modelling approaches; (2) the definition of the influence of dynamic failure modes, which may be different from those understood within the context of rigid body ship dynamics; (3) the lack of consensus on the definition of representative design or extreme operational conditions; (4) limited understanding of methods that can be used to model the influence of extreme events on fatigue accumulation based on data from in-service experience.

Local Slamming Loads

Local slamming loads are severe transient and may cause local structural damage during extreme events (Hirdaris et al., 2014). The phenomenon was first recognized by Yamamoto et al. (1985), who reported damages due to bow flare slamming on an 819 TEU container ship in cyclone conditions. At the time, the authors concluded that an 840 kPa impact pressure in the way of a 13.7 m circular area might lead to structural damage.

In the early days, theoretical research was driven by von Karman (1929) and Wagner (1932). A comprehensive research summary on ship-slamming physics is presented by Kapsenberg (2011). Wagner's model is based on the potential flow theory. It applies within the context of ideal and incompressible fluid flow that is generally used to estimate the pressure distribution on ideally stiff wedges. Zhao & Faltinsen (1993) solved the similarity flow for wedges by a nonlinear boundary element method with a jet flow approximation. Their results agreed with the simple asymptotic solution by Wagner (1932) for small deadrise angles. Faltilsen et al. (1996) extended this approach to 2D arbitrary geometries. These papers provided important research output regarding the value of analytical formulations and potential flow-based simulations, and the ideas presented are implemented in classification guidelines (DNVGL 2021).

With the advent of super-computing power, advanced numerical methods have been employed to better understand the influence of fluid-induced nonlinearities and strong fluid-structure interaction. On the hydrodynamics front, numerical models are based on the Arbitrary Lagrangian-Eulerian (ALE) scheme (Stenius et al., 2007, 2011; Wang & Guedes Soares, 2014; Wang & Soares, 2012), the Finite Volume Method (FVM) (Southall et al., 2014, 2015), Smoothed Particle Hydrodynamics (SPH) (Alexandru et al., 2007; Farsi & Ghadimi, 2016; Veen & Gourlay, 2012), and the Volume of Fluid (VOF) method (Southall et al., 2014). Recently published work by Tavakoli & Hirdaris (2023) confirms that accurate numerical modelling of the time-dependent nature of hydroelasticity-induced slamming, along with violent fluid-structure interaction and free surface evolution, remains challenging. The authors suggest that plate deformations may significantly affect dynamic response, especially in oblique conditions. This is because rolling free surfaces and waves may influence the distribution of hydrodynamic loads.

Strong coupling FSI methods are used to study the influence of flexible fluid–structure interactions on wedge-shape structures. In their traditional format, they combine the Boundary Element Methods (BEM) or Reynolds Averaged Navier Stokes (RANS), Computational Fluid Dynamics (CFD) and FEM (Yan et al., 2022c), see Fig. 5. More advanced numerical schemes such as ALE (Stenius et al., 2011; Wang & Guedes Soares, 2014) and SPH (Panciroli & Porfiri, 2015) may also be coupled with FEA.

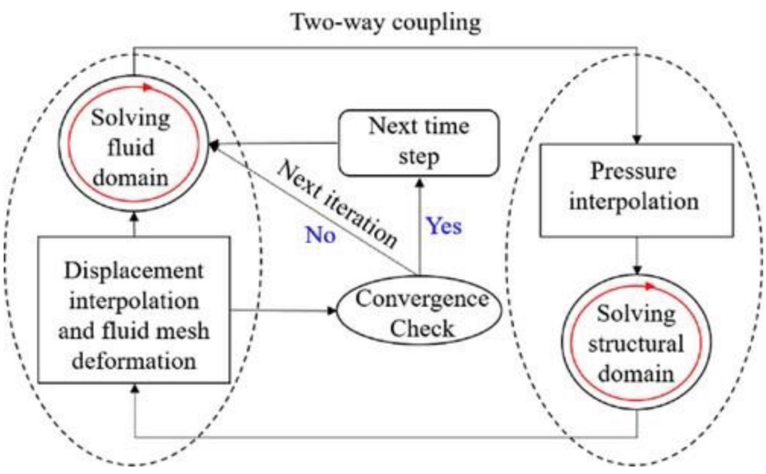

Fig. 5. Two-way coupled FSI modelling method as per (Yan et al., 2022b)

Recently, a benchmark study for flat stiffened plates by Truong et al. (2021) reviewed uncertainties associated with modelling and computation. Yan et al. (2022a) and Yan et al. (2022c) presented a detailed validation of two-way coupled Finite Volume (FVM) and FEA methods. The authors studied the complete history of the flat plate water entry problem. Experimental and numerical uncertainties were analyzed according to the ASME V&V method (ASME 2009) and confirmed the validity of the simulation-based approach. A sequel study compared the water entry fluid actions for the cases of a flat plate impinging on the water at different velocities and the case of a symmetric wedge idealizing slamming at different deadrise angles. In this study, numerical predictions have been compared against available experimental data by Tödter et al. (2020) for flat plates and the hydrodynamic pressure design curves implemented in classification guidelines for wedge-like structures (DNV-GL (2015)) as shown in Fig. 6. The results generally showed good agreement. This work confirms that a two-way coupled FVM-based CFD-FEA modelling procedure does not change the trend of pressure design curves already implemented in classification rules for stiff wedges. The smaller the deadrise angles, the larger the differences in fluid pressures and forces between stiff and flexible structures. The similarity in the pressure distributions of flexible wedges is not obvious.

Because of the complexity of three-dimensional flows, such as fluid separation, fluid breaking, and bubble flows, the accurate prediction of local slamming loads in three dimensions is still very limited. Recently, Xie et al. (2024) presented results from drop experiments idealizing the asymmetrical slamming load characteristics of a truncated ship bow under the combination of heel and pitch orientations. In this work, an angle device was used to independently adjust the heel and pitch orientation of the test model. The results suggest that air cavities and jet flows may cause multiple oscillatory pressure peaks. Abnormal pressure characteristics appear in some locations, where the pressure decreases with the increment of water entry velocity.

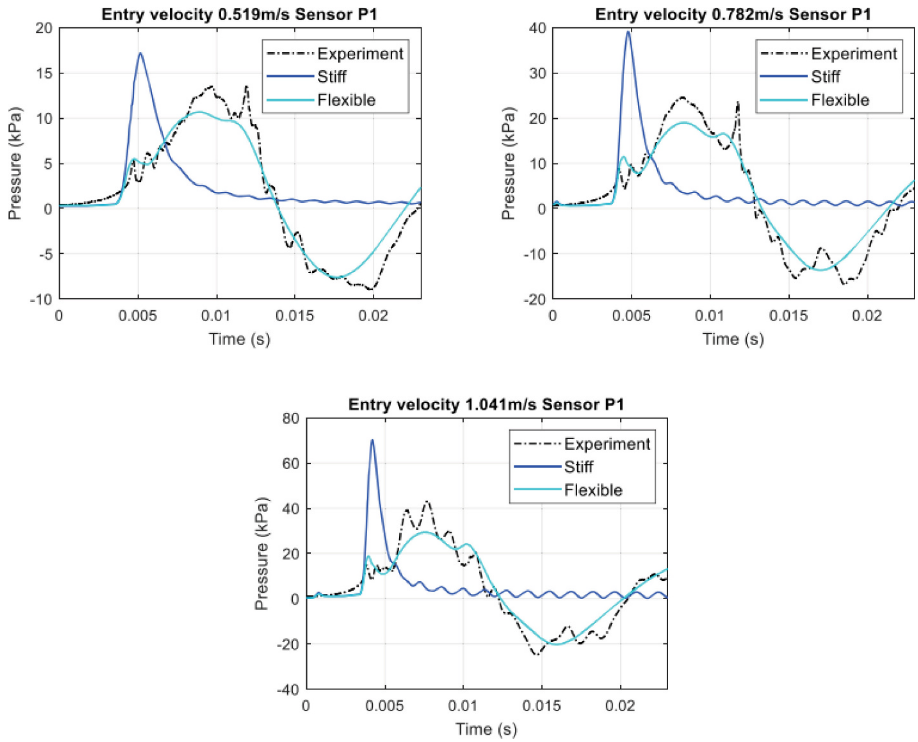

Fig. 6. Comparison of stiff and flexible plate simulations carried out by Yan et al. (2022c) with experimental (flexible plate) results presented by Tödter et al. (2020)

Severe green water effects coupled with slamming events in confused seas are rarely researched. This is because of the complexity associated with strong nonlinear interactions between waves and ships. Recently, Liu et al. (2022c) presented comparisons against theoretical and experimental data to verify the reliability and accuracy of their time domain method. Results indicate that the response of peak pressures in the bow and deck area was affected by high-frequency components, while peak pressures in the way of the superstructure were affected by low frequencies. Ha et al. (2024) presented a numerical model for predicting slamming impact loads on the bow flare of a ship-type floating production storage and offloading (FPSO) model under breaking waves. To investigate the relation between the slamming impact load and the free motion of the FPSO model, the breaking impact simulations were performed under fixed positions and the free motion of the FPSO model.

Since slamming is primarily a local loading event, it may affect the seakeeping qualities and strength of high-speed crafts. For example, high-speed ferries typically have operational limitations based on maximum motions, accelerations and slamming occurrence. Monohulls tend to suffer high slamming pressures near the lowermost chine from the bow up to 1/3 of the hull length and towards amidships (Kapsemberg & Brizzolara, 1999). Past analyses of the slamming loads on fast ferries operating at as-built conditions concluded that fluid-structure interactions were not affecting local pressure loads for hulls built in aluminum or steel. However, fluid-structure interactions may indeed play an important role for high-speed hulls built in reinforced plastic (e.g., see Honey et al. (2021)). Cross-deck bottom slamming is an important design constraint for high-speed catamarans, which can be equipped with wave-piercing bows. Shabani et al. (2018) mitigate slamming loads and to avoid large clearance from the waterline. (Hosseinzadeh et al., 2023b, 2023a) present two-part companion papers that deal with the experimental and numerical studies of the impact-induced loads and structural responses of a three-dimensional non-prismatic aluminum wedge with a stiffened panel during free-fall water entry. The effects of water impact velocity, deadrise angle, mass of the wedge, and bending stiffness on the slamming pressures and structural responses are discussed in detail. Two-way coupling methods are assessed and used to simulate the water entry problem. Initially, an explicit nonlinear finite element method with a Multi-Material Arbitrary Lagrangian-Eulerian (MMALE) solver is employed to evaluate the elastic response of the structure following a free-fall water impact. Subsequently, the hydroelastic slamming problem is modelled using a two-way coupled technique with a k-ε turbulence model and implicit unsteady solver for both the fluid and structural domains (Star-CCM + /ABAQUS). The importance of FSI simulation is assessed using a hydroelasticity factor (R_F), which is found to have a significant effect on the unstiffened bottom for all impact velocities studied. For a stiffened bottom panel, hydroelasticity is only significant at high-impact velocities.

In another recent study (Tavakoli et al., 2024) confirmed that local slamming loads can also be important to the seakeeping performance of planning craft. This is because, as the speed increases, the hydrodynamic lift forces that support the weight of such vessels magnify, and buoyancy gradually converges to zero while the displaced volume diminishes. In rough sea conditions, this can result in relatively large wave-induced motions and vertical accelerations that can be way greater than gravity. During what is known as the unsteady planning phase, large slamming forces may also arise, causing strains (see; (Gilbert et al., 2023; Hosseinzadeh et al., 2023b, 2023a; Tavakoli et al., 2023), and this may damage the vessel's bow region. Monohedral planning craft configurations (i.e., crafts with constant deadrise angle along their entire length) are subject to low deadrise angles in their rear part and larger toward the bow, where slamming loads can also be excessive. A solution can be given by developing optimal step hull configurations (see Bonci & de Jong (2023)). Recently, advanced numerical methods such as the 2D + t model introduced by Garme (2023) were used to account for the influence of one-way coupling in design. A two-way coupled method using unsteady Reynolds-averaged Navier-Stokes equation is presented by Diez et al. (2022), who also applied multidisciplinary design optimization (MDO) for the estimation of loads on a deep-V planning-hull grillage panel subject to slamming loads in regular waves. Notably, the effects of one-versus two-way coupling are negligible for both the original/traditional and optimized grillages (as per the hydroelasticity factor R). In contrast, the impact of FE boundary conditions on the analysis and optimization outcomes is significant, confirming the need for proper calibration of the FE model in FSI and MDO studies.

Slamming-Induced Whipping Loads

Zou et al. (2024) conducted an experimental investigation using a segmented model to determine bow flare slamming loads and whipping responses of a ship in regular waves. A continuous wavelet transform was employed to capture temporal variations in the harmonic components. Their study revealed that the whipping responses significantly increased the asymmetry of the vertical bending moment (VBM) at amidships at high sailing speeds.

Lu et al. (2023) introduced a 3-D nonlinear time-domain hydroelastic analysis method for ship wave loads considering asymmetric slamming. The hydrodynamic idealization is based on a 3-D Rankine panel method and structural dynamics are implemented by FEA. The interaction between the hull structure and the flow field was considered to predict the hydroelastic response of the hull girder. The motions and sectional loads of the ship are expressed by modal superposition. After calculating the asymmetric slamming loads using the Modified Logvinovich Model (MLM), the hydroelastic response of a 21,000-TEU container ship was analyzed. This incorporates the horizontal bending-torsional coupling vibration.

Li et al. (2022a) presented an experimental investigation of stern slamming and global whipping-induced responses using a segmented model test of a cruise ship with a scale ratio of 1:60. Experimental random uncertainty was analyzed by considering the model responses in a series of regular waves. It is found that different types of response have different levels of dispersion. In a sequel study, Li et al. (2024a) developed a time-domain hydroelastic numerical model for investigating the slamming and whipping loads imposed on a ship travelling at different forward speeds. The numerical model integrates a beam model, the 3-D Rankine panel model, and the 2-D modified Logvinovich model. The tilt angle of the 2-D profile in the slamming model is determined by the direction of relative velocity, which considers the forward sailing speed. It is shown that the first-order elastic mode mainly affects the dynamic response. The authors conclude that slamming forces may be sensitive to the longitudinal interval of the slamming profiles, especially in the way of the vessel's stern.

Parunov et al. (2024) presented a benchmark study on motion and global wave loads for the case of a Canadian Patrol Frigate in regular waves. Nine institutions participated in the benchmark with six codes, quantifying the hydroelastic responses. The seakeeping methods employed include non-linear strip theory, 3D boundary element method formulated in frequency and time domain, and computational fluid dynamics (CFD). Euler and Timoshenko beams are used to model the hull girder stiffness. Experimentally based methods, CFD and momentum theories, are employed to calculate slamming loads. It was found that fully coupled CFD and finite element method (FEM) provide results consistent with measurements, but such simulations are prohibitively computationally expensive.

2.1.6 Sloshing

Sloshing is a physical phenomenon that is to be considered for any moving vehicle or structure containing a liquid with a free surface. This is a vast topic covering many applications: propellant slosh in spacecraft/plane tanks and rockets, liquid slosh for trucks, offshore units and ships transporting liquids. For ships transporting liquids, sloshing is a large-scale phenomenon involving some very small-scale effects. Indeed, overall volume and geometries, fluid densities come into play as well as many local parameters such as local geometry of the tank's boundaries gas/liquid physical and thermodynamic properties (density ratio, surface tension, compressibility, phase change).

Following this physical description, one can identify two main topics: global (overall liquid motions within the tank) and local flows (impact pressures). The first topic, global flow, is of primary interest since the internal liquid motions inside the ship tank(s) may influence the ship's motions. Experimental and numerical calculation aspects will be covered. In addition, sloshing mitigation techniques will be presented. The second topic deals with local flows (free surface, kinematics) and impact pressures that may occur during liquid impacts. These impact pressures need to be quantified, especially for ships transporting cryogenic liquids. Indeed, loss of containment (due to extreme impact pressure) could have severe consequences for the crew and the ship. Also, numerical calculations and experimental results are covered.

Global Flow

The first topic deals with the evaluation of the global flow within the tank(s) in order to assess the possible influence of these internal liquid motions (and their forces) on the ship's stability and motions. The loss of stability due to liquid motions is usually calculated by the (analytical) evaluation of the free-surface correction of the metacentric height, and no dynamic calculation is required. One exception concerns the ore carrier. Indeed, due to recent major accidents involving ships carrying liquefied solid bulk cargoes, work has been carried out to better understand the fluidization of these solid cargoes, which can lead to capsizing. A transparent material was developed to be a substitute for iron ore (non-transparent) that allows to better visualize and understand this fluidization process through further sloshing model tests Chen & Zhang (2024).

For seakeeping applications, the influence of the internal liquid motions on the ship motions (or floating unit) depends on the tank's shape, dimensions, position, arrangement (internal structures or not), and liquid density. Going in order of increasing complexity, here are different configurations that have been studied in the literature.

First, for small tank's dimensions, for instance, a swimming pool (typically 20m) with respect to the ship ones (typically 200m), the influence of the internal liquid motions on seakeeping can be neglected (Wu et al., 2023b). These (very) different dimensions lead to a decoupling between the swimming pool natural periods and the ship motions ones resulting in quasi-static motions of the free surface. Thus, for small ship motions, a linear numerical model (neglecting nonlinear effects) was developed and has shown to be applicable by giving results close to CFD results (Qi et al., 2023). For such a linear model, the damping (due to bottom friction) can be approximated by a linear equivalent damping, which depends on the fluid velocity squared (Neugebauer et al., 2023).

The second configuration is related to large tanks such as spherical or prismatic LNG tanks (but without large internal structures such as baffles). These large tanks have a significant influence on the ship motions (Caputano & Goodwin, 2023; Wang et al., 2023e, 2024c). In Wang et al. (2023e), a typical FLNG equipped with three (prismatic) tanks was studied (usually, one or two tanks were considered). It was shown that the most conservative roll RAO (for a large range of frequencies) was associated with three tanks equally filled: changing one filling level in one of the three tanks significantly reduced the roll RAO. This result, which needed to be confirmed for other fillings distributions than the tested ones, was interesting since it confirmed that the iso-filling assumption made for the LNGC/FSRU/FLNG sloshing analysis was conservative. Regarding numerical methods that can adequately handle such type of coupling effects for large tanks (without internal structures), potential flow theory (frequency and time domain) and CFD (volume of fluids + VOF, Smooth Particle Hydrodynamics (SPH)) are widely used for both interior (liquid motions inside the tank(s)) and exterior problems (seakeeping), and are in excellent agreement with the model tests (Jiao et al., 2024; Wang et al., 2024c).

The last configuration for coupled seakeeping is related to tanks with internal structures such as anti-roll tanks. Kapsenberg & Carette (2023) showed that Free-Surface anti-roll tanks were more efficient than U-tanks (larger damping over a broader range of frequencies). The fluid flow characteristics inside such anti-roll tanks (traveling bore and the complex internal flow including flow separation due to the internal baffles) explained why CFD methods were required, and potential methods were unreliable. Finally, the Effective Gravity Angle (EGA, a combination of the local acceleration and the roll angle) was introduced and proved to be a governing parameter for such anti-roll tanks.

Local Flow

The second topic deals with the evaluation of the local flow (free surface, fluid velocities and impact pressures) within the tank(s). The final objective of such investigation is to assess the design loads to be considered for the design of the tank and ship's structures. To do this, sloshing model tests and numerical calculations considering water and air are reviewed. Indeed, for the sake of simplicity, many sloshing model tests (and so the corresponding CFD calculations) were carried out using the most straightforward available fluids, water and air. In Bardazzi et al. (2024), comparisons between sloshing model tests on a quasi-2D tank and one-phase SPH calculations were carried out. The studied filling level was close to the critical depth for which the resonant sloshing dynamics changed from "hard spring" to "soft spring" as filling increased. Very good agreement between CFD and experiments was observed for the free-surface elevation time series and the complex sloshing regimes (doubling frequency, tripling frequency bifurcations, asymmetric and chaotic regimes). Their study confirmed that even one-phase CFD calculations captured the global flow, the detailed local flow, and the complex sloshing regimes.

Other sloshing model tests focused on the free-surface profiles that can lead to significant impact pressures (Shen et al., 2024). It was confirmed that flip-through impacts (transition between liquid impact with an air pocket and wave running up along the wall) gave rise to the most significant pressures and stresses. However, pressure measurements showed poor repeatability, and impact pressures needed to be studied statistically. This stochastic nature of sloshing impact pressures and the complexity of the liquid impact physics explained why discrepancies were observed between experimental and numerical sloshing impact pressures (Pilloton et al., 2022). This led to original experimental sloshing campaigns using different fluids than air and water to study, among others, the effects of gas-to-liquid density ratio and phase transition on impact pressures. The first consisted of small-scale model tests using a non-flammable liquid with a boiling point of 34 °C at atmospheric pressure (Lee et al., 2021a). Condensation was observed, but the authors estimated that the influence of density ratio was more dominant than the effect of phase transition on the modification of impact pressures. In parallel, a larger-scale experimental campaign (named SLING) was launched. The objective was to better understand the source of variability and the main governing parameters (gas-to-liquid density ratio, compressibility, phase change) of the sloshing impact pressures (Ezeta et al., 2023). A flume tank (equipped with a wave maker) was installed in a high-end autoclave to study phase change during sloshing impacts. This multiphase facility also allowed the disentangling of the influence of the gas-to-liquid density ratio and the gas compressibility parameters. The first results confirmed the importance of the influence of the gas-to-liquid density ratio on sloshing impact pressures (the higher this density ratio is, the lower the pressures). The final aim of these studies was to improve the representativeness of the sloshing model and so the scaling of the sloshing model tests (Fan et al., 2024; Jain et al., 2021; van der Meer, 2022). However, in these model tests, raised edges (such as corrugations) were rarely represented due to small-scale issues. To circumvent this issue, dedicated numerical calculations were carried out to better understand the loads acting on these raised edges (Audiffren et al., 2024). In the studied configuration, the most significant loads occur on the first hit corrugation. In addition to these numerical calculations, machine learning approaches, based on the existing sloshing model tests database, were applied to predict sloshing activity that ship operators can use. Finally, the statistical post-processing of the sloshing impact pressures is the last step of a sloshing analysis. It was shown that discrepancies existed among the different mathematical formulations for the long-term pressures (Ahn, 2023; Ahn et al., 2024). Also, the importance of considering the hydro-elastic responses of the containment system and the supporting hull structure was highlighted (Malenica et al., 2022; Park et al., 2024).

2.1.7 Data-Driven Methods

Introduction

Recent technology developments facilitate the possibility of creating large datasets throughout a ship's lifetime. From the early design phase to the operation at sea, designers and operators have nowadays the possibility to utilize the information in this data to acquire new knowledge. The data can generally come from different sources, e.g., numerical simulations, model tests or full-scale measurements. Traditionally, ship designers have used experience and data from previous projects as well as regression-based empirical methods to create a preliminary design that fulfils the client's requirements and regulatory boundary conditions. Data-driven methods allow for more efficient, systematic utilization of large datasets for such tasks. Ship owners are under pressure to fulfil IMO emission regulations for their fleets. Due to rapidly advancing sensor and telemetry technology onboard ships, many ship owners possess large amounts of ship operational data. Data-driven methods, often based on Machine Learning (ML), offer significant potential for more efficient, safer, and environmentally friendly ship operations. Furthermore, operational data provides valuable input for the design of the next generation of ships. Several methods are available to efficiently and systematically exploit a given data resource, and new approaches are under development.

A general review of currently available ML approaches for application in the ship design process was given by Huang et al. (2022e). It shows the different ML application fields in ship design and operation. While the applications for routing and fuel consumption prediction were rated relatively mature, autonomous shipping was highlighted as a developing field with an increasing need for algorithm development. When it comes to ship design, it was found that most models so far focus on resistance reduction as the standard optimization goal. For example, Ao et al. (2023) proposed a deep-learning neural network model to predict the total resistance of KCS hull form variations. Using geometry modification parameters and Free-Form Deformation (FFD) techniques, the authors created a dataset to train and test the model, which is capable to predict hull resistance during preliminary design. The research concluded that deep learning enhances hull design efficiency and accuracy in the early design phase. However, there are not many application cases where data-driven methods have been applied for other important design aspects, such as stability and structural integrity so far. As highlighted in Fig. 7, approaches that can be classified as supervised and reinforced learning are among those that are best suited for wave load applications. In contrast, unsupervised learning algorithms are well suited for performance predictions such as fuel consumption.

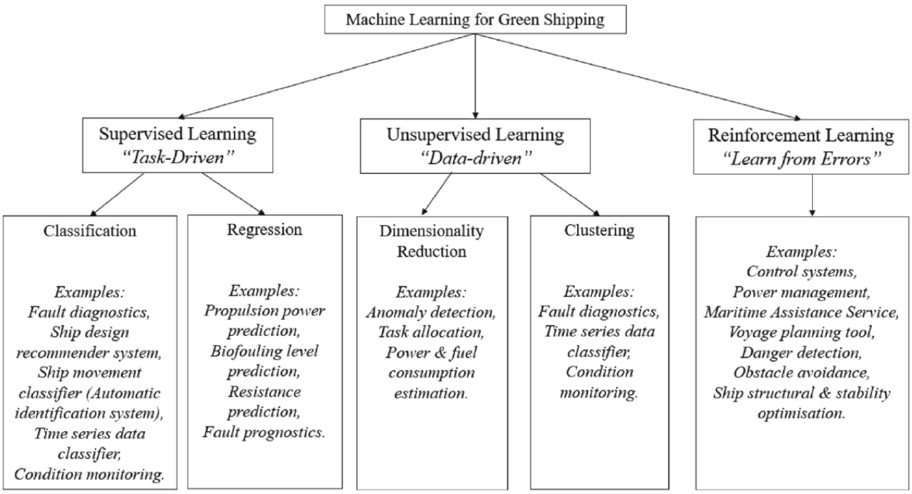

Fig. 7. ML strategies and application examples as a toolbox towards 'green shipping' from Huang et al. (2022e)

However, there have been early notable studies on ML applications in this field, such as Rogers et al. (1998), who developed an approach based on neural networks to determine dynamic bending moments without knowledge of the actual wave parameters. Their method is based on input from the ship's heave and pitch motion. Another early example is the optimization of a bulk carrier with two conflicting objectives (weight and fatigue) performed by Cui et al. (2012) where a simple reinforced learning approach called Q-learning was used. Based on a combination of multi-objective particle swarm optimization, reinforced learning, and CAE software, the authors were able to provide an improved design with respect to the original design for every chosen objective.

A review of recent research activities shows that the work on data driven methods for the estimation of the impact of wave loads on structural responses is still rather sparse. However, there is an increasing number of activities related to applying ML algorithms to predict the seakeeping performance of ships from simulations, model tests, or full-scale measurements. Besides offering possibilities and advantages in selected applications, data-driven approaches require special care regarding data pre-processing. This topic has become more critical as it has become easier to access large amounts of data via sensors and black box algorithms.

Structural Responses

In ship structural design, the prediction of the vertical bending moment (VBM) and the total longitudinal stress (TLS) is crucial. Current state-of-the-art methods offer approaches to determine these properties at different fidelity levels. Low-fidelity methods provide efficient and practical applications with low accuracy, and vice versa for high-fidelity methods. A study from Jiang et al. (2023a) introduced a multi-fidelity regression model using an artificial neural network (MF-ANN), which combines low-fidelity data for initial modelling and high-fidelity data for corrections, significantly enhancing prediction accuracy while offering efficiency and robustness. The proposed model was successfully validated through VBM predictions, while TLS predictions demonstrate that even minimal high-fidelity data can achieve high accuracy.

In another example, Wang et al. (2024b) investigated a real-time prediction method for wave-induced hull girder loads using ship motion data as input. Two Recurrent Neural Network (RNN) models were developed to predict VBM, horizontal bending moment (HBM), and torsional moment (TM) at the mid-ship of a large container ship. An improved model incorporating an error correction strategy was also explored to enhance prediction accuracy. The authors investigated the influence of RNN parameters such as the window length of the time series, optimizer, number of layers, and neurons on the prediction accuracy. Their study found that a 3-layer GRU network is optimal for TM and HBM, while a single-layer LSTM network is better for VBM, highlighting different data relevance. LSTM (Long Short-Term Memory) models were designed to effectively capture long-term dependencies in sequential data by using memory cells and gating mechanisms to regulate the flow of information. They are particularly useful for tasks involving time series data and other sequences where context from previous inputs is crucial for accurate predictions. GRU (Gated Recurrent Unit) models simplify the LSTM architecture by combining the forget gate (which determines what information to discard from the previous state) and the input gate (which decides what new information to incorporate) into a single update gate, making it computationally more efficient while still effectively capturing dependencies in sequential data. They can also be used for time series data, providing a balance between performance and complexity. Verification showed that prediction models perform best under the same irregular sea state conditions, with RMSE below 5.2%, and perform less accurately with varying sea conditions. The error correction strategy significantly improved the models, reducing RMSE for HBM from 10.1% to 6.8% and for TM from 7.5% to 5.8%. The improved prediction models show enhanced performance across different conditions.

A data-driven approach that does not use ML but can estimate long-term extreme values of wave loads on a ship along a defined route involving hindcast wave database and ship operability analysis was shown by Petranović et al. (2021). In their approach, the authors determined the transfer functions of wave-induced motions and loads through closed-form expressions. It identifies the most probable extreme wave loads for short-term sea states, calculates annual maximum values, and fits them to a Gumbel distribution. These distributions were then statistically combined along the route, considering sea states as either independent or fully correlated. This method aids in determining probable wave loads for long return periods, which are essential for ship structural design. The results closely align with other long-term distribution methods when assuming statistical independence among sea states. It also allows for considering wave zone correlations and the sensitivity of wave loads to operational criteria. Numerical results indicate that operability criteria are not met in 2–4% of sea states. Avoiding these reduces extreme bending moments by a factor of 2, reducing ship speed in these states cuts bending moments by 20%, and assuming complete correlation among sea states reduces bending moments by 8–21%.

Motion Responses

Over the last few years, there has been some noticeable development of data-driven methods to predict the impact of wave loads on the motion behaviour of ships. Three application scenarios can be distinguished: Purely data-driven models, physical-informed models and calibration models for low-fidelity software tools. The following selected examples highlight the progress in these fields.

A data-driven framework introduced by Ren et al. (2023) can identify 6-degree-of-freedom (DOF) ship models based on ship motion measurements and corresponding wave load estimations. The proposed model incorporates hydrodynamic coefficients, thruster inputs, mooring systems, and wind and wave excitation loads. Sparse regression was utilized to fit these measurements, ensuring that the reduced-order system captures the main features of the system's dynamics while maintaining the physical integrity of the candidate functions. The authors verified their method through experiments and comparative studies, demonstrating its potential for application to other floating structures. This work highlights the importance of balancing model accuracy and complexity and shows that the algorithm can achieve satisfactory short-term motion predictions through direct integration. However, the real-time application requires significant improvements in computational speed. Future research is suggested to focus on enhancing estimation accuracy, reducing computation time, and improving robustness against noisy measurements, especially in scenarios involving time-varying speeds and headings.

Another recent example is a study by Lee et al. (2023), where an integrated artificial neural network system was developed to predict ship motions in varying sea states. The system combines an LSTM encoder-decoder to capture motion-induced wave effects with a convolutional neural network (CNN) for analyzing spatiotemporal wave-field data. The LSTM encoder processes historical motion data to encode the memory effects of radiated waves. At the same time, the LSTM decoder utilizes this encoded information along with anticipated wave field data to predict future ship motions. Validation using a physics-based seakeeping program demonstrates the system's robustness in making deterministic predictions in new sea states.

While purely data-driven methods can provide satisfactory results, physics-informed neural networks (PINN) offer greater accuracy in many application cases. PINNs integrate principles from physics into the architecture and training of neural networks. They are designed to directly enforce physical laws, such as conservation principles or governing equations, into their learning process. By embedding prior knowledge of physical behaviour, PINNs can effectively learn from limited data and generalize to new scenarios more robustly. This approach not only enhances the interpretability of neural network predictions but also improves their accuracy by constraining solutions to adhere to known physical constraints. One recent application example is the study by Schirmann et al. (2022), who investigated the effectiveness of linear response regression (RR) and nonlinear neural network (NN) models in predicting vessel heave, pitch, and roll using multidirectional wave data. The inclusion of physics-based motion predictions in these models was highlighted, demonstrating improved performance in reducing the Mean Squared Error (MSE) compared to models without physics-based inputs. Their work revealed that NN models outperform RR models when physics-based information is included. This can be attributed to their ability to capture nonlinear relationships. However, physic-informed RR models can predict heave and pitch motions reasonably well.

Another field where research activities are observed is the application of ML algorithms to enhance the accuracy of low-fidelity software results by using training data from low- and high-fidelity codes. Kim et al. (2023a) developed a method to improve the accuracy of efficient ship motion models. In their study, they calibrated low-fidelity models, which use constant coefficient ordinary differential equations using data from high-fidelity simulations. Forced motion calculations determined radiation forces, and fixed-body calculations assessed diffraction forces, which were then regressed to obtain appropriate coefficients for the low-fidelity models. The proposed calibration method significantly improved the performance of low-fidelity models, ensuring their outputs align closely with high-fidelity models through penalized regression techniques to stabilize coefficients.

Data Processing

Large amounts of data offer new possibilities for ship owners and designers to improve both the operation of current ships and the design of the next generation of ships. However, especially on-board and weather data pose significant challenges regarding data quality and availability, directly impacting ML model results. The methodologies proposed by ISO19030 alone might not be sufficient to address these issues. While the significance of the field grows, not much focus has been put on this in terms of research so far. A study by Jabary et al. (2023) discussed the development and implementation of a data processing system for ship operational data. The system integrated raw operational data from multiple sources, such as onboard measurements and external data, into a unified database. To ensure data quality, the raw data underwent pre-processing steps, including data filtering and imputation, to address missing values and outliers. Data quality issues like missing data, outliers, and different data formats and frequencies presented significant challenges, which were mitigated through the pre-processing procedures. The processed data was then used for performance analyses, with the aim of optimizing ship operations for critical performance indicators. The general observations and conclusions regarding data quality and availability also apply to other ML applications, such as wave and structural loads.

2.2 Wave Loads on Offshore Structures

Significant advancements have been made in understanding and analysing wave loads on offshore structures, driven by the growing demand for accurate and reliable design tools to ensure the efficiency, robustness, and safety of these structures operating in complex marine environments. This section reviews state-of-the-art developments, organized into key thematic subsections as in Sect. 2.1. Unlike ships, offshore structures are designed to maintain a fixed position during operation. While the fundamental theoretical principles may overlap with those applied to ships, the specific requirements for offshore structures introduce unique challenges related to wave-induced phenomena and their modelling. For instance, first- and second-order wave and current loads are critical for the design of mooring systems and station-keeping. In contrast, ship design focuses more on calm water resistance and added resistance in waves, which are essential for seakeeping and manoeuvrability. These distinctions highlight the specialized approaches for analysing and simulating wave loads on offshore structures.

2.2.1 Potential Theory Method

Potential flow theory has been exploited to calculate the exciting wave loads on such structures and their response to the wave interaction with fixed and floating structures. Concerning ships, different boundary conditions are considered for offshore structures, such as the stiffness of the station-keeping system, to determine the dynamic response of offshore structures. Moreover, structures supporting offshore energy systems, such as floating solar panels, can be very large, including hinged modules tethered to the sea bottom (Zheng et al., 2024). Eventually, the time-domain response of offshore structures is required to approximate the coupled dynamics of offshore structures, and correspondingly, the nonlinearity of wave loads on the offshore structure must be considered for studying the resonance modes.

Linear and Weakly Nonlinear Potential Flow Theory.

Hao & Pan (2022) used Green's function of submerged pulsating singular points to implement a panel method solver for computing potential flow due to wave interaction with offshore structures with a thin shell geometry. Dipole elements were employed to model the body boundary condition on the thin shell geometry as a drop of the potential, which can be exploited to include porosity-related effects. Moreover, numerical studies on a two-layer panel model with small gaps suggest that the mesh size requirement in DNV-RP-C205 needs revision. Hence, the linearized free surface boundary conditions and the linear body boundary conditions are satisfied in the solution. The diffraction and radiation potential functions have been calculated in the frequency domain, which imposes the constant water depth condition. The image method has been deployed to address the sea bottom boundary condition and linearized free surface boundary conditions.

A comprehensive study was conducted by Cong et al. (2021) on the wave run-up on the bottom-mounted cylinder subject to bi-directional irregular waves using the second-order potential flow model. The second-order velocity potential induced by the sum and difference pairs of wave components was computed through Quadratic Transfer functions (QTF). Prior experimental and numerical studies had verified the solution for the single cylinder, and the model was here used to determine the second-order wave elevation near the cylinder near the wall. A comparative study was presented to demonstrate the second-order wave run-up on the cylinder, as shown in Fig. 8. The significance of representing the free surface to the second order is remarkable in the free surface's evolution and the surface elevation's magnitude. The impact of the second-order terms is amplified for oblique sea heading angles where the interference of directional frequency pairs is considered.

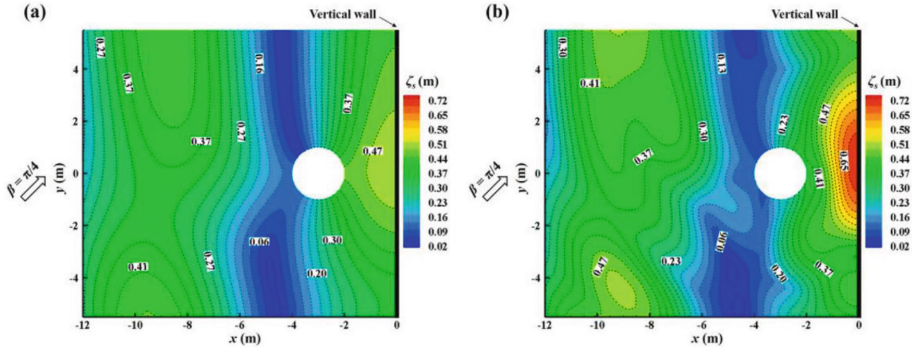

Fig. 8. Comparative study of the wave elevation amplitude distribution around the cylinder near the vertical wall for linear solution (a) and second-order solution (b) in a regular wave (Ka = 0.48)

For an array of truncated cylinders in a row distributed in equal space, the solution of the second-order velocity potential was computed by (Huang et al., 2021) to estimate the wave elevation within the cylinder and sum and difference wave forces due to frequency pairs of irregular waves. Indeed, Huang & Teng (2020) work was extended for bi-chromatic incident waves, and some improvements in the numerical algorithms were included where the wave propagating and evanescent modes were derived. Since the up- and down-wave vertical surfaces are allowed to be placed close to the body, the calculation of the free surface integral can be performed in a small region, and an analytical method was developed to directly evaluate the up- and down-wave vertical surface integrals. After solving the boundary integral equation, the sum- and difference-frequency radiation and diffraction potentials were computed explicitly. Numerical results for the quadratic transfer functions of the second-order free surface elevation, pressure and force were demonstrated for a series of geometries in channels.

The effect of incident waves on the piston-like behaviour of the free surface between two fixed barges was investigated by Gao et al. (2022)). A linear potential model using a higher-order boundary element method (BEM) was employed to determine the effect of the incident wave angle on the resonant fluid motion within the gap for two fixed square corner barges. An adaptive Gaussian method was used to improve the accuracy for nearly singular integration. The results show that gap resonant peaks at other incident wave angles would be more critical than the beam sea case, which has been widely deemed the most crucial case. Moreover, the second mode peak value can overcome the first mode peak value at specific conditions. The resonant frequency and peak value increase while the gap width decreases.

Fully coupled aero-hydrodynamic modelling of floating offshore wind turbines was simulated by Deng et al. (2023), in which the time-domain second-order potential model was developed to introduce the instantaneous hydrodynamic pressure and corresponding wave loads in the equation of motion. The free surface was included in the boundary integral equation, and the perturbation approach was implemented to calculate the second-order velocity potential. Furthermore, the time-domain second-order wave loads associated with the aerodynamic load were introduced into the equation of motion, with the stiffness matrix of the mooring line taken into account on the left-hand side of the equation of motion.

A coupled-dynamic approach of a modularized design of a Tension Leg Platform (TLP) structure which supports the power transmission plant for a wind farm was studied by Abbasnia et al. (2024). A three-dimensional linear potential model was developed to study the buoyant de-centralization of modules on the response of the TLP structure in long-crested waves, with slackline occurrence being considered as a design criterion.

The potential flow model has also been implemented to approximate resonance modes in fixed and floating Wave Energy Converters (WEC) of the type Oscillating Water Column (OWC). Since the free surface inside the OWC chamber may be influenced by the Power-Take Off (PTO) system through the pneumatic pressure of the trapped air, the efficiency of the OWC devices has become a point of interest to study the performance of OWCs for various geometrical properties of OWC chamber, sea-bottom variations and the PTO mechanism. Srinu et al. (2024) developed a two-dimensional linear potential flow to study the performance of a fixed OWC for a wavy sea bottom. The linear pneumatic model was used to solve the velocity potential inside the chamber, and the resonance mode of the piston-like free surface was investigated. Moreover, George et al. (2021) used the two-dimensional potential flow model to optimize the U-shaped oscillating water column (U-OWC) device based on an artificial neural network model.

Fully Nonlinear Potential Flow Theory

The resonance mode of the free surface within the trapped free surface among the double-body structure was investigated by developing a 2D fully nonlinear NWT in which a high-order finite element method (FEM) was employed to solve the potential flow (Huang et al., 2022b).

Kim et al. (2021) developed a 3D, fully nonlinear numerical wave tank (NWT) to approximate the response of a freely floating cylinder in nonlinear waves. The decomposition method was used to calculate the time derivative of the velocity potential implicitly, and the linear BEM formulation was used to calculate the kinematics of the water particles. The results were compared to prior studies to demonstrate the range of validity of the NWT. A FEM solver was developed to solve the fully nonlinear potential flow for twin-cylinder oscillating in currents to find out modes of resonance of the free surface. Similarly, a two-dimensional fully nonlinear model was developed by Abbasnia et al. (2022) based on a high-order BEM to determine the dynamic response of a twin-cylinder supporting a floating solar panel. The numerical model was verified by a set of experimental records.

Abbasnia et al. (2021) developed a two-dimensional, fully nonlinear model to simulate free surface elevation within a fixed Oscillating Water Column (OWC) device. The spring-like behaviour of the trapped air due to the PTO mechanism was taken into account for the chamber free surface. A series of investigations were made to study the dynamic response of a floating pontoon OWC near the breakwater in coastal zones using the three-dimensional, fully nonlinear potential model (Cheng et al., 2022b, 2022a). The results were compared with experiments to verify the numerical results.

Cong et al. (2024) conducted a feasibility study for enhancing the wave energy capture of OWC devices through the utilization of Multi-Chamber Multi Turbine (MCMT) technology. Unlike traditional single-chamber OWCs, MCMT OWCs comprise multiple chamber modules that can coordinate during different wave phases to optimize wave energy cultivation. By considering coupling effects in a linear reciprocal relationship between the air pressure and air-flow movement in different chamber modules, a numerical model was developed to assess the functional performance of three-dimensional MCMT OWCs of arbitrary geometric shapes using a fully nonlinear higher-order BEM. The study focuses on representative MCMT OWC designs with annular or rectangular cross-sections. Two specific scenarios were investigated: an annular MCMT OWC integrated into the monopile foundation of an offshore wind turbine and a rectangular MCMT OWC integrated into a barge-type breakwater. Numerical analyses revealed that dividing the chamber into multiple modules can convert sloshing-mode free-surface movement into separate piston-mode movements, thereby enhancing wave energy capture.

2.2.2 Field Methods

Field methods provide various techniques and tools for solving the Navier-Stokes equations, which are essential for simulating wave-structure interactions in ocean and coastal engineering. These methods are categorized into Lagrangian, Eulerian, and Lagrangian-Eulerian combined techniques. Modelling wave-structure interactions poses significant numerical challenges due to highly deformed, moving interfaces with complex physics such as wave breaking and fluid turbulence. Additionally, intricate interactions occur between waves and both rigid and flexible structures, as well as non-linear interactions between fluids and solids with different physical properties. Eulerian methods, which depend on a mesh grid, have been extensively developed and applied, with tools like *OpenFOAM*, *Star-CCM* +, *REEF3D*, *ANSYS/Fluent*, and *ANSYS/CFX* being prominent examples.

The use of *OpenFOAM* has significantly advanced the study of hydrodynamic loads on offshore structures through various complex interactions and modelling techniques. Researchers have effectively investigated wave-structure interactions, including the examination of nonlinear wave fields and amplification harmonics around fixed tandem cylinders, as well as the development of improved screen force models for hydrodynamic loads on net panels for fish cages and offshore fish farms (Mohseni & Guedes Soares, 2022a, 2022b; Wang et al., 2022b). Coupling methods between potential and viscous flow solvers have enhanced computational efficiency while accurately capturing hydrodynamic loads (Robaux & Benoit, 2022). Studies on floating structures have validated models for floating body motion with mooring dynamics, providing critical insights into the dynamic responses of barge-type platforms and the significance of nonlinear drag forces (Chen & Hall, 2022; Otori et al., 2023). Hydrodynamic coefficients and induced flows around heave plates have been determined with high accuracy (Pinguet et al., 2022). Empirical and numerical methodologies, such as the Morison approach and domain decomposition strategies, have been assessed for predicting hydrodynamic forces (Aliyar et al., 2022; Clément et al., 2022). High-fidelity Computational Fluid Dynamics (CFD) models have been created for WECs in extreme wave conditions and dual-chamber oscillating water column devices, demonstrating robustness (Gadelho & Guedes Soares, 2022; Katsidoniotaki et al., 2023). Additionally, research into wave loading on TLP-type floating wind turbines and wake interactions between spar-type floating offshore wind turbines has underscored the capability to predict dynamic responses and aerodynamic loads (Mohseni & Guedes Soares, 2024). Moreover, novel methodologies based on *OpenFOAM*, such as *qaleFOAM* for simulating focusing waves and their interactions with fixed/moving cylinders, and the *FOWT-UALM-SJTU* solver for coupled aero-hydrodynamic simulations of Floating Offshore Wind Turbines (FOWT), have been developed to address specific challenges in modelling complex offshore systems. (Gong et al., 2021; Huang et al., 2023b; Yu et al., 2023c).

Similarly, the application of *STAR-CCM+* has provided significant insights into the hydrodynamic loads on offshore structures. Researchers have extensively explored wave-structure interactions and the effects of platform motion on the aerodynamic performance and wake properties of FOWTs, employing advanced techniques such as Dynamic Fluid Body Interaction (DFBI) and Volume Of Fluid (VOF) methods(Alkhabbaz et al., 2024; Califano et al., 2023). The influence of hydroelastic effects on wave-induced forces and structural responses has been highlighted through flexible structure modelling and fluid-structure interaction (FSI) simulations, demonstrating the significant impact of hydroelasticity on the overall load and bending moments of monopile structures (Gu et al., 2023; Thome et al., 2023). Investigations into nonlinear difference-frequency wave loads on semi-submersible FOWTs have underscored the importance of accurate uncertainty quantification and the impact of higher harmonics on overall hydrodynamic loads (Wang et al., 2021a; Zeng et al., 2023). Advanced aero-hydrodynamic analyses have demonstrated the benefits of novel biomimetic and fractal designs in improving the stability and efficiency of semi-submersible platforms, as well as optimizing WECs integrated with floating wind turbines, showing significant improvements in power generation efficiency through heaving viscosity damping correction (Huang et al., 2023a; Zhang et al., 2022f). The hydrodynamic responses of floating platforms under irregular waves have been validated using coupling approaches between High-Order Spectral (HOS) and CFD models, enhancing the accuracy of low-frequency responses and improving the predictive capability for extreme wave conditions (Zhang et al., 2023f) (Fig. 9).

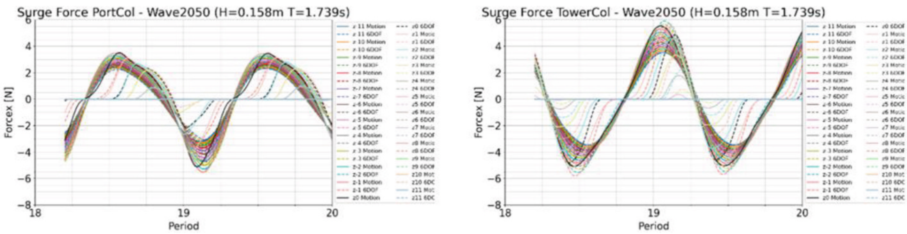

Fig. 9. Comparison of the sectional surge force on the port (left) and tower (right) column of a FOWT floater in Califano et al. (2023)

Building on the strengths of these established tools, *REEF3D* and *ANSYS/Fluent* have also been instrumental in advancing hydrodynamic studies of various offshore structures. *REEF3D* has been employed to investigate hydrodynamic characteristics and responses under oscillatory flow conditions, providing insights into parameters such as blockage ratios and Keulegan–Carpenter numbers on square cylinders (Dutta et al., 2022). It has also been used to analyze the dynamic responses and mooring forces of submersible steel-frame offshore fish farms under regular wave conditions, highlighting the sensitivity of surge motions to wave parameters and the effects of structural variations on motion responses and mooring forces (Wang et al., 2022c). *ANSYS/CFX* been also applied to assess the impact of wind and wave loads on floating photovoltaic systems, where numerical simulations and finite element analysis were conducted to evaluate stress distributions and ensure the structural integrity of these systems under various conditions (Choi et al., 2023).

In addition to commercial and open-source tools, in-house codes have also played a crucial role in advancing our understanding of hydrodynamic behaviour. A hybrid model combining fully nonlinear potential flow and Navier-Stokes equations has been developed to simulate complex wave-structure interactions in large domains, achieving good agreement with experimental data and showcasing the advantages of such hybrid models (Saincher & Sriram, 2022). Another study utilized a two-dimensional RANS CFD model with a VOF method to investigate hydrodynamic interactions between adjacent floating bodies, highlighting the sensitivity of hydrodynamic coefficients to the displacement of floaters (Jiang et al., 2024). Additionally, the hydrodynamics of a submersible steel-frame offshore fish farm in regular waves was analyzed using an open-source CFD code coupled with an in-house FEM code, demonstrating the accuracy of the coupled CFD-FEM approach in predicting the response of floating offshore wind turbines under regular wave conditions (Wang et al., 2022h).

Furthermore, particle-based methods have significantly advanced the study of wave-structure interactions and hydrodynamic loads on offshore structures. The particle-based method has been enhanced for 3D simulations, enabling accurate modelling of wave interactions with fixed structures through a hybrid approach combining potential and viscous flow models such as Meshless Local Petrov-Galerkin method with Rankine source function (MLPG_R) model (Agarwal et al., 2021). The SPH framework has been validated for various applications, including the DeepCwind semi-submersible floating platform, demonstrating high fidelity in predicting hydrodynamic loads and capturing nonlinear behaviours under different wave conditions (Tagliafierro et al., 2023). SPH simulations have also accurately modelled the interactions between steep and breaking waves with vertical cylinders, revealing complex relationships between wave phases and peak forces (Yang et al., 2023d). Further, SPH studies on sea access roads and floating boxes have provided detailed insights into horizontal and uplift wave forces, validating the method's accuracy against experimental data (Chen et al., 2022f; Vineesh & Sriram, 2023). The SPH method has shown potential for full-scale applications, accurately simulating the hydrodynamics of floating offshore wind turbines and capturing the dynamic responses and mooring line forces under various wave conditions (Tan et al., 2023). Additionally, SPH modelling of wave interactions with multi-float structures has offered valuable insights into the hydrodynamic performance and structural responses, demonstrating its capability in engineering practice (He et al., 2023).

Finally, the Boussinesq equation has been effectively applied to study hydrodynamic loads and wave interactions with offshore structures, leveraging its ability to handle nonlinear and dispersive wave effects efficiently over large domains. A mathematical model using higher-order Boussinesq equations was developed to analyze solitary wave interactions with a floating pontoon, validated against CFD simulations using *OpenFOAM* and *OceanWave3D*, demonstrating good agreement and highlighting the model's ability to capture complex wave profiles and pressure distributions (Mohapatra et al., 2022). A hybrid modelling approach that couples a finite-element Boussinesq model (FEBOUSS) with a Meshless Local Petrov-Galerkin model (MLPG_R) for Navier-Stokes equations efficiently simulates wave-structure interactions, especially for directional waves, by combining the strengths of both models (Agarwal et al., 2022). The near-trapping phenomenon in a four-cylinder array was investigated using a Boussinesq model with a cut-cell technique, accurately predicting high free surface elevations and wave loads, which are critical for the safety assessment of offshore structures (Ning et al., 2022).

2.2.3 Wave-Current Interaction

Floating structures are affected by various environmental factors such as waves, currents, and winds. In many cases, the hydrodynamic performance of floating structures has been focused only on waves. Nevertheless, in recent years, the current effects have been thoroughly studied in the literature.

The importance of considering wave-current interaction effects of wave loads on cylindrical bodies has been investigated (Ghadirian et al., 2021; Xin et al., 2023; Yang et al., 2021). It was shown that waves in the presence of opposing currents are causing a nonlinear effect of the free surface elevation and inline force component. In contrast, current colinear waves are the most linear, causing a wave height decrease with increasing current velocity. Furthermore, the coupled effects between surface waves and subsurface current play a more important role in the hydrodynamic loads than the surface elevation. A higher-order FEM has been applied by Huang et al. (2022b) to analyze the nonlinear wave resonance generated by oscillations of twin cylinders in a uniform current. They concluded that the resonance which is caused by wave-current effect occurs at all first-order resonant frequencies for both symmetric and antisymmetric motions of the cylinders.

Offshore Wind

Offshore wind energy harnessing is a major renewable energy technology. During the design process of an offshore Wind Turbine (WT), it is necessary to properly predict the energy yield and structural loads. Offshore WT foundations can be categorized as gravity-based foundations, suction caissons, monopiles, and floating structures with mooring systems. Of these foundations, monopiles have been the most widely used for shallow water, either as isolated bodies or as part of Jacket foundations. Regarding their wave-current interaction phenomena, numerical models taking into consideration different wave-current interaction angles and focusing on the stress inside the seabed and the liquefaction area around the pile have been considered in the literature (Lin & Guo, 2022; Wei et al., 2022). The Reynolds-averaged Navier-Stokes equations with the k-ε turbulence model have been used, and Biot's poro-elastic theory has been applied to simulate the transient seabed response. As far as floating structures with mooring systems are concerned, the nonlinear stationary response of a spar-type WT under current and wave interactions has also been examined (Silva et al., 2021). These interactions have been estimated using statistical quadratization theory, which describes the nonlinear system as an equivalent polynomial of quadratic order. The main advantage of the theory is the low computational cost, which is lower than corresponding time domain simulations while producing accurate estimations of the platform's responses. Additionally, a semi-submersible floating platform, encompassing either a WT or a WT and a fish cage, under the actions of wind, current and wave loads has been studied (Fan et al., 2023; Zou et al., 2023). The hydrodynamic responses of the platform, under the action of aero-hydrodynamic coupling, have been evaluated, highlighting their interaction with the aerodynamic loads of the blades. Concerning the effect of the fish nets on the platform's displacements, these can suppress the low-frequency motions but have almost no influence on the wave-frequency motion. A vertical cylindrical body can also be applied as a monopile for offshore wind turbine support. Buljac et al. (2022) determined the environmental load effects on a monopile concurrently subjected to wind, wave and currents. They showed that the wind predominantly causes surge direction structural loads at the natural frequency of the wind turbine, whereas currents enhance the dynamic loads at low frequencies due to nonlinear hydrodynamic interactions.

Aquaculture

Fish cages, which operate individually or as an array, are increasingly being considered to be deployed in open sea areas to have higher water quality and fewer conflicts with other maritime activities. Therefore, the development of a fish farm which can withstand the current and wave loads is a prerequisite for the industry. The wave-current interactions with the mooring system of a fish cage have been studied in Cheng et al. (2021) and Liu & Guedes Soares (2023). These analyses concluded that for a current velocity of less than 0.5 m/s, the mooring forces are still within the safe range even if a mooring line breaks, whereas in order to avoid cage volume reduction due to large current velocities, the weight of the bottom ring of the cage and/or the net solidity should be selected appropriately.

Nevertheless, an increase in the ring's weight results in larger mooring loads, whilst a decrease in the net solidity may lead to the fish escape. Regarding the type of netting materials and their connections, numerical studies have been conducted focusing on the axial forces on the connection points between the net and ropes/steel connectors (Føre et al., 2022; Hu et al., 2022b; Slagstad et al., 2023; Xie et al., 2023b). Findings from these studies include that for large stiffness of the connectors, the vibration displacement of the net becomes small. On the other hand, with small stiffness, the motion of the rope becomes significant which increases fatigue damage.

Tidal Energy

Tidal energy is a renewable and predictable energy source for which pre-commercial type models and full-scale devices have been developed. Recently, many studies have focused on various forms of tidal current turbines. Specifically, attention has been paid to tidal rotors undergoing prescribed uncoupled surge, heave, and pitch motions in the presence of regular waves concluding that the heave motion reduces the mean power coefficient by about 9%, whereas the pitch motion causes periodic fluctuations in the damping coefficient of the power coefficient (Huang et al., 2022a; Wang et al., 2022g). Also, several studies have reported that the frequency and amplitude of the surging motion can increase the power output of a horizontal-axis tidal turbine (Wang et al., 2021c; Zhang et al., 2023e). Furthermore, Zilic de Arcos et al. (2023) applied a coupled model for the force-motion interactions between a tidal rotor and a floating platform. Their analysis showed load fluctuations due to phase interactions between waves and platform motions, which, at certain ranges of wave periods, can cause a reduction in fatigue damage and improve the quality of power delivery. A parametric study on the dynamic loads of a tidal current turbine with and without considering wave-current interactions, using higher-order theories coupled with a modified BEM, has been developed by El-Shahat et al. (2021). From their analysis, it was concluded that maximum loading ranges were 170% of the average out-of-plane bending moment and 99% of the average in-plane bending moment without interactions, whereas with wave-current interactions, these values were reduced to 110% and 69% for out-of-plane and in-plane bending moments, respectively. In addition to the developed tidal turbines, a hybrid wave and current energy converter has been presented to harvest energy from both ocean wave and current simultaneously (Chen et al., 2022d). This device can improve the electric power output by 38% - 71% for regular- and 79% for irregular- waves compared to a WEC.

Submerged Tunnels

Submerged floating tunnels are innovative deep-water transportation infrastructures for crossing waterways. Compared to coastal bridges subjected to strong winds and waves, submerged tunnels have a more significant potential for development in a strait or bay area with high tropical cyclone activity (Chen et al., 2023b; Xu et al., 2023). However, like other coastal structures, floating tunnels are subjected to wave-current actions. In this regard, several studies involving segment tests and numerical simulations were conducted to examine the motion response of a submerged floating tunnel under wave-current actions (Jeong et al., 2022; Won et al., 2021; Yang et al., 2023e; Zhou et al., 2023a). The horizontal response of a submerged floating tunnel is significantly amplified when the wave force direction is the same as the direction of the current force, whereas non-uniform terrain may mitigate the displacement distortion at both ends of the tunnel (Xu et al., 2023). Furthermore, with respect to combined earthquake and wave-current actions, recent studies have shown that the response of the submerged tunnel is strongly affected by the direction of the earthquake action (i.e., horizontal earthquake action increases the responses of the system compared to the vertical). Additionally, waves can weaken the tension amplification of earthquakes by up to 10% and increase the maximum horizontal acceleration of the tunnel by 40% (Luo et al., 2021; Wu et al., 2021).

Floating Bridges

Floating bridges are often located in exposed areas and are subjected to combined environmental loads. Analyses have shown that the hydrodynamic loads of wave-current combined flow are much larger than those of the wave-only flow, while when waves and currents are travelling in the same direction, the responses of the bridge are significantly amplified (Huynh et al., 2023). Specifically, under 1-year load cases, the amplifications in the standard deviations of the acting loads and bending moments are 30%–52%. On the other hand, under 100-year load cases, these values are doubled (Dai et al., 2022). Huang et al. (2022g) concluded that the hydrodynamic pressure on the structure caused by the earthquake increases with increasing water depth, whereas the combined effect of seismic and waves differs from that of only seismic action. Hence, the influence of the travelling wave effect cannot be ignored. It should be noted, however, that the vertical displacements of the bridge pontoons caused by heavy moving loads (vehicle loads) are significantly larger than those caused by environmental loads (Miao et al., 2021). In addition, several studies have been presented recently which are focused on basin tests of a scaled floating bridge model under the combination of wave, current, and wind loads (Rodrigues et al., 2022; Viuff et al., 2023; Xiang et al., 2023). From the experimental analysis, it was concluded that, generally, the current reduces the bridge's pontoon motion responses related to the horizontal motion of the bridge, while the vertical pontoon motions are amplified. Figure 10 shows floating bridge experimental model tested by Rodrigues et al. (2022). The model was subjected to concurrent waves and current and prescribed wind loads time series. The wind pre-computed loads were obtained from numerical simulations and applied using cables connecting each pontoon to an individual actuator.

Mooring Buoys

Cylindrical and spherical buoys have also been used as catenary anchor leg mooring buoy structures which interact with waves, underwater currents, and wind. Amaechi et al. (2022) conducted a numerical study to evaluate the buoy's motion responses. Regarding the effect of the current speed on the body's hydrodynamics, it was concluded that the buoy's motions are influenced by the increase of the current, which also increases the effective tension in the mooring lines.

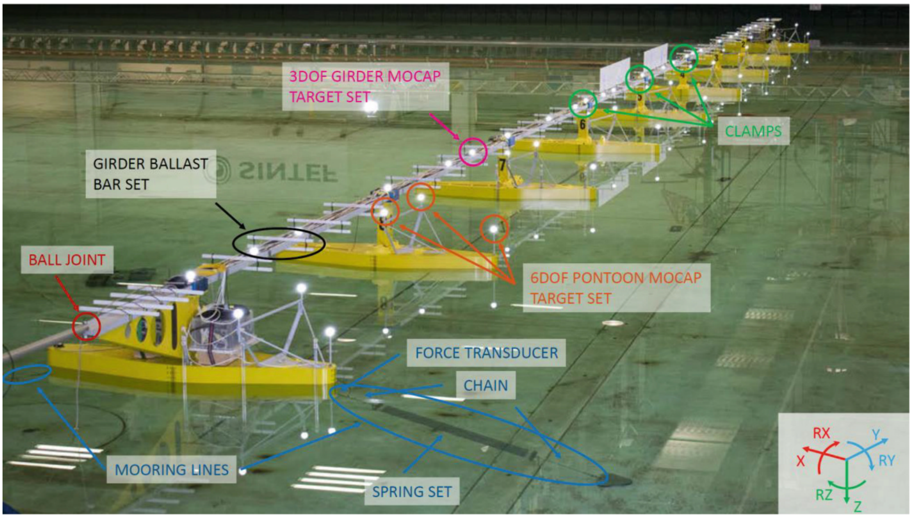

Fig. 10. Photo of the floating bridge experimental model from Rodrigues et al. (2022)

2.2.4 Airgap and Wave-in-Deck Loads

The structural safety of offshore platforms is critically dependent on understanding and managing of the airgap and Wave-In-Deck (WID) loads. Recent studies have mainly focused on quantifying these factors to enhance platform design and safety protocols. This review synthesizes the findings from multiple studies conducted between 2021 and 2024, highlighting advancements in modelling and risk assessment procedures related to WID in offshore structures.

Airgap refers to the vertical distance between the lowest part of an offshore platform's deck and the crest of the highest expected wave. This gap is critical for preventing WID occurrences, which can lead to severe structural damage. WID loads are the forces exerted on the platform's deck when waves exceed the airgap. These loads can be extremely high, especially during storms or in regions with harsh ocean conditions. The impact can be divided into three phases: the initial impulsive force phase, an oscillatory phase, and a subsequent negative pressure phase. These phases can cause both global and local structural damage, including denting, cracking, and, in severe cases, platform collapse.

A Complex Phenomenon

WID loads are inherently highly non-linear, not only due to the complex nature of the wave forces but also because of the intricate fluid-structure interaction caused by the irregular geometry of the structures subjected to these loads, such as the topsides of oil and gas rigs. As a result, simplified methods are often employed in practice, as outlined in standards like the silhouette method from the American Petroleum Institute recommended practice (API, 2014).

However, these procedures are extremely conservative, potentially leading to an over-estimation of the loads on structures by as much as 30%–75%, as reported by Wang et al. (2023c). This emphasizes the value of applying high-fidelity numerical methods, such as Smoothed Particle Hydrodynamics (SPH), to capture better the complex nonlinearities involved. These advanced methods can effectively handle phenomena like air compressibility effects (de Oliveira Costa et al., 2021), the influence of platform deck appendages such as balconies (Fonseca de Carvalho e Silva et al., 2023), and the accurate modelling of freak waves (Huo et al., 2021; Luo et al., 2022). Interestingly, the application of data-driven methods remains largely absent in direct WID load predictions.

One ought to keep in mind that the ultimate goal of assessing WID loads and conducting airgap studies is to ensure the structural integrity of the offshore unit while protecting its crew and cargo in the most efficient way possible, typically by reducing costs. While this may seem obvious, it is crucial to recognize that the assessment must be robust enough to allow for generalization and quick design iterations based on its findings, yet not overly conservative, as this could lead to unnecessary waste of resources and materials. With this approach in mind, some researchers have revisited traditional procedures – "recipes" for WID loads assessment, which are found in recommended practices (API, 2014; DNV-GL, 2019), among others – to develop more efficient and robust methods.

Procedural Aspects of Assessment of WID Loads

The accuracy and effectiveness of the methods applied are crucial for the industry, particularly for operators, in decision-making processes and in outlining action items as part of their business risk management, as noted by Azman et al. (2021). These authors employed pushover analysis, also known as Ultimate Strength Analysis, to determine the Reserve Strength Ratio (RSR) of an offshore platform, incorporating WID loads into the analysis in accordance with ISO (2020). Similarly, Lihin et al. (2022) proposed a revised methodology for assessing fixed offshore structures under WID loading, using the silhouette method calibrated with field measurements from a structural health monitoring system installed on the structure. To improve the reliability assessment of offshore structures concerning WID loads, Ma & Swan (2023b) presented findings that enhance the physical understanding of waves occurring in realistic design sea-states, highlighting that many 'design wave events' will involve breaking waves, regardless of water depth. Their analysis of a large database of WID events revealed that recommended practices consistently under-predict the maximum WID loads. Additionally, these researchers argue that their recently developed Lagrangian Momentum Absorption (LMA) model provides highly accurate predictions by integrating fully nonlinear wave inputs with the structural openness/porosity (Ma & Swan, 2020).

Application of Nonlinear Potential Flow Methods

To support further advancements in assessment methods and procedures, various approaches have been employed in recent years to calculate air gap responses and WID loads. Higher-order potential field methods remain highly relevant for the numerical modelling of these problems. For example, Wang et al. (2022e) used the Green-Naghdi potential flow theory to study the airgap of a structure up to the second order. Similarly, Ren et al. (2021) conducted a study on wave surface elevation around a multi-column offshore structure, investigating wave run-up and peak surface elevation caused by wave interaction with rounded-corner square columns of different corner ratios. Additionally, Wei et al. (2023) compared the Newman approximation with the Pinkster approximation for computing second-order wave loads, which influence the air gap calculation for a semi-submersible platform.

In the specific case of FOWTs, Arya & Ranjan Behera (2023) studied freak wave impacts on a SPAR platform using a potential flow theory-based numerical model in the time domain. The motions of the SPAR FOWT and airgap effects were analyzed using the *FAST* software, although the study did not include the effects of non-linear wave loads, viscosity, or drag force. Despite these limitations, the study provides a valuable foundation for further development.

Field Methods

The application of field methods for calculating airgaps remains a prevalent research focus, particularly concerning WID flow and the corresponding loads in wave-structure interaction problems. Numerical formulations based on Smoothed Particle Hydrodynamics (SPH) are particularly popular due to their meshless nature, which is advantageous when dealing with discontinuous fluids. For instance, Fei et al. (2024) derived a relationship between wave forces and characteristic velocity during wave impacts on deck structures using SPH-based simulations. Similarly, Sasikala et al. (2021) employed Weakly Compressible Smoothed Particle Hydrodynamics (WCSPH) with two types of boundary conditions—Repulsive and Dynamic—to solve the slamming problem on a horizontal deck.

In general, Computational Fluid Dynamics (CFD) studies, including but not limited to SPH, are often validated against experimental data, with observed errors ranging from 3% to 15%, as noted by (Nizamani et al., 2022). These studies typically focus on detailed geometries of existing designs or case studies involving simple boxes or plates. They almost invariably conclude that existing standards are conservative regarding WID loads and offer alternative formulations for key variables.

Several examples illustrate the current state of the art. Deng et al. (2023b) investigated slamming on the wave-ward side of a deck box on a semi-submersible subjected to an extreme wave, finding the loads to be much lower than standard predictions. Yao et al. (2023b) found a correlation between the significant incident wave height on a mooring-stabilized semi-submersible and the peak pressures experienced by the platform, consistent with findings from Huo et al. (2021), who reported a dramatic increase in wave slamming pressure, particularly for freak waves.

In many cases, a dam break problem is used to approximate WID loads on topsides or in geometries suitable for calibrating numerical models, as demonstrated by Mu et al. (2023). However, this approach is not always appropriate for modelling WID (Hernández-Fontes et al., 2021). Zago et al. (2023) emphasized the need to distinguish between two main classes of flow, each requiring distinct modelling approaches. The first class involves an essentially two-dimensional flow with a single wave front traversing the entire deck, which can be modelled using a linear wave theory-based dam break approach to predict the type and propagation of the overtopping wave. The second class, involving multiple wave fronts originating from all sides of the platform, is better handled using a 3D SPH method.

Model Tests

The required test durations for achieving converged short-term wave and impact extreme value statistics are crucial factors in designing model test campaigns, as recently investigated by (Scharnke et al., 2023). Model tests are typically used to validate or calibrate numerical solvers for specific configurations, especially concerning extreme sea states. They also serve to explore novel phenomena or designs and to draw conclusions about the parameters governing these phenomena.

For the first type of test, several recent studies are noteworthy. Fonseca de Carvalho e Silva et al. (2023) analyzed loads on a balcony structure subjected to extreme wave impacts, investigating alternative configurations that could attenuate these impact loads (see Fig. 11). Studies on flare barriers and wave run-up (Liu et al., 2022b, 2023a), along with experimental validations (Nizamani et al., 2022; Yao et al., 2023b; Zago et al., 2023), also stand out in this context.

Regarding the exploration of novel phenomena, notable examples include the findings of Hernández-Fontes et al. (2021) on flow classification, Guo et al. (2021b) on the classification and comparison of wave impact modes on semi-submersibles, Mohajernasab et al. (2023) on the effects of air pockets and Ma & Swan (2023a) on the influence of topside porosity.

Additionally, it is important to highlight some studies that are significant for their comprehensive test campaigns or their focus on real structures, regardless of whether they fit into the aforementioned categories: AlMashan et al. (2021), Nam et al. (2022), Zhang et al. (2022), and (Luo et al., 2022).

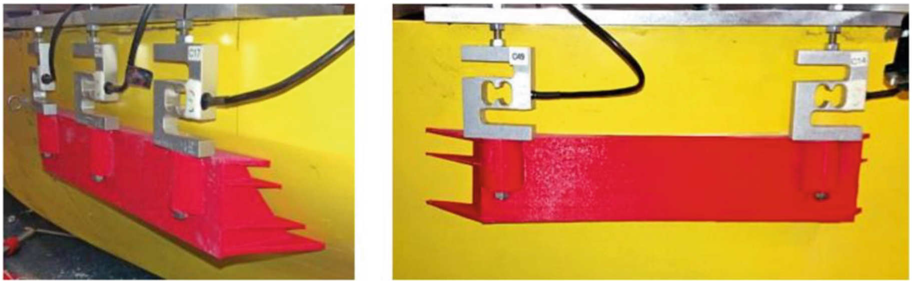

Fig. 11. 3D printed mooring balcony attached to the scaled model for wave tank experiments vie load cells to capture impact loads in Fonseca de Carvalho e Silva et al. (2023)

2.2.5 Mooring System

Station-keeping systems are required for floating structures to limit their excursion and orientation of the structures under the action of wave, current, and wind environmental loads. Several studies have been presented in the literature in recent years, focusing on the design, analysis, and simulation of different types of mooring systems.

Moored FOWTs form the leading innovation in the ocean energy sector. Shared mooring lines are a method to reduce the station-keeping cost of floating farms due to a reduced number of anchor deployments. Specifically, the mooring lines situated in the interior of the farm connect directly between adjacent floating platforms rather than extending to individual anchors (Wilson et al., 2021). Shared mooring systems can exhibit higher platform offsets compared to individual ones (Gözcü et al., 2022; Munir et al., 2021), whereas the responses of the system cannot be independent due to the hydrodynamic coupling between the floating structures. However, shared moorings can offer some benefits in fatigue and failure tolerance compared to a conventional mooring approach, which is captured under mooring coupled dynamic analysis since quasi-static analysis may lead to overestimation of the durability of shared moorings (Lozon & Hall, 2023; Zhang & Liu, 2023). As far as isolated floating FOWTs are concerned, recent studies have focused on the NREL 5MW OC4 semi-submersible FOWT (Huang & Yang, 2021; Liu et al., 2022a; Neisi et al., 2022; Xu et al., 2021b) with different mooring line materials, mooring components (clump weight and buoy) and anchors (drag embedment anchor and suction anchor) under various conditions of wind gust and average wind speeds. In addition, Zong et al. (2023) conducted a sensitivity analysis on the structural damage and deformation of the floating WT under bow and side impact from vessels. They concluded that although the FOWT may not be critically damaged by ship impact, the equipment inside may fail to work properly.

Moreover, the IEA 15MW WT mounted on the UMaine VolturnUS-S reference platform was also examined in the literature (Chueh et al., 2023; Wang et al., 2023b). Specifically, attention has been paid to effectively improving the survivability of the WT by proposing a novel constant tension mooring system, instead of a conventional catenary chain, for shallow waters and a power-control strategy which reduces the displacements of the platform. Regarding recent advances in the simulation and analysis of floating FOWTs, the developed models deal with the wind, wave, mooring dynamics, platform motions, and turbine structural dynamics. Coupled aerodynamic-hydrodynamic modelling has commonly been undertaken using fully coupled aero-hydro-servo-elastic-mooring tools *FAST* and *OpenFAST* developed by NREL which are applied either to numerical software, i.e., *ANSYS AQWA*, *WAMIT*, *OrcaWave*, *DNVGL WADAM* etc., or *STAR-CCM+* and *OpenFOAM* CFD simulation tools (Pillai et al., 2022; Ramzanpoor et al., 2023; Subbulakshmi & Verma, 2023; Wang et al., 2022d; Yan et al., 2023). Nonetheless, other hybrid potential-viscous flow models have been developed with excellent correlation with commercial software (Yu et al., 2023c). Also, Ferri et al. (2022) have developed a numerical model to optimize platform and mooring system characteristics towards the reduction of the dynamic response of a 10 MW FOWT.

The investigation of the technological and economic feasibility of multi-purpose floating structures, which combine offshore wind turbines with WECs, is a promising alternative for reducing the levelized cost of energy and enhancing the performance of renewable technologies. Although offshore multi-purpose floating systems have not yet achieved comprehensive commercial maturity, the feasibility of combining a floating wind turbine and a WEC has already been investigated. Specifically, a floating structure which encompasses an array of Oscillating Water Column (OWC) devices, moored with tension tethers, and supports a 10MW FOWT has been numerically simulated using an in-house developed servo-hydro-aero-elasto-dynamic formulation for installation in a North Sea or Mediterranean Sea location (Konispoliatis et al., 2021, 2022b). The same hybrid FOWT has been considered by Kardakaris et al. (2023) with a catenary chain line instead of a TLP mooring system to examine the effect of the mooring type on the system's power efficiency. Also, the chain mooring characteristics of a hybrid system which encompasses a 5MW WT and three-point absorbers WECs have been examined by Men et al. (2023). Their analysis showed that although the mooring tensions at the windward side chain increased, they did not seem very sensitive to the converter's size.

Apart from steel-wired mooring systems, hybrid lines composed of synthetic fibre and steel ropes (Yu et al., 2023a) as well as fully synthetic lines (da Cruz et al., 2023;

Nguyen & Thiagarajan, 2022; Pillai et al., 2022) have been considered for mooring applications in offshore structures. Polyester fibre ropes offer a reduced cost per breaking strength and better fatigue properties than steel lines. However, in damaged conditions, the residual strength of ropes decreases with the increase of the damage level (Lian et al., 2022). Regarding the mechanical characteristics of the fibre rope, the focus has been given to rope stiffness under empirical and neural network predictions (Zhang et al., 2023b) and different model practices (Sørum et al., 2023a). When compared to polyester moored systems, nylon ropes have the potential to reduce the mooring cost by increasing their fatigue life and reducing their cross-section area compared to fibre lines (Sørum et al., 2023b; Verde & Lages, 2023), whereas they (nylon moorings) also allow greater motion responses which interfere optimally with wave energy harvesting activities (Depalo et al., 2022; Xu et al., 2021a, 2021c; Xu & Guedes Soares, 2023).

Regarding wave energy absorption, recent studies have focused on the effect of mooring types (i.e., taut, catenary, TLP) on wave power efficiency. Concerning floating point absorber WECs, TLP moorings are proven to be more suitable for long-wavelength installation locations, whereas taut moorings seem suitable for locations dominated by short and medium wavelengths (Meyer et al., 2023). Regarding oscillating water column (OWC) devices, taut moorings have attained the best performance, followed by the TLP and the catenary moorings (Gubesch et al., 2022b). However, TLP moorings can be prone to a brief loss of tension, leading to large snapping forces of short duration on the tendons, a phenomenon presented by Miškov et al. (2023). A taut mooring line is also qualified to moor an attenuator-type WEC. Nevertheless, elastic mooring cables seem preferable to inelastic ones due to their ability to reduce the snap loads of the converter (Stansby et al., 2022; Zhao et al., 2023). Nonetheless, independently from the specific nature of the converter and the mooring type, a crucial aspect in wave energy extraction regards the implementation of optimal control strategies. In this context, model-based control techniques towards the maximization of power capabilities have been performed by Papini et al. (2023), Windt et al. (2021), and Carapellese et al. (2022).

Moored porous structures such as fish cage systems and permeable floating bodies have been dealt with in the realm of potential flow theory using a Boundary Element method (BEM) to simulate the wave effect and the discrete lumped-mass model for the determination of the mooring dynamic behaviour (Konispoliatis et al., 2022a; Ma et al., 2022b, 2023). Here, the mooring line is discretized into a number of finite elements, the forces on which are determined and assembled into a symmetric banded global system. Due to the increased interest in CFD modelling, which typically solves the fluid flow problem using Navier-Stokes equations, several authors have studied the importance of including viscosity in moored structures. Specifically, focus has been given to *OpenFOAM* and its coupling with *MoorDyn* (Aliyar et al., 2022a; Chen & Hall, 2022; Jiang & el Moctar, 2023) as well as with improved *MoorDyn* solvers for nonlinear effects simulation (Jeon et al., 2023). In addition, apart from commercial software, in-house FEMs have been incorporated with CFD (Huang et al., 2022c)), allowing accurate solutions for dynamic interactions between structures and their mooring systems. Nevertheless, although high-fidelity CFD models attain the best agreement with measured experimental data, low-fidelity linear wave theory models can predict values within the same order of magnitude of CFD and experiments with much lower computational time (Engström et al., 2023).

Furthermore, the research was also focused on moored floating breakwaters. These are built to protect water areas from wave attacks. Compared to the bottom-seated breakwater systems, floating breakwaters have an easier installation, are less expensive in deep water applications, and are less dependent on the seabed conditions. Regarding the applied methodologies for the analysis and simulation of moored breakwaters, mesh-based CFD models (Chen et al., 2022c; Wei & Yin, 2022), Boundary Elements Method (BEM) (Liang et al., 2022b), and Smoothed Particle Hydrodynamics method (SPH) have been applied for the simulation of the free surface, the flow and the wave breaking. The latter method was widely adopted due to the flexible free-surface boundary condition. In this approach, the fluid is discretized into a set of Lagrangian particles, which are entitled with physical quantities such as density, pressure, etc. (Cui et al., 2022; Han & Dong, 2023). However, the solid boundary implementation is adversely affected by the Lagrangian nature and kernel interpolation. Hence, various algorithms have been proposed for floating breakwaters and have been verified experimentally. The fictitious particles method has been developed to construct solid boundary by placing fictitious (or virtual or ghost) particles in the solid domain (Chen et al., 2023c). Each fixed ghost particle corresponds to an interpolation point in the fluid domain, the velocity and pressure of which are evaluated from the fluid particles around the interpolation point. Unlike the latter approach, the dynamic boundary particles (DBP) keep stationary relative to the solid boundary and participate in the same equations of state and continuity as fluid particles. A modified DBP was implemented in a floating breakwater with taut, slack and hybrid mooring systems (Guo et al., 2022).

Lastly, fatigue assessment of mooring systems involves considerable uncertainties with respect to both load and capacity. To better understand and quantify the fatigue capacity and degradation of mooring lines, several original fatigue tests on mooring chains of different material grades under artificial or natural corrosion conditions, with or without cathodic protection, have been performed in recent years to study the effect of the corrosion condition on fatigue resistance (Aursand et al., 2023; Lone et al., 2023; Qvale et al., 2021, 2022; Zhang et al., 2022h). The results proved that the corrosion has a detrimental impact on fatigue resistance, whilst fatigue capacity increases as the mean loads are reduced. Furthermore, extended S-N curve formulations have been proposed by Mendoza et al. (2022)), accounting for not only prior and future fatigue loads but also mean load and corrosion effects (Lone et al., 2022a, 2022b). Also, the mooring fatigue performance of a typical semi-submersible platform using chain and wire ropes has been numerically simulated by He et al. (2022) and Yang et al. (2023a)), who highlighted the decrease of fatigue life under the increase of corrosion rates. Apart from fatigue analysis, the failure of a mooring line is of utmost concern due to uncertainty in the line's behaviour and lack of structural robustness. Mooring line failure conditions have been recently examined for offshore fish cages (Hou et al., 2022; Tang et al., 2022a), wind turbine structures (Sun et al., 2023b; Zhang et al., 2022b), semi-submersible (Mao et al., 2022), and TLP platforms (Wu et al., 2022). Probabilistic assessment methodologies and deep neural network approaches have been developed, indicating that the failure of one mooring line significantly affects the probability of failure of the remaining mooring lines due to the increase of the structure's motions and tensions in the remaining lines. Aiming to reduce the number of short-term simulations needed to evaluate multi-dimensional fatigue damage integral, a univariate dimension-reduction method has been developed by Ibarra et al. (2022) that transforms the environmental conditions into standard Gaussian variables for fatigue damage determination. Also, Shao et al. (2023) studied the power performance of a wave park of two types of heaving WECs and the accumulated fatigue damage of their mooring lines, using relative tension-based fatigue analysis and rainflow counting methods. Their analysis has focused on the effect of the wave heading angle and the arrangement of the lines towards the incoming wave train in the amount of fatigue damage accumulated by mooring lines.

2.2.6 Model Tests

Advanced model testing remains an indispensable approach in studying wave loads on offshore structures. These empirical assessments provide crucial insights that directly inform the iterative design and validation of theoretical models and engineering practices. Incorporating these empirical results into data-driven methodologies underscores their critical role in the evolving technological landscape of marine engineering.

Research on classical offshore platforms has focused on the hydrodynamic impacts of wave-induced slamming and breaking waves, which is critical for understanding structural loads during extreme sea states. For instance, an investigation into the effects of freak waves on floating platforms through a series of flume experiments examined various air-gap conditions, identifying four distinct wave impact patterns that revealed how wave interactions with the platform could result in significant motions, tension forces in tethers, and impact pressures at various points on the structure (Luo et al., 2022). Further research explored the interaction between internal solitary waves (ISWs) and FPSOs, focusing on oblique wave impacts. Through experimental testing combined with numerical simulations, the primary forces exerted by ISWs were identified, leading to the development of a simplified prediction model. This study provided regression formulas for the friction coefficient and correction factors, crucial for accurately predicting wave-induced loads on FPSOs, thereby offering valuable data for improving FPSO design and operational strategies in ISW-prone environments (Zhang et al., 2022). Additionally, a comprehensive experimental study under the Norwegian SLADE KPN research project simulated steep, breaking waves to analyze their impact on offshore platforms and wind turbines, focusing on local structural responses by measuring pressure and strain to characterize hydroelastic effects. These findings are instrumental in refining safety standards and design guidelines for offshore structures subjected to such conditions (Ahani et al., 2022).

Research has highlighted the importance of mooring system integrity under varying environmental loads in FOWTs, with models for those needing to be properly validated. For example, flume experiments on a 5 MW barge-type FOWT under mooring line failure scenarios showed that traditional models often overestimate dynamic responses, underscoring the need to account for damping effects in design (Tang et al., 2023a). Similarly, the hydroelastic response of FOWTs has been a focal point of investigation, particularly concerning the nonlinear and higher-order hydrodynamic loads that can induce significant vibrations. A study on a spar-type 10 MW FOWT with a flexible tower and platform demonstrated that second-order hydrodynamic loads could lead to pronounced springing and ringing effects, which are critical considerations for the design of future, larger-scale systems (Leroy et al., 2022). Experiments also revealed that aerodynamic loading influences FOWT hydrodynamics by suppressing pitch resonance and amplifying surge frequency vibrations, offering insights for optimizing FWT designs (Wen et al., 2022). Research on TLP configurations, such as the CENTEC-TLP, has shown that these designs can effectively minimize system responses to wave loads, even under extreme conditions, thereby enhancing the overall structural resilience and reliability of FOWTs (Hmedi et al., 2022).

Additionally, experimental studies on concurrent wind, wave, and current loads on monopile-supported OWT models demonstrated significant discrepancies when these loads were analyzed in isolation, emphasizing the need for comprehensive assessments considering their combined effects (Buljac et al., 2022). The adaptability and performance of mooring systems have been further explored through model tests and numerical simulations, particularly under cyclic loading conditions typical in marine environments. These studies have provided critical insights into fatigue life and failure mechanisms, essential for developing more resilient mooring designs (Fonseca et al., 2022). Finally, research on the hydrodynamic effects of heave plates, commonly used in semisubmersible FOWTs, provided critical data on parameters like KC numbers, oscillation frequencies, and plate geometries, informing design improvements (Zhang et al., 2023d).

The exploration of WECs, particularly Oscillating Water Columns (OWC), has advanced the understanding of efficient wave energy capture, with extensive experimental work driving these advancements. Studies integrating OWC systems into multifunctional marine structures, such as floating breakwaters, have employed scale models to optimize geometric configurations for maximum energy extraction. These tests have demonstrated these systems' dual functionality, which can both extract energy efficiently and provide robust coastal protection under varying marine conditions (Cheng et al., 2022a). Research has also focused on the shape optimization of back-buoy oscillating water columns, using both numerical simulations and experimental validation to improve primary conversion efficiency by examining the effects of various bottom-corner geometries (Jalani et al., 2022). Furthermore, model tests have been crucial in assessing the operational efficiencies and energy transduction capabilities of OWC installations, offering detailed performance metrics that are critical for optimizing these systems (Gubesch et al., 2022a). Studies on the nonlinear wave loads on quad-OWC devices, validated through wave tank experiments, have provided critical insights into optimizing the spatial arrangement of OWC arrays to reduce wave forces and improve platform stability (Zhou et al., 2023b).

Studies on aquaculture structures have meticulously quantified the effects of wave-induced motions using physical model tests, offering insights to enhance structural integrity and stability. For instance, experiments on gravity fish cages under regular wave conditions yielded valuable data on hydrodynamic loads and motion responses, crucial for improving aquaculture design and safety (Liu et al., 2023d). In-depth analyses of hinged multi-body aquaculture platforms have revealed how different stiffness and wave periods affect their dynamic behaviour, offering guidance on optimizing mooring configurations and structural designs (Ma et al., 2022a). Further research has explored the design and implementation of robust mooring systems, which are essential for ensuring the survivability and operational efficiency of aquaculture platforms in harsh marine environments. Comparative investigations between closed and semi-closed fish cages under various wave conditions provided insights into their hydrodynamic performance, highlighting differences in global responses and survival under extreme conditions. These studies underscore the importance of experimental validation in understanding the complex interactions between aquaculture structures and their marine environments, providing a foundation for developing more resilient and efficient designs (Shen et al., 2022).

Investigations into the hydroelastic behaviour of Very Large Floating Structures (VLFS) under low-frequency loads have utilized scale models to assess performance and stability under various sea states, ensuring their deployment in maritime applications. For example, model tests of hydroelastic truncated floating bridges provided critical insights into the dynamic response of these large structures, highlighting the importance of careful experimental design and system identification for accurately replicating the behaviour of full-scale structures (Rodrigues et al., 2022). The dynamic responses of other floating platforms to marine conditions have also been critically examined through a combination of model tests and numerical simulations. For instance, research on semi-submerged cylinders under combined steady and oscillatory flow conditions shed light on the hydrodynamic forces acting on these structures, with empirical models developed to predict these forces accurately (Hu et al., 2023). Studies have explored the impact of marine growth on the hydrodynamic behaviour of cylinders, using experimental methods to quantify the effects of different types of roughness, such as mussels and corals, on drag and inertia coefficients under wave and current loading (Marty et al., 2022). Additionally, experimental and numerical investigations on wave impacts on box-girder bridges provided detailed analyses of wave-induced forces and moments, contributing to the development of robust design strategies for coastal bridge structures (Zhu et al., 2022). Moreover, long-term model testing has been pivotal in evaluating the durability and safety of VLFS under cyclic and extreme loads, offering guidance for their long-term deployment in marine environments (Scharnke et al., 2023). Figure 12 shows the convergence test results of non-dimensional wave crests and impact force peaks for a wave tank model test case study from Scharnke et al. (2023). N is the number of seeds, and the lines denote the different test cases denoting different severities and duration of the seastates.

Studies on kinematic behaviour using advanced techniques like Particle Image Velocimetry (PIV) have provided detailed insights into structure-fluid interactions. For instance, experiments on internal solitary waves interacting with horizontal cylinders in stratified fluids, validated through PIV, advanced the understanding of wave-flow coupling and led to accurate force models for these interactions (Wang et al., 2022f). Physical model tests combined with PIV have also been employed to investigate the effects of solitary waves on elastic submerged plates, successfully capturing detailed turbulence fields and wave loads. Measurements of surface elevation, plate motion, velocity, and turbulence fields have allowed for a comprehensive understanding of the hydrodynamic behaviour of different plate materials under solitary wave conditions (Hsiao & Hsiao, 2022).

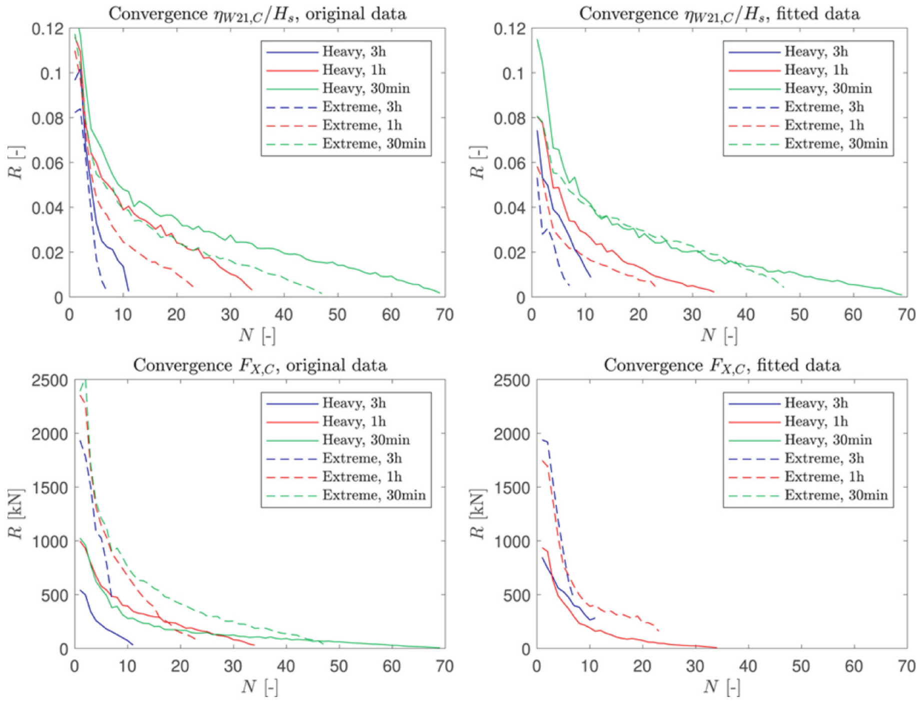

Fig. 12. Results for the convergence study from Scharnke et al. (2023)

2.2.7 Data-Driven Methods

The integration of data-driven methodologies in marine hydrodynamics and offshore engineering has significantly increased in the last three years. Previous efforts, such as those by Sclavounos & Ma (2018) and Pena-Sanchez et al. (2020), have already shown the value of applying machine learning techniques in predicting and modelling wave loads on offshore structures. These studies highlighted the potential of integrating artificial intelligence (AI) and machine learning with traditional marine engineering practices to enhance predictive accuracy and computational efficiency.

In 2021, Guo et al. (2021a) introduced a Long Short-Term Memory (LSTM) based model focused on predicting the heave and surge motions of semi-submersible vessels. The study emphasized the importance of real-time, accurate predictions for offshore operational safety and efficiency, demonstrating the model's capability to predict future motions with an average accuracy close to 90%. The use of LSTM, a recurrent neural network, was particularly notable for its ability to process time-series data, making it well-suited for predicting the dynamic responses of offshore structures to wave loads. Ma & Sclavounos (2021) studied the use of Support Vector Machines (SVM) in modelling nonlinear hydrodynamic loads on fixed cylinders in shallow water by analyzing experimental data from which (nonlinear) transfer functions were established. This work illustrated the potential of SVM regression methods in capturing complex marine hydrodynamic loads, offering insights into the field's understanding of fatigue and extreme statistics analysis for offshore structures. Pena & Huang (2021) presented the application of deep learning, specifically Generative Adversarial Networks (Wave-GAN), for predicting nonlinear regular wave loads and run-up on fixed cylinders. The study demonstrated Wave-GAN's ability to accurately predict wave-induced pressures for unseen wave conditions, by utilizing Computational Fluid Dynamics (CFD) simulations to generate training and testing datasets. A "grey-box modelling" approach by Pitchforth et al. (2023)), which aimed to enhance the accuracy of wave loading predictions on offshore structures, was published in the same year. By integrating Morison's equation with a data-driven Gaussian process NARX model, the study achieved significant improvements in predictive accuracy and model extrapolation capabilities, especially in scenarios with limited data coverage. The work underscores the value of merging physics-informed machine learning with traditional offshore engineering practices.

In 2022, the research on applications of data-driven methods continued to diversify. Katsidoniotaki et al. (2022) developed a digital twin to predict extreme loads on a wave energy conversion system's mooring system under harsh wave conditions, demonstrating the digital twin model's ability to predict mooring force with high accuracy and drastically reduced computation time, while Li et al. (2022b) introduced a Temporal Convolution Network (TCN) model for predicting wave runup on semi-submersible platforms, employing a data-driven approach to establish the nonlinear mapping of wave-structure interactions, optimizing the input tensor space considering both temporal and spatial dependencies. Liang et al. (2022a) combined Computational Fluid Dynamics (CFD) with Deep Reinforcement Learning (DRL) to investigate wave dissipation by actively controlling flat plate breakwaters against regular waves. Utilizing an in-house NWT to simulate fluid-structure interactions, the model applied an Artificial Neural Network (ANN) to learn wave dissipation strategies through continuous wave-plate interaction. The study demonstrated the model's adaptability and ability to learn control strategies automatically, presenting a significant advancement in the application of AI techniques for enhancing coastal protection measures.

In 2023, (Chen et al., 2023a) presented an Auto-Regressive model for forward predicting surface wave elevations and the motions of offshore floating structures (see Fig. 13). The model, validated with numerically synthesized wave data, indicated that band-pass filtering could improve prediction accuracy considerably, especially with narrower spectral bandwidths (as would be expected). Other studies further advanced the application of machine learning in predicting mooring line tensions and the motions of moored barges, respectively, using reservoir computing models (Yang et al., 2023b, 2023c).

In summary, the last three years have been characterized by a rapid expansion in the application of advanced data-driven methodologies and machine learning techniques in marine hydrodynamics and offshore engineering. These developments build upon the preliminary work established previously and showcase a notable shift towards more sophisticated, accurate, and efficient predictive models. This progression signifies a promising future for the integration of AI and machine learning in enhancing the design, analysis, and operation of offshore structures, ensuring their resilience against the dynamic challenges posed by marine environments.

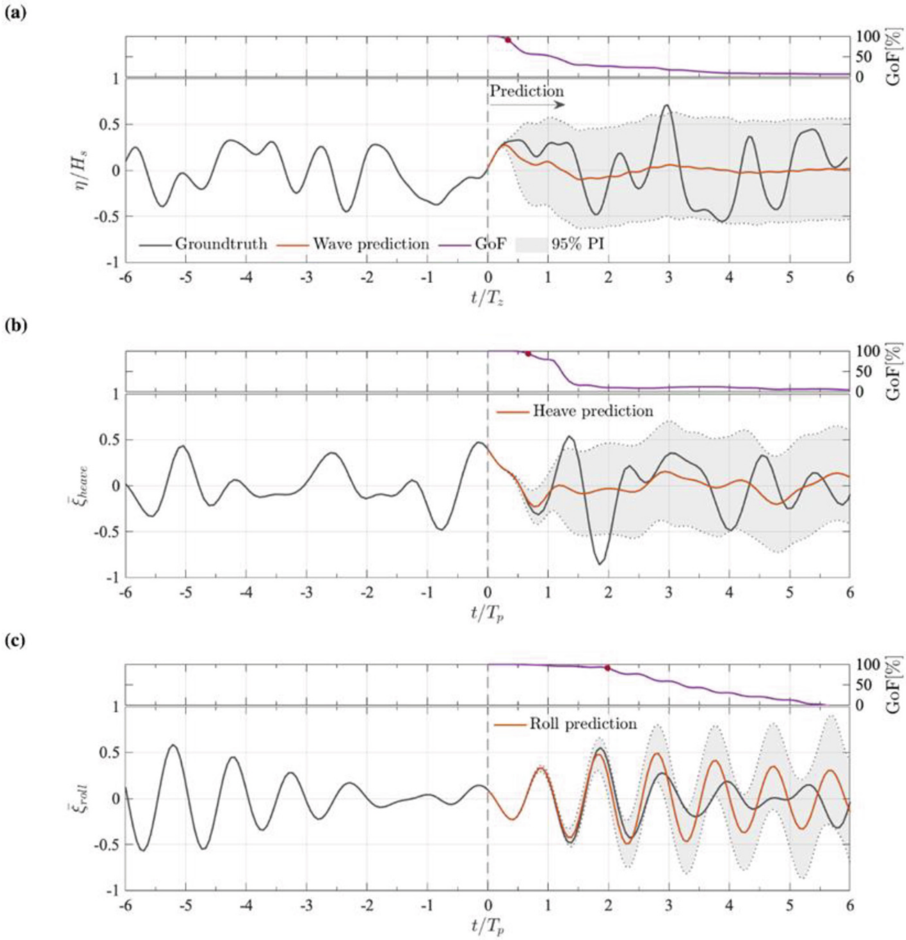

Fig. 13. Wave tank data prediction results on (a) surface wave elevation (b) heave motion, and (c) roll motion of a scaled model in a wave tank under the action of waves in Chen et al. (2023a).

3 Current Loads and Wind Loads

Historically, the main loads attributed to current and wind acting on ships and offshore structures are the drag forces (ahead or lateral/oblique) and the yawing moment in the free surface plane, first considered according to a static or quasistatic nature. From this perspective, the key impacts of these loads are the mean drift and their role in providing damping for the slow drift because waves coexist. To estimate these loads and assess their impact on the system (whether it is a ship or an offshore structure), methods derived from detailed experimental research, such as those proposed by API

(American Petroleum Institute), DNV (Det Norske Veritas), or OCIMF (Oil Companies International Marine Forum), are commonly employed. These methods determine the forces and moments experienced by the system because of its movement relative to the translational velocity induced by currents or wind speeds. In fact, an additional drag force may be considered because of the yaw rate, which is particularly significant for the components of systems operating in water.

Inaccuracies in estimating the current and wind loads on ships can lead to an imprecise calculation of their power requirements, difficulties in maintaining position during manoeuvres or cargo handling, increased reliance on tugboats for port operations or near other structures, and an increased risk of incidents and shortcomings during certain tasks. On the other hand, inaccuracy in estimating these loads on offshore systems, usually anchored, can lead to the impairment of the mooring system itself, the catastrophic failure of subsystems and lines of prospection and production (drills, risers, and umbilicals, mainly), as well as the imposition of additional difficulty in their operations assisted by PSV, for example.

Due to the growing dimensions of modern ships and offshore structures, there is an increased need to meticulously consider the force and momentum coefficients resulting from wind and/or current effects, particularly in conjunction with wave dynamics and varying environmental conditions at operational sites such as ports enclosed by tall structures, sheltered areas, and shallow-water channels. In the study by Torre et al. (2021), a large cruise ship anchored in a port was examined with its force and momentum coefficients in a wind tunnel to assess the potential impact of nearby civil engineering works on the reduction of these coefficients.

Furthermore, the growing scale of the systems has also impeded purely experimental studies in towing tanks or wind tunnels because of the requirement for progressively smaller models. On the other hand, this difficulty opens space for decisive support of investigations based on CFD simulations, recognized as increasingly complete and precise, as found in Yoo et al. (2022), where wind loads on the FPSO side by side with a shuttle tanker are evaluated by simulations using Reynolds-averaged Navier-Stokes (RANS) equations and the SST k-ω turbulence model; as in El Moctar et al. (2023), where the effects of wind are examined through experimental and numerical methods (URANS and two turbulence models), demonstrating that the configuration of deck structures significantly impacts aerodynamic forces and moments.

Another recent scenario that has received significant attention is that current and wind are considered in offshore wind power generation systems; see Edwards et al. (2024). In contrast to typical issues, the loads in this situation exhibit dynamic features, often cyclic, that may result in resonant and/or unstable dynamic effects. According to these aspects, the crucial problem currently refers to the aerohydrodynamic behaviour of floating offshore wind turbines (FOWTs), investigated numerically and experimentally from the point of view of the wind turbine, for example, in Chen et al. (2022a) and Wang et al. (2023d), and for the floating platform as found in Yin et al. (2022).

As pointed out in Bandizadeh Sharif et al. (2023), the large class of fluid-structure interaction (FSI) problems includes flow-induced vibrations (FIV), which come from the significant influence of marine currents and winds on a series of offshore structures; see Fig. 14.

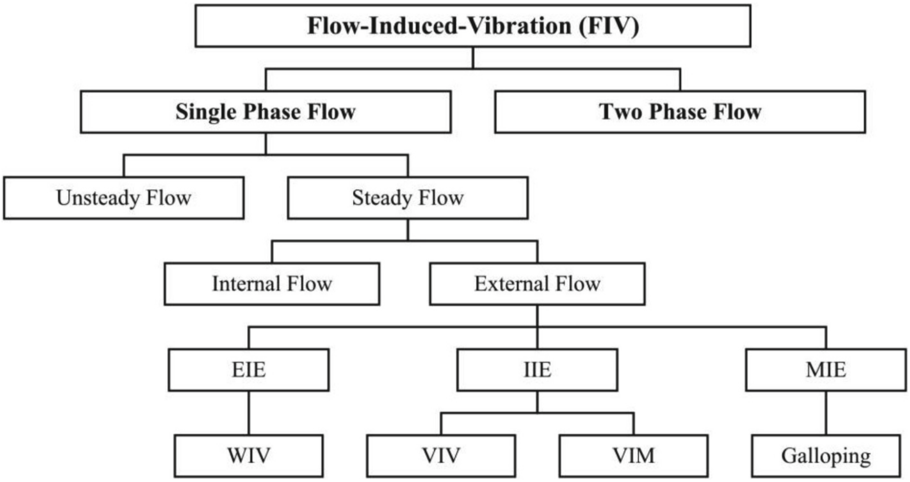

Fig. 14. A possible FIV classification, as proposed in Bandizadeh Sharif et al. (2023).

Focusing solely on single-phase flows in a steady external regime, FIV can be associated with extraneously induced excitations (EIE), for instance, the wake-induced vibration (WIV) phenomenon, with instability-induced excitations (IIE), mainly vortex-induced vibrations (VIV) and vortex-induced motions (VIM); and with motion-induced excitations (MIE), as those found in the galloping phenomenon. This presents a challenging situation since excitations do not occur in isolation, and the required design approach may vary from destructive, when the objective is to reduce the damaging effects caused by these phenomena, to useful, when FIV is used for renewable energy generation; see Fig. 15.

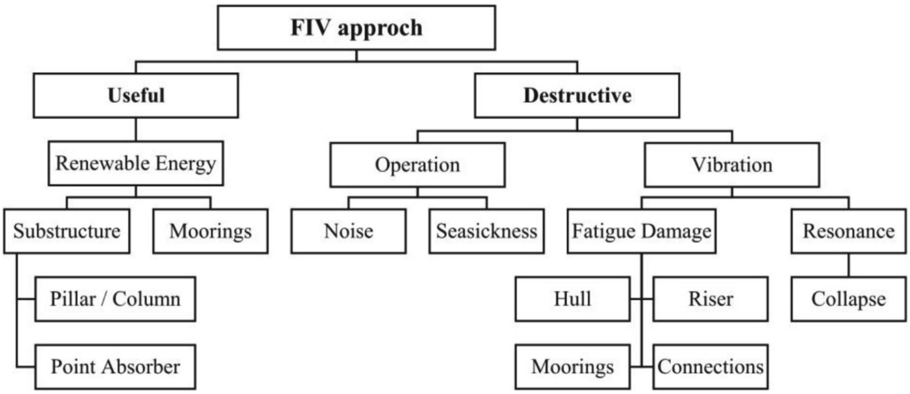

Fig. 15. The two main approaches concerning FIV in designs, according to Bandizadeh Sharif et al. (2023), are useful and destructive.

More information on the analysis of current and wind forces on ships and offshore structures is provided in the following subsections.

3.1 Current Loads

As previously stated, the need for more accurate predictions of current loads associated with the greater size of vessels has driven investigations where tests in towing tanks and/or wind tunnels are specifically conducted to validate increasingly accurate and more comprehensive CFD simulations. This method is exemplified in the work of Mauro et al. (2023), where the authors proposed an initial design phase of drill ships using high-fidelity CFD calculations. The results were comparable to those obtained using conventional methods, namely API-1984, DNV-GL2018, and OCIMF-1994/2010. The need for greater safety in the manoeuvring or dynamic positioning of ships in the current has required intense research to achieve an increasingly accurate determination of force coefficients, as presented numerically in Kim et al. (2022a), Aydın et al. (2022), Song et al. (2023), and analytically in Zhang et al. (2023a), where the results showed the important influence of this environmental agent on the manoeuvring performance of ships.

The unpredictable nature of currents poses a risk to structures in marine environments, shortening their lifespan by hastening existing failures or causing faster deterioration over fewer cycles due to material fatigue. This is why investigations of the effects of marine currents are so important for the design of offshore lines (mainly risers, umbilicals, and mooring lines).

In the study by de Carvalho et al. (2022), theoretical models were used to calculate the tension in mooring lines and the compression of the fenders on the dolphins within a port infrastructure. The authors suggested that utilizing a nonlinear model could be beneficial for engineers and analysts in estimating the forces and dynamic amplification coefficients needed in the simplified (linear static) approaches outlined in the standards. Also, in analytical terms, according to Amouzadrad et al. (2023), a moored structure offered enhanced stability compared to a free-edge structure, as it exhibits greater deflection than the free structure. Structural displacements increase as current speeds increase, which is caused by elevated hydrodynamic loads on the structure in the upstream region. As the current speed increases, the increase in transmission coefficients is due to the more significant current generating larger hydrodynamic forces, resulting in increased displacements that cause more wave energy to pass beneath the structure. Furthermore, the number of resonating patterns decreases as the wavenumber increases, which is expected as the wave reflection decreases in the upstream region. In addition, the floating structure became more stable for lower current speed values and higher mooring stiffness.

During the fatigue life of offshore lines, plastic deformation accumulates from the multiaxial stress-strain response of the material, subsequently resulting in cyclic accumulation of plastic damage. Marine currents, as well as concomitant waves and winds play an important role in analyzing accumulated damage. For example, using FEM-based commercial software, Gemilang et al. (2021) investigated the catenary lines' low cycle fatigue in a spread mooring configuration from an FPSO unit. The comparison between the SN method and the low cycle analysis showed that the first method was conservative only when the average load was 20% below the minimum breaking load.

It also showed that increasing the spreading radius of lines could exacerbate the fatigue problem and lead to faster failure. The significance of marine currents is also suggested in the study by Zhang et al. (2022g), in which the authors performed fatigue assessments on oil offloading lines (OOL) that connect an FPSO to a catenary anchor leg mooring (CALM) buoy.

As an alternative to commercial software, Sivaprasad et al. (2023) proposed an artificial neural network (ANN) to estimate fatigue damage in a top-tensioned riser (TTR) subjected to vortex-induced vibration (VIV). Although it is a 2D analysis that does not consider waves, wind and material variations, as well as considering a uniform current and a linear soil model, the validated ANN model showed acceptable performance, with a maximum difference of 9.6%. In the same sense as the alternatives in Wu et al. (2023a)), a cluster analysis based on the Gaussian mixture model (GMM) was applied to analyze the responses of the full-scale riser. The method can adequately separate 242 measurement events into 12 clusters, reducing the parameter dimensions so that the underlying physics can be better understood. Furthermore, Sun et al. (2022a) introduced a technique that relied on the average conditional exceedance rate (ACER) method for a precise estimation of extreme values of current loads.

When considering the production of sustainable energy, the potential to harness marine currents is also taken into account. The behaviour of a submerged turbine exposed to sea waves and currents was studied by Lloyd et al. (2021), using the numerical CFD method and experiments in a test tank to confirm the results. Five different flow conditions were examined, including two conditions that involved both current and waves, and three conditions involving only current. The variability in loads was considerably higher when looking at waves and currents, with the maximum loads aligning with the peaks and troughs of the wave surface. The results also showed that when waves were included, the amplitude of thrust/torque fluctuation was 35 times greater than in tests with currents alone.

Wind turbines are another source of clean energy generation and are usually installed in places where regular currents and tides can be significant with respect to flow-induced vibrations (FIV).

Fujarra et al. (2022) investigated the basic principles regarding how initial roll or pitch angles influence the flow-induced motion (FIM) amplitudes of a low aspect ratio floating circular cylinder. The 6 DOF amplitude response, coupling trajectories, and frequency spectra were analyzed. Experiments with four initial angles demonstrated that the initial pitch influences the yaw motion, leading to geometric asymmetry that enhances the yaw displacements. The yaw motion increased as the reduced velocity was increased, making it essential to correctly model and analyse VIM on floating offshore wind turbines (FOWT).

The complexity associated with the design of the FOWT was discussed in Edwards et al. (2024), where the authors emphasized the importance of employing a combined numerical and experimental methodology to develop such systems. The intricacy is inherent in the experimental method due to the significant interaction between the wind turbine's aerodynamics and the floating offshore structure's hydrodynamics, making it challenging to fully model at a smaller scale.

The study by Otter et al. (2022) offered a review of modelling approaches for FOWTs, with an emphasis on numerical techniques and software tools. The authors noted that the selection of a computational method was based on the balance between accuracy and computational efficiency. Low-fidelity methods were used during the preliminary design phase, mid-fidelity techniques were suitable for analyzing global dynamics, and high-fidelity approaches were necessary for detailed examinations. In addition, full-physical and hybrid test methods were used to validate and calibrate the numerical models, depending on factors such as testing facility, budget, and uncertainty; see Fig. 16. Full-physical tests can model all aspects of the wind turbine, including aerodynamic damping, but are expensive and require a dedicated model for each turbine design. Hybrid testing is cheaper, more versatile, and does not require bulky wind generation equipment, allowing for the simulation of turbines at various scales. Trends and gaps in current research are identified, such as comparative studies and improving the accuracy of numerical engineering tools. The paper also concludes that the traditional modelling approach remains essential for FOWT designs.

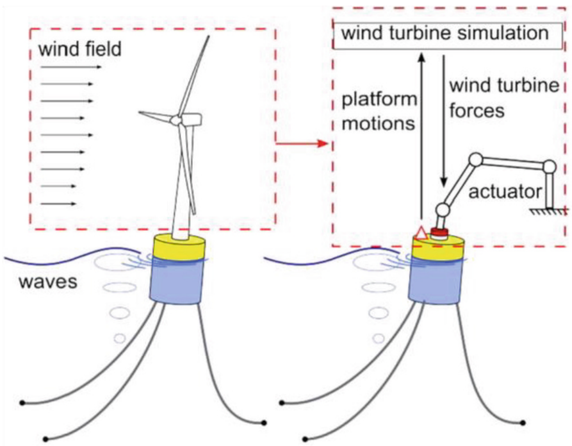

Fig. 16. The two approaches for testing FOWT according to Otter et al. (2022): (left) full-physical versus (right) hybrid testing.

Sergiienko et al. (2022) examined and evaluated scale-down methods within the same framework of the FOWT, considering data from 9 reference wind turbines and eight semi-submersible platforms (SSP) for 5–15 Megawatts to identify trends and scaling laws related to their physical properties. The mass, power and thrust forces of the wind turbine scale quadratically with the diameter of the rotor, and these characteristics do not depend on the design of the drive train. The main challenge for larger wind turbines was tower design, as the "soft-stiff" tower design was not applicable to floating offshore wind energy systems with power ratings higher than 10–12 Megawatts. Existing SSPs have a variety of design solutions, with a draught of less than 20 m and natural frequencies of around 20 and 30 s. However, the crucial geometric factor influencing the design is not associated with its waterplane area but with the product of the offset column diameter and the distance to the offset column.

Based on a practical approach to reduce FIV, Bandizadeh Sharif et al. (2023) provided an extensive review of both numerical and experimental studies on suppression systems in circular cylindrical marine structures, focusing on devices such as strake, spoiler, fairing, splitter plate, shroud, dimple, ribbon, bump, and travelling wave wall to reduce vortex shedding. According to the authors, the helical strake was the most widely used suppression device, demonstrating the most effective performance in reducing such vibrations. The optimal design could reduce FIV by 95–100%, therefore reducing the fatigue damage of these structures.

The mitigation aspects were also investigated in Gonçalves et al. (2023a), where based on small-scale experiments, the authors emphasized the critical role of the design of the heave plate (HP) in reducing flow-induced motion (FIM) and indicated that only the largest HP positively reduces dynamic behaviours due to wave and current incidences, making it essential for FOWT developments. In Gonçalves et al. (2023b), the impact of draught, pontoon height, and column face length on the FIM of an SSP with four square section columns was experimentally investigated. The findings indicated that a reduction in the column-pontoon ratio resulted in lower transverse motion amplitudes.

Fluid-structural interactions such as FIV can happen with wave excitation, a co-existence that is crucially important for offshore system design. This issue was experimentally investigated by Du et al. (2022), considering a large-scale model of a tension leg platform (TLP) towed at different velocities concomitant to irregular waves. The study found that 0.32D transverse amplitudes were highest at Vr = 7.0 (where Vr is a nondimensional parameter usually applied for FIV studies), while the inline and yaw motion experienced increasing amplitudes with reduced velocities. The most significant responses were at 0 and 22.5 degrees of heading, while no critical heading was recognized for surge motion, and the VIM amplitudes were significantly suppressed under nonlinear stiffness and greater damping. In a similar sense, Rueda-Bayona et al. (2023) took into account the VIV excitation concomitant to those coming from winds and irregular waves, proposing a methodology based on the design of experiment (DOE), the analysis of variance (ANOVA) and the near-hydrodynamic field analysis to correctly evaluate the damped natural periods and responses due to the nonlinear fluid-structure interactions.

Two FOWTs were numerically investigated in Li et al. (2023) (SSP-type and barge) using OpenFOAM and an in-house model to consider the simultaneous wave and current excitation. The primary findings indicated that waves could amplify VIM when there was a significant angle between the current and the wave and that the highest wave height during lock-in was not the most hazardous scenario. Rather, a smaller wave height with a longer period could provoke even greater motion. Three-dimensional CFD simulations with an SSP-type FOWT in model and full-scale were also studied by Jiang et al. (2023b), indicating a significant influence of scale and highlighting the improved effectiveness of the CFD method for VIM studies. The FOWT based on the OC4 platform (SSP of three columns without pontoons) was numerically investigated under different headings in Liu et al. (2023c), revealing that the VIM "lock-in" and transverse response persist up to the nondimensional reduced velocity of 30, with a maximum of 0.8D in amplitude, for incidences of 0 and 90 degrees, while smaller amplitudes were observed for 180 degrees due to the interaction between the upstream vortices and the downstream side column. A similar approach was used by Zhao et al. (2022), considering CFD simulations of a four-column SSP with pontoons and revealing the differences between VIM at 0 and 45 degrees of current heading. The aspects of strake mitigation were numerically investigated by Kharazmi & Ketabdari (2022) for a large-scale spar platform, mainly discussing the arc angle and the number of entrances of these helical strakes with respect to VIM attenuation.

Still, in the context of FIV (or FIM) experiments, an unconventional measurement technique was presented by Leal et al. (2023) and Fujarra et al. (2023) based on the usage of inertial measurement units (IMU). The authors stated that the frequencies and amplitudes of FIV measured with the cost-effective IMU method closely matched those obtained using a significantly pricier optical motion capture system. They reported an average relative error of less than 2.8%, which supports the validity of using inexpensive hardware, although it requires more advanced signal processing techniques.

3.2 Wind Loads

3.2.1 Wind Loads on Ships

Kobayashi et al. (2022) stated that numerical simulation was increasingly employed with wind tunnel testing and regression formulas in the ship design phase to predict the wind load acting on ships (vessel and superstructure). The numerical approaches, however, required more secure, standardized procedures that addressed the clarification of computational variances depending on simulation conditions, particularly regarding the blockage effect, the computational estimation capacity for stationary and non-stationary regimes, wall functions applied to the ship surfaces, the difference of wind profiles recovered by the normalization based on the momentum integration in a shear flow, and the effect of Reynolds number.

Considering this need for verification and validation (V&V), Deng et al. (2022) studied the wind loads on a large container ship both experimentally and numerically under various conditions to assess aerodynamic performance and find methods to decrease wind resistance. A similar approach based on wind tunnel tests and CFD simulations was conducted by Dao et al. (2023) to study wind loads on the topsides of a liquefied natural gas carrier (LNGC), a floating production storage and offloading ship (FPSO) and a jack-up platform (JUP). Overall, favourable validation outcomes were obtained, indicating that the reliability of the experiments and CFD models can be used as a benchmark for future research on offshore wind loading.

A fully numerical investigation of the aerodynamic drag of navy ships in different positions was presented by Islam et al. (2022). Considering the full and model scales, this study showed that the scale effect was negligible for the surge and sway forces but more pronounced for the yaw moment. Although this was possible, the authors concluded that further in-depth investigation remains necessary, including comparison with experimental results and sea trials. In Van He et al. (2023), the wind loads on an original passenger ship were also investigated only by considering CFD simulations. Based on the pressure and velocity distributions around the hull, several new geometries with different frontal accommodation shapes were evaluated to reduce wind drag and improve aerodynamic performance.

Therefore, recent studies allow one to conclude that CFD simulations can provide reliable data for aerodynamic loads acting on ships, which are usable for continuous improvement of aerodynamic performance and manoeuvres under the action of wind.

Research on wind loading on ships was also intensified in the last period due to the IMO resolution (International Maritime Organization (IMO) (2023)), which aimed to reduce ship emissions and achieve net zero greenhouse gas emissions from international shipping by around 2050. Consequently, the maritime industry and commercial transport by ships strove to quickly minimize overall emissions using all available means. In addition to alternative solutions such as cleaner fuels and enhanced ship designs, the resurgence of wind-assisted ship propulsion (WASP) was notable, including those based on rigid sails and towing kites, but mainly using Flettner rotors. As discussed in Khan et al. (2021), theoretical advances in performance prediction programs (PPPs) were notable in this context but still lacked parameters and validation from experiments. This represented one of the future challenges for WASP, along with the precise assessment of environmental and economic impacts and the often-overlooked structural consequences.

In this sense, a methodology based on the application of previously computed wind forces in CFD to a small-scale model using a cable-driven parallel robot (CDPR) was presented in Sauder & Alterskjær (2022) to test the Flettner rotors installed in a very large ore carrier (VLOC) under highly controlled wind loads, still due to a simplistic aerodynamic model. Changes in vessel speed, roll angle, drift angle, and rudder operation in response to the incoming wind angle and speed were recorded and found to qualitatively agree with earlier WASP studies. As expected by the authors, this methodology allowed for a comprehensive validation of the hydrodynamic performance of these new designs. In addition, it facilitated quick comparative evaluations of different configurations, setups, or sail reefing/control strategies. Other factors that could be investigated using this method included course stability when using sails, reduction in manoeuvrability with sails, the positive impact of sails on damping wave-induced motions, and the effect on added resistance in waves.

Kume et al. (2022) also evaluated the aerodynamic characteristics of a ship with Flettner rotors, comparing results from wind tunnel tests and CFD simulations. RANS-based results of the WASP scaled by Reynolds number (*Re*) agreed qualitatively and quantitatively with those of the wind tunnel tests. Moreover, as proposed by previous works, the CFD results conducted at full-scale *Re* indicated an excellent performance in numerically predicting wind loads on a full-scale rotor if the L_{pp}-based *Re* was more than one million.

An investigation based on systematic simulations of Flettner rotors applied as WASP was found in Monteiro (2024). A wide range of spin ratios α (relations of velocities in the cylinder wall and the far field was considered under bi- and three-dimensional CFD models. Regardless of the approach, three flow regimes were observed for different spin ratios. For a spin ratio of 2.5, the 2D lift coefficient (C_L) results aligned closely with those of other studies. However, at higher spin ratios, C_L values were significantly overestimated, whereas the drag coefficients (C_D) were for the 2D discrepancy (particularly focused on the amount of flow deflection), although there was no significant improvement in C_D. The torque coefficients were underestimated but followed the same pattern of experimental results, and changes in domain heights did not significantly alter the results.

3.2.2 Wind Loads on Offshore Structures

The energy available over the sea is highly suitable for power generation, as offshore winds are quite abundant with high speeds near the surface, enabling efficient harnessing of this source. As mentioned in Buljac et al. (2022), accurate estimation of energy production and loads in offshore wind turbines (OWTs) is crucial during the development of new offshore wind farms. Frequently, a beneficial increase in wind power and an advantageous increase in wind energy production, with respect to the size of the turbine and its support system leads to a decrease in structural loads. In this scenario, the researchers have examined small-scale tests conducted at the Wind-Wave-Current Tank (WWCT) laboratory at Newcastle University, UK. The combined effects of waves, currents, and wind on a monopile-supported OWT model were investigated more realistically, as this structure remains the most widely used in the industry. As a result, the current was the main contributor to the overall mean load, with a lower mean wind contribution, while waves dominated load fluctuations. Moreover, (Buljac et al., 2022) found how much influence the tower had on environmental loads, which was generally prominent for prototype OWTs in the cutoff wind speed range and beyond. At the natural frequency of the turbine, the wind primarily induced structural loads in the surge direction, whereas currents amplified dynamic loads at lower frequencies because of non-linear hydrodynamic interactions.

More discussion of significant advances in OWT technology was found in the review by Asim et al. (2022), where critical aspects were assessed to identify knowledge gaps and to facilitate future efforts to understand the intricate behaviours of these systems, mainly those regarding aerodynamic characteristics, dynamic response, structural integrity, mooring cable design, ground scouring, and cost modelling.

Another important concern for OWTs is the structural integrity of their support structures, mainly in terms of failure mechanisms and physics-based modelling techniques. Yeter & Garbatov (2022) reviewed the structural integrity of the OWT support structures, covering a historical background, fatigue and fracture phenomena, crack estimation, and models to predict the remaining life. The paper reviewed influential studies on structural integrity and reliability, which are essential for evaluating the remaining life and managing the lifecycle. It also discussed a risk-based framework for assessing structural integrity, considering the uncertainties of modelling, loads, and material properties.

As a conclusion point on wind and current loads, it is crucial to recognize that innovative methods to enhance the efficiency of sea-based energy production are continuously being developed and evaluated. An example of research in this direction can be found in the numerical investigation of El Beshbichi et al. (2022), which compared the dynamic performance of multirotor FOWT on a spar, SSP and TLP. Six different load scenarios were analyzed, revealing that yaw motion was crucial for these systems, especially for the spar-type FOWT. However, in the SSP and TLP cases, this motion was although the high standard deviations in tower base bending moments heightened the fatigue damage risk in the TLP configuration. In addition, significant tendon loads can raise fatigue-related issues and limit state performance. The sizeable mean pitch angle and yaw standard deviation can decrease the quality of the electric power output. Severe storm conditions lead to a substantial rise in the response standard deviation, particularly affecting SSP-type FOWT.

4 Ice Loads

4.1 Ice Loads on Ships

Reliable prediction of ice loads remains a critical issue for the design and safe operation of ships navigating in the Arctic and ice-infested waters. While navigating through ice, ships are expected to encounter a variety of sea and glacial ice features, requiring the estimation of ice loads. These ship ice loads can be categorized into global and local ice loads. The global ice loads, also known as ice resistance, are important for evaluating overall ship performance, whereas local ice loads are crucial for assessing structural integrity and safety. During this reporting period, researchers have continued to use various modelling techniques, model-scale laboratory experiments, and full-scale trials and measurements. Most of these efforts build on previously developed modelling approaches and are primarily based on existing and published experimental and trial data. The COVID-19 pandemic may have indirectly affected the research type during this reporting time.

4.1.1 Full-Scale Measurements and Trials

Full-scale measurements and trials provide realistic and reliable ice load data by capturing actual environmental and operating conditions experienced by ships. They also serve as benchmarks for validating and calibrating various analytical, numerical and semi-empirical ice load models and model-scale test results.

Sinsabvarodom et al. (2021) analyzed full-scale test data of a station-keeping vessel operating in drifting ice in the Bay of Bothnia in March 2017. The study employed an ice resistance method to estimate global ice loads and determine short-term extreme mooring loads for the vessel under various ice management scenarios.

Influence Coefficient Matrix (ICM) is an ice load prediction method based on a coefficient matrix and is widely employed to convert strain data into ice pressures. This method is often used to estimate the ice loads experienced by ships during full-scale trials. Böhm et al. (2021) investigated the effect of ICM on the accuracy of shear strain-based local ice load measurements onboard the SA Agulhas II. Using a numerical model of a ship grillage system, consisting of a plate and five frames, under various ice load conditions, the study revealed that the number and location of strain gauges significantly affect the ICM and, consequently, the accuracy of the ice load measurements. While the common instrumentation practice is suitable for measuring ice loads within the instrumented area, the study emphasized the importance of optimizing instrumentation setups to achieve improved ice load measurements across various loading scenarios.

The far-field identification method is another approach to predicting ice loads in full-scale measurements. Wang et al. (2023a) employed a radial basis function neural network (RBFNN) based far-field identification method to monitor the ice-induced strains onboard the RV Xue Long 2 during a research expedition. The effect of noise on the identification results of ice loads on the RV Xue Long 2 bow shoulder was investigated numerically and eliminated using a noise injection learning algorithm. The method's feasibility was verified through a model-scale test, where the testing bow shoulder panel was rigidly fixed on a pedestal and loaded with a hydraulic tensioning jack. The method requires further elaboration and full-scale validation. He et al. (2021) utilized Green's function to monitor the time history of far-field dynamic ice loads onboard a ship during the full-scale measurement of Tianen's 2019 Arctic voyage. The study indicated that the Green's function strongly depends on the strain signal intensity. They employed a regularization method to avoid ill-posed problems and to obtain a numerically stable solution.

4.1.2 Model-scale Experiments

Model-scale experiments are often preferred over full-scale measurements and trials as they provide a cost-effective, controlled, and detailed analysis of ice loads and the underlying physics of the ship-ice interaction process. Several model-scale experiments were conducted to explore ship ice loads during this reporting period.

Wan et al. (2023) conducted model-scale ice tests on an Arc7 ice-class LNG carrier to investigate ice resistance under various ice and operating conditions. The tests involved towing the model LNG carrier with a dynamometer through level ice, broken ice and brash ice fields to analyze ice failure modes and ice-hull interaction characteristics. Meanwhile, Xue et al. (2024) utilized a combined experimental and numerical approach to predict ice resistance in broken ice fields. The study employed synthetic polypropylene model ice, and tests were conducted in the conventional non-refrigerated towing tank. The test results were incorporated with CFD-DEM-based simulations to account for the fluid effect, such as the changes in fluid velocity and ship waves. Both studies compared their ice resistance results with existing empirical and semi-empirical formulas.

Li et al. (2021) performed model-scale tests to analyze the escort performance of ships navigating through narrow ice channels created by icebreakers. The test results were then utilized to benchmark numerical simulations of ten sample ships performing escort operations. The study explored the effect of channel width and ice thickness on the resistance and attainable speed.

Sun & Huang (2021) and Müller et al. (2024) investigated ice impact loads in model-scales. Sun & Huang (2021) assessed spatial and temporal variations of ice loads during ship-ice glancing impact tests in an ice tank. The study analyzed tactile sensor data from the test results to classify various local ice failure processes such as pure crushing, spalling and non-simultaneous crushing. It proposed an approach to generate migrating non-uniform ice loads based on Gaussian functions. Müller et al. (2024) investigated the influences of initial ice contact shape on the ice failure modes and resulting impact loads against a rigid steel plate through small-scale drop tower experiments conducted at the Hamburg University of Technology. The study considered 27 cylindrical ice specimens with varying end shapes of cone, dome, wedge, ellipse and other shapes. The experiments were conducted at a ship-ice interaction speed of 2000 mm/s.

Guo et al. (2023) evaluated the ramming performance of an icebreaking research vessel (IRV) model in thick artificial ice at different ship speeds. While these tests may not capture all aspects of the ship ramming process, they provided valuable data for future studies on ramming performance.

4.1.3 Modelling and Simulation Effort

Nowadays, modelling and simulations are the primary research tools for investigating ship-ice interaction processes and predicting ice loads for ships operating in ice. During this reporting period, these modelling and simulation efforts have been predominant in predicting ice loads compared to full-scale and model-scale approaches. These efforts included a range of analytical, semi-empirical, numerical and probabilistic methods.

Analytical and Semi-empirical Approach

Various analytical and semi-empirical approaches, including several machine learning algorithms for predicting ship resistance and global ice loads in different ice features, were employed by several studies (Cai et al., 2022; Ryan et al., 2021; Sun et al., 2022b; Uto et al., 2024; Zhou et al., 2022). Uto et al. (2024) proposed a ship resistance methodology that coupled the World Meteorological Organization (WMO) egg code to account for the natural variability of sea ice. The methods derived mean, maximum and minimum resistances assuming three independent sub-ice regimes in each ice regime. The thickness and size of the ice floes within the ice regimes were estimated based on the stage of development and form of the sea ice in the WMO egg code. The methodology was validated against the full-scale thrust measurement data from the ice trials onboard the icebreaker P/V SOYA.

Sun et al. (2022b) applied an Artificial Neural Network (ANN) model based on 140 data sets from 18 sea trials and model-scale tests to develop a ship resistance model. The study found that seven features related to ship design and ice mechanical properties (ship length, ship breadth, ship draft, stem angle, ship speed, ice thickness and ice flexural strength) along with a Radial Basis Function-Particle Swarm Optimization algorithm (RBF-PSO), could provide a generalized prediction model for ice resistance. Similarly, Ryan et al. (2021) utilized a set of existing ice resistance formulas along with open-water resistance, and fuel consumption formulas to develop an Arctic Ship Performance Model (ASPM). The ASPM was implemented in the MATLAB platform using a machine learning algorithm and validated against full-scale measurement data from the previous Arctic Cargo ship voyage across the Northern Sea Route (NSR). Sazonov & Dobrodeev (2021) proposed a modified semi-empirical method to predict ice resistance in level and broken ice channels for large vessels. The method was validated against model test data from the ice basin of the Krylov State Research Centre.

Cai et al. (2022) employed an image analysis technique to estimate the circumferential crack size of broken ice, a vital parameter to simulate different level ice-breaking processes. The study adopted a deep learning YOLACT model, an instance segmentation model, for improved detection of broken ice floes in the images. A new image processing algorithm was used to analyze the detected ice floes that quantifies the circumferential cracks. Zhou et al. (2022) also used a semi-empirical “circumferential crack model” to calculate the dynamic global ice load in level ice. The study statistically processed the measured ice properties data using the Nataf Transformation to derive the ice parameters required for numerical simulation.

Jiang et al. (2023c) investigated the effect of sea waves and hydrodynamic interaction on added mass and, consequently, on ice impact loads under various sea states. Added mass was estimated with and without accounting for hydrodynamic interactions using a multi-body hydrodynamic code and Potential flow theory, respectively. The Pierson-Moskowitz Spectrum (P-M Spectrum) was applied to evaluate added mass in various sea states. The added mass was then integrated into Popov's model for estimating ship ice impact loads. The results indicated that the sea waves affect the ice loads, while the influence of hydrodynamic interactions is minimal. The study also considered wave-induced motions on ice loads.

Nan et al. (2021) proposed a Long Short-Term Memory (LSTM) networks-based model as an alternative to traditional time and frequency domain inversion models to invert ice loads experienced by ships. The refined grey wolf optimizer algorithm was utilized to optimize the structures of the LSTM networks. The model was trained with ice load data generated by the finite element method.

Numerical Approach

Li & Huang (2022) comprehensively reviewed existing numerical approaches for simulating the ship-ice interaction process and predicting ship performance and local ice loads in broken ice fields. The study analyzed the efficiency and accuracy of these approaches and highlighted the need for further research in ship-ice interaction simulation. Han et al. (2021) presented a simulation technique combining FEM and CFD to predict icebreaking performance in pack ice conditions. This study modelled the pack ice as a rigid body with real-time control of hydrostatic and hydrodynamic forces acting on the pack ice. The hydrostatic force was expressed as a nonlinear restoring force, while the hydrodynamic force was determined using a drag coefficient validated through CFD. Chen et al. (2021a) investigated continuous-level icebreaking using traditional FEM and cohesive element methods (CEM). The FEM was employed to simulate bending fracture, while CEM was used to model the ship-ice interaction process. When compared to existing empirical formulas and model test results, the combined FEM and CEM method demonstrated better accuracy for thinner ice than for thicker ice.

Several studies employed the coupled CFD-DEM method in analyzing ship resistance in ice. DEM defines ship-ice and ice-ice contacts in this coupled method, while CFD captures the hydrodynamics. Zhang et al. (2022d) and Watanabe et al. (2023) applied this method to study ship resistance in brash ice. Zhang et al. (2022d) used the VOF method to simulate the free surface of the water, whereas the latter study applied the lattice Boltzmann method (LBM). Both studies compared their results against model tests and FSICR empirical formulations. Xie et al. (2023a) also used the CFD-DEM coupling approach to study the self-propulsion performance of an ice-strengthened bulk carrier model, which was towed by a carriage with a running propeller in brash ice. Tang et al. (2022b) and Xiong et al. (2023) implemented the coupled CFD-DEM method in STAR-CCM + to investigate ship resistance in pack ice with various ice concentrations and ship speeds for the KRISO Container Ship (KCS) model and the icebreaker Xue Long 2, respectively. Huang et al. (2022d) employed the CFD-DEM approach to study pre-sawn ice resistance, whereas Hu et al. (2022a) utilized an in-house sphere-based DEM combined with CFD to simulate the ship performance in the Arctic marginal ice zone (MIZ).

Ren & Park (2023) developed a numerical model based on the moving particle semi-implicit (MPS) method to predict the ice resistance of a model icebreaker during continuous level icebreaking. The model assumed the level ice to be a continuous isotropic elastic material with a maximum tensile stress failure criterion for the bending and part of the crushing fractures. Crushing fracture due to the shear stress was ignored.

Chen et al. (2023d) numerically investigated the effect of the ice flexural strength on the level ice resistance for icebreakers. The study considered an ice material model previously developed by Sazidy (2015). It changed the critical simulation parameters within the model to achieve different flexural strength values and to analyze their effect on the ice resistance. The study employed a value criterion of the influencing parameters such as the plastic failure strain, Young's modulus, and compressive yield strength within a three-dimensional data space and then applied this criterion to a numerical simulation of an icebreaker running in level ice. The simulation results were compared with semi-empirical models of ice resistance.

Xuan et al. (2021) and Xuan et al. (2023) numerically investigated the global ice load characteristics during manoeuvring captive motion for the icebreaker Xue Long in level ice and broken ice fields, respectively. The model in Xuan et al. (2023) combined DEM and a drag model, while the later-level ice load model utilized a traditional FEA approach with an element erosion technique to simulate ice failure. Both the models were validated against towing test data from the icebreaker Araon model. Yang et al. (2024) simulated the turning and Zig-Zag manoeuvring motions in broken ice fields by coupling the non-smooth discrete element method (NDEM) with the 3-DOF Maneuvering Modeling Group (MMG) model. They investigated the effect of ice concentration, size, thickness, ship speed and rudder angle on the ship's manoeuvring trajectory and steering flexibility.

Gu et al. (2022) applied a circumferential crack fracture-based numerical model to analyze the turning performance of icebreaker AHTS/IB Tor Viking II in level ice. The model was based on the previous research and enhanced accuracy by incorporating ice bending and crushing failure processes. Liu & Ji (2021) investigated the ice resistance of ships in escort operations in level ice using the dilated polyhedron-based DEM (DPDEM), which applied an improved bond-failure criterion to enhance the stability of the simulation for the sea ice-breaking process. Erceg et al. (2022) provided a numerical model to predict local ice loads resulting from ship-ice interaction in level ice, using a dedicated contact algorithm that included contact detection, force evaluation and cusp formation for arbitrary bow shapes at the waterline. The ice sheet was modelled as a homogeneous plate resting on an elastic foundation.

Ni et al. (2024) used the Cohesive Element Method (CEM) to simulate ship collisions with rafted ice. Considering the freezing strength and porosity of ice, the rafted ice was modelled as a multilayer isotropic elastoplastic material. The numerical results were compared with model-scale data from ice-freezing strength experiments conducted at the Svalbard University Laboratory. In a separate study, Ni et al. (2022) modified the length-to-thickness ratio in the original cohesive zone formulation based on several J-integral assumptions and existing research, providing an enhanced formula for simulating Mode I type crack propagation in ice. The accuracy of this formula was assessed using an FEA model of a double cantilever beam and experimental results. Liu et al. (2023b) also investigated the fracture behaviour in level ice using a couped bond-based peridynamic and traditional FEA (PD-FEA) through simulations of the cantilever beam and Mode I crack failure. Yu et al. (2023b) also employed a cohesive element formulation for modelling a wedge-shaped ice indenter within a user-defined subroutine VUMAT in ABAQUS/EXPLICIT to study the dynamic responses of the stiffened panel against the indenter impact. The tri-axial ice model was considered as an isotropic, rate-dependent, elastic-plastic material that fails in a quasi-brittle manner.

Jin et al. (2021) numerically simulated the low-speed icebreaking process for a hovercraft based on a simplified circumferential icebreaking pattern. The model was compared against existing model test data, and the influence of ice thickness and bending strength on ice loads was examined.

Statistical Approach

Zhang et al. (2023c) employed a bivariate reliability approach to analyze bow ice load data for an oil tanker operating in the Arctic environment. The data were derived from simulations of collisions between the oil tanker bow and 2D crushed ice fields with randomly distributed ice debris. The crushed ice fields were modeled using a cellular automata model. The results were then compared against Asymptotic and Gumbel logistics models.

Zhong et al. (2023) developed a methodology to monitor ice-induced hull pressure for ships navigating through ice floe fields. The methodology is based on statistical analysis of ice pressure data from ice model tests and coupled CFD-DEM numerical simulations. The model tests were carried out in the towing tank at Harbin Engineering University (HEU), where the ice model was made of non-refrigerated synthetic polypropylene, and the ice pressure was measured using tactile pressure sensors. The methodology was applied to a single-ship case study; however, further investigation is required to verify its robustness.

Li et al. (2024b) provided a combined statistical and numerical approach to predict extreme ice loads on various parts of the icebreaking hull. The study utilized a rejection sampling technique to generate stochastic ice fields that account for the variability of sea ice thickness. The interaction between the icebreaking hull and these stochastic ice fields was then numerically simulated to estimate extreme ice loads. The numerical results were validated against existing ice tank test data from the Xue Long 2 model.

4.2 Ice Loads on Offshore Structures

4.2.1 General

Ice load is a common force experienced by offshore structures located in the Arctic or ice-infested regions. Many factors, such as environmental conditions, ice properties, and structural characteristics, influence the ice load acting on an offshore structure. The mechanical properties of ice are complex, and the physical processes and failure modes of ice interaction with different offshore structures vary. The variable failure modes of ice and its complex mechanical properties make it challenging to estimate the ice load on offshore structures. Ice loads can cause significant damage to offshore structures. When a structure collides with ice, a dynamic impact load is generated, resulting in structural damage. Continuous pulsating loads can cause vibrations in the structure, which may lead to fatigue failure over time.

The comprehensive interaction between ice and structures is still challenging to predict. However, specific characteristics of ice forces have been observed in model-scale or full-scale tests. Crushing failure is the primary failure mode between ice and vertical structures. The ductile failure of ice typically occurs at a relatively low velocity, and ice loads in time histories exhibit saw-tooth patterns. At a high velocity, the brittle failure occurs, and spalling or flaking propagates on the periphery of the contact interface, inducing a "line-like" ice load in the centre of the interface. For the inclined structure, bending failures also occur during interaction.

Currently, numerical simulations and experiments remain two pivotal approaches for studying ice loads on offshore structures. In numerical simulations, two main methods are used: one simplifies the ice-offshore structure interaction process into a mechanical model, and the other simulates the detailed ice-structure interaction based on a specific numerical algorithm. Experimental research primarily focuses on model-scale tests, while full-scale observations have become relatively rare in recent years.

4.2.2 Modelling Effort (Analytical, Numerical and Statistical Approach)

Theoretical models are classical approaches for dealing with ice and structure interactions. They are derived from analytical models or data from full-scale or model-scale tests. These methods enable rapid prediction of ice resistance and are often used in the initial stages of engineering design and load prediction. Yu and Low (2022) developed a phenomenological model based on a stress-strain relationship equation that captures ductile-brittle transition phenomena under different strain rates. The model was validated against rigid indentation tests, and the predictions were found to match the experimental data well regarding effective pressure, peak pressure, and the time series of ice loads.

Because of the increasing computational power in recent years, numerical simulations have become the most popular approach to investigate ice loads on offshore structures. Truong & Jang (2022) developed a numerical model for level ice-structure interaction problems and validated it by comparing the estimated results with relevant ice collision test data as well as existing simulation results. Using this model, the effects of strain gauge arrangements and corresponding load cells on the estimation of local ice pressures acting on actual offshore structures were investigated. These efforts can improve the accuracy and reliability of the Influence Coefficient Method (ICM), which is an ice load prediction method based on a coefficient matrix, as described earlier. Makarov et al. (2022) reviewed various ice load calculation methods for simulating ice-structure interaction. By comparison, the authors concluded that numerical methods such as FEM and DEM were the most frequently used and provided recommendations on the use of SPG (Smooth Particle Galerkin Method) for the ice-structure interaction modelling. Song et al. (2023) used the nonlinear FEM to investigate the dynamic response of monopile-supported offshore wind turbines. The dynamic response of ice-structure interaction was analyzed, and the influence of ice drift velocity and average wind speed was examined using a statistical method. The simulation results were compared with the ISO 19906 and International Electrotechnical Commission (IEC) standards to gain insight into ice loads. The predictions obtained by the proposed method agreed well with these two international design standards, especially for the maximum ice load.

With the increasing demand for energy and the development and utilization of renewable energy, the advantages of offshore wind energy have become increasingly prominent, especially in polar areas, due to the abundant and high-quality wind. However, building offshore wind turbines in these regions also faces unprecedented challenges because extreme ice loads often lead to collapse or damage to structures. Therefore, in recent years, many researchers have conducted in-depth studies about the effect of ice loads on the structure of offshore wind turbines (OWTs).

Ji & Yang (2022) presented a coupling model of the discrete element method (DEM) and the finite element method (FEM) to study the impact of ice loads and ice-induced vibrations on the monopile foundation of OWT in the process of ice crushing. The results demonstrated that the ice thickness was positively correlated with the ice force on the structure, which was the intuitive representation of the ice load energy. The effect of speed on the ice force model appeared only for large ice thicknesses. Liu et al. (2022d) studied structures' dynamic response and damage during the ice-structure interaction using the fully coupled model with the fluid-structure interaction (FSI) method. The numerical results were consistent with the calculated ice force from the ice force spectrum fitting method. They also showed that the existence of fluid affected the collision process as well as the ice-crushing behaviour. Wang et al. (2022a) established a fully coupled model of a monopile OWT structure with an anti-ice cone. The dynamic response of the OWT under the combined wind and ice load was studied by using the cohesive element method (CEM). The angle of the anti-ice structure had an important effect on the dynamic ice load and motion response of the OWT structure. Changes in the cone angle could influence the pattern of ice destruction, and the optimal ice-breaking cone angle for the OWT in the operating state is 60°. Barooni et al. (2022) constructed a fully coupled numerical model of a floating OWT. Its dynamic response to ice-induced loads was investigated comprehensively using several simulation studies. The ice load had little effect on the output power when the wind turbine operated at rated wind speeds. Shi et al. (2023) used a numerical method based on the three-dimensional interaction model to predict the ice dynamics and structural responses. The area damage rate and fatigue damage rate of the monopile foundation were proposed for further study under wind and ice loads. The results showed that the ice thickness had a more significant effect on OWT damage and fatigue than ice speed. Wu et al. (2024) introduced an OWT dynamic analysis framework that included soil-structure interaction (SSI), random ice loads, and aerodynamic loads. The results showed that when considering SSI, the OWT with a flexible foundation demonstrated notably greater tower-top displacements in comparison to a fixed foundation when subjected to ice loads. The bending moment at the mudline of the OWT under combined ice-aerodynamic loads exhibited an increasing trend compared to the cases of individual ice or aerodynamic loads.

In addition to wind resources, the Arctic region is also rich in oil and gas resources, so the development and utilization of these resources have significant development prospects. Global warming has accelerated the melting of ice and snow in this region, creating favorable conditions for oil and gas exploration. However, the impact of ice loads on offshore platforms also poses challenges to the exploitation of these resources. At present, some progress has been made in the research of offshore platforms under ice loads, mainly aiming at the floating offshore platform adapted to the polar environment. Zhang et al. (2022a) adopted a fully coupled time-domain algorithm to study the dynamic performance of semi-submersible platforms under ice and wave conditions. The paper indicated that the optimized structure could significantly reduce the peak and average ice load, the surge motion and pitch motion of the platform, and the tension of the mooring system. Zhu & Ji (2022) presented the spherical discrete element method (DEM) to simulate and estimate the ice load and mooring force on the moored structure during the ice-structure interaction. The numerical results were compared with nonlinear finite element calculations as well as model-scale experiments. It was demonstrated that the maximum ice load and mooring force had a linear correlation with the ice thickness. The mean and maximum values of the structure's motion also increased as the ice thickness increased. Han et al. (2022) constructed a numerical simulation model of a large-volume gravity-based structure (GBS) towing process assisted by multiple tugs in polygon-shaped broken ice floes. The dynamics of the towing system demonstrated that ice characteristics such as ice thickness, ice concentration and floe size affected the ice load of the multi-body coupled towing system. The forward speed of tugs and GBS also decreased with the increase in ice thickness, ice concentration and floe size.

4.2.3 Model-Scale Experiments

Compared with full-scale measurements, the cost of model-scale tests can be significantly lower, and they can be repeated to explore the influence of different parameters. Herrnring et al. (2021) performed ice extrusion and double pendulum tests and compared the results with the maximum ice force and contact pressure obtained from numerical simulations. The finite element numerical model was based on the Mohr-Coulomb node splitting (MCNS) model to simulate the ice-structure interaction problem dominated by crushing and focused on the brittleness of the ice model. In the process of verification, the MCNS model agreed well with the experimental results. Lemström et al. (2022) conducted laboratory-scale experiments on ice-structure interaction processes in shallow water by pushing a ten-meter-wide ice sheet against an inclined structure of the same width. The results showed that the ice loading process on the inclined structure in shallow water consisted of two distinct phases: the initial phase with a linearly increasing ice load due to an increase in ice mass above the water line and the steady-state stage with an approximately constant load. Tian et al. (2022) carried out model tests to investigate the ice-loading mechanism on a typical structure. They analyzed the failure behaviour of level ice as well as the influence of ice loads on the structures. Numerical simulations based on the cohesive element model were adopted to evaluate the effects of the crack propagation and the crushing process of level ice. From the study, they found that the global ice load of a vertical structure was random, while the global ice load on an inclined plate structure presented a distinct pulsation characteristic and strong periodicity due to the relatively constant frequency of the bending failure. Hendrikse et al. (2022) conducted model tests at the Aalto University's ice tank. They collected a large amount of data on ice-structure interaction, mainly from ice failing against a vertically sided cylindrical pile. The dataset included various model test results from offshore wind turbine structures, structural models representing a series of single- and multi-degree-of-freedom oscillators, scaled dynamic models of the Norströmsgrund lighthouse, and the Molikpaq caisson structure. The results of the experiment provided a reference for the subsequent relevant research. Van den Berg et al. (2022) analyzed the structural responses during intermittent crushing through an experiment of ice-structure interaction. The structural model was represented by a hybrid test device that combines physical and numerical components to simulate the behaviour of a specific test structure in real time. The experimental results showed that the median ice forcing frequency was linearly related to the ice drift velocity. Owen et al. (2023) investigated the peak load-velocity dependence of the model ice used at Aalto University's ice tank. The development of frequency lock-in and intermittent crushing in the model ice was analyzed using a single-degree-of-freedom (DOF) structure. The study found that peak loads on compliant structures cannot exceed peak loads on rigid structures in the same ice conditions, with the only difference being that the peak loads on compliant structures occur at higher ice drift speeds in the far field due to the change in relative velocity.

4.2.4 Full-Scale Measurement and Trials

Due to the difficulty and high cost of full-scale measurements in harsh conditions, relevant studies are rare, making the data extremely valuable. These data can be utilized to inform new designs, analyze important phenomena, and validate new methods. Wang and Zhang (2023) designed and installed an isolation cone system on a mooring dolphin platform in the Bohai Sea. Field tests showed that the acceleration of the ice-induced vibration of the platform structure decreased significantly and that the isolation cone system significantly reduced the ice-induced vibration of the structure.

4.2.5 Ice-Induced Vibration

In cold regions, ice loads constitute a significant factor affecting structural safety. Ice-induced vibration can be harmful to offshore structures and their associated equipment. Model-scale experiments are an important method for studying these issues, as they provide valuable data and verify the effectiveness of new designs and numerical methods. Hammer et al. (2023) conducted an experimental study on ice-induced vibrations of an offshore wind turbine on a monopile foundation. A real-time hybrid test setup was used to incorporate the specific modal properties of an offshore wind turbine at the point of ice action. Experiments showed that the vibration caused by ice depended on the speed of ice drift. The interaction at low-speed results in intermittent crushing, and the multi-modal interaction regime gives rise to the largest bending moments of the support structure. Liu et al. (2023) studied two platform designs to reduce ice-induced vibration and improve the platforms' self-centering ability. Both platforms were tested in the laboratory, and the data were used to develop numerical simulations. The results showed that the ice-induced vibrations of the two novel jacket platforms with concrete-filled double-skin legs were reduced under ice load conditions, and the self-centring offshore platform with concrete-filled double-skin legs had a better control effect. Hammer and Hendrikse (2023) experimentally investigated the effect of wind and ice loading direction inconsistency on the development of ice-induced vibration in offshore wind turbines. The test results showed that misaligned scenarios result in the development of sustained ice-induced vibrations in the direction of the ice load. Furthermore, steady-state high-amplitude ice-induced vibrations could grow more efficiently in a misaligned scenario than in an aligned scenario.

Several researchers have studied the ice-induced vibration problem using various mathematical or numerical methods. Abramian et al. (2022) presented a mathematical analysis of an extended model describing a sea ice-induced frequency lock-in for vertically-sided offshore structures. The results showed that a frequency lock-in regime occurred during ice-induced vibrations when the dominant ice force frequency was close to the natural frequency of the structure. Gagnon (2022) used LS-Dyna to develop a full-scale three-dimensional numerical simulation model of ice-induced vibrations in structures and applied it to the Molikpaq facility for an ice encroachment event in the Beaufort Sea. The ice model was made of crushable foam material incorporating regular spallation events. The model manifested typical characteristics of ice-crushing in the brittle regime. A narrow horizontal hard zone (relatively intact high-interface-pressure ice) was present in the mid-height region of the ice-edge contact area. The model could be configured for various types of structures (offshore platforms, offshore wind turbines, moored structures, etc.) that interact with ice sheets or other ice masses. Long et al. (2023) used the discrete element method (DEM) and the parallel bond model to investigate the interaction between sea ice and offshore wind turbines (OWTs). They analyzed the ice-induced vibration of OWTs at various ice velocities. The results showed that brittle failure of sea ice occurred at higher ice drift speeds, leading to random structure vibration. At lower ice drift speeds, both brittle and ductile failure of sea ice resulted in self-excited vibrations. Zhang et al. (2024) used the cohesive element method (CEM) to analyze the ice-induced vibration of offshore structures. They studied the vibration response of the sea ice-jacket platform under both unprotected and protected conditions with ice-breaking cones. The results showed that the motion response of offshore platforms exhibits a positive correlation with the impact speed of the ice, while the sensitivity of this impact was found to be minimal. Furthermore, the influence of different ice directions on the vibration response of multi-leg offshore platforms was significant, and the shielding effect had a major impact on the platform's response.

With the development of interdisciplinary numerical models, machine learning methods have also been applied to simulate ice-induced vibration phenomena and predict the structural response. Zhang et al. (2022b) used gated recurrent neural networks (GRNN) to predict and suppress the response of offshore platforms under ice loads. The numerical results showed that the ice-induced vibration response prediction method based on the Gated Recurrent Unit Network (GRU) can predict the structural response with satisfactory accuracy. The ice-induced vibration response control method based on the Long-Short-Term Memory Network (LSTM) and GRU network effectively learns the Linear Quadratic Regulator (LQR) method and achieves a significant control effect. Chen et al. (2023) optimized a short-term prediction model for structural response using machine learning theory. A prediction model was established based on the field monitoring data from the Bohai JZ20-2MUQ platform. By utilizing the strong self-learning ability of neural networks for data prediction, the ice-induced vibration (IIV) response prediction model for a specific platform can be realized with high prediction accuracy, relying solely on theoretical analysis and engineering experience for sample feature extraction.

5 Uncertainty

Uncertainty quantification in the evaluation of loads on ships and offshore structures covers several different aspects. In the reviewed literature, uncertainty estimation is carried out for numerical methods, model-scale, and full-scale experiments. Various available standards for the quantification and expression of uncertainty have been used, such as ISO (ISO/IEC Guide 98-3:2008 - Uncertainty of Measurement—Part 3: Guide to the Expression of Uncertainty in Measurement (GUM:1995), n.d.) (ISO/IEC Guide 98-3:2008 - Uncertainty of Measurement—Part 3: Guide to the Expression of Uncertainty in Measurement (GUM:1995), n.d.) standards, ITTC standards, ISSC standards, and American Society of Mechanical Engineers standards.

5.1 Ships

5.1.1 Slamming Loads

The quantification of slamming loads with full-scale measurements is quite a challenging task. For such a reason, model-scale tests and numerical simulations are the most common way for slamming load evaluation. The complexity of fluid-structure interaction simulations and experiments requires a careful estimation of the uncertainties. In (Yan et al., 2022c), a systematic comparison of experiments with fluid-structure interaction (FSI) simulations for flat plate water entry was presented. Particular focus was attributed to hydroelasticity and air trapping effects, quantification of the experimental and numerical uncertainties, and the validity of modelling assumptions for the prediction of bottom slamming-induced loads. Verification and validation to estimate errors were carried out using the American Society of Mechanical Engineers standard. The experimental part was carried out using an electrically driven, vertically moving platform made of polyoxymethylene copolymers (POM-C).

The platform had three pressure sensors, one accelerometer inside the test body, and two strain gauges at the bottom. The numerical simulation followed the two-way fluid-flexible-structure interaction (FFSI) implicit coupling scheme introduced by Lakshmynarayanana & Hirdaris (2020). The FSI was modelled using the STAR CCM + /ABAQUS interface. Generally, good agreement between experiments and numerical simulations was found for both the rigid and hydroelastic cases. The influence of air entrapment was investigated by monitoring the presence of air during experiments with a high-speed camera. The uncertainty estimation for both the experimental and numerical parts was carried out. The uncertainty estimation comprised the accuracy of the sensors, the acquisition system, and the uncertainties due to the repetition of experiments (30 repetitions were performed). Discretization uncertainties were quantified using the Grid Convergence Index (GCI) method. The errors were lower for quantities not influenced by local effects (forces) in comparison with pressures and strains that were affected by larger errors. The authors used the American Society of Mechanical Engineers standard for "Verification and Validation" to estimate the errors in both the experimental and numerical parts. The main findings and suggestions were: for local slamming, a high number of experiments was recommended; the validation uncertainty depended on the parameters taken into account; the percentage validation uncertainty tended to be smaller for higher impact speeds in the case of pressure and was roughly independent of the velocity in the case of force.

Regarding a purely numerical simulation, Wang et al. (2021b) presented an analysis of numerical uncertainty due to discretization in the Arbitrary Lagrangian-Eulerian (ALE) Finite Element method for the prediction of water-slamming loads. The paper quantified uncertainty using two ITTC-recommended methods, which used the independent grid and time-based discretization as well as a constant Courant-Friedrichs-Lewy (CFL) number-based discretization approach. The study found that the uncertainty values obtained from the free-falling models were closer to those from experiments. The same conclusions regarding the better accuracy of the Courant-Friedrichs-Lewy (CFL) method in comparison with the ITTC method were drawn, but with a different application, as shown in Islam & Guedes Soares (2021).

5.1.2 Global Loads

Global loads on ships can be due to waves, grounding, or collision. The study of global load effects can be carried out by numerical simulations, considering the hull girder as either a rigid body or a flexible structure and taking into account both linear and non-linear effects. On the other hand, experimental model-scale tests can be carried out in dedicated facilities. The main uncertainties are related to the transfer function evaluation for linear effects, while the correct simulation of hydroelasticity, whipping, and springing effects are the challenges for non-linear effects estimation. Regarding experiments, the number of repetitions and the generation of waves are the main topics.

Regarding linear effects, the results of a benchmark study organized by the ISSC-ITTC Joint Committee on global linear wave loads on a container ship with forward speed were presented by Parunov et al. (2022). When linear effects were considered, the main uncertainties were linked to evaluating transfer functions. To address this, the paper analyzed different seakeeping codes and their impact on the long-term extreme vertical wave bending moments. Fifteen seakeeping codes were tested, belonging to one of the three methods: strip theory, 3D frequency-domain method, and 3D time-domain method. Quantification of the uncertainty of the transfer functions was carried out in the form of the Frequency Independent Model Error (FIME) given by the Eq. (1).

$$\varphi = \frac{\sum_i \widehat{H}_i H_i}{\sum_i H_i^2} \tag{1}$$

where, $\widehat{H_i}$ are the measured transfer functions $\widehat{H_i}$ is the calculated transfer function as Total Difference, as Kim & Kim (2016) determined. The uncertainty of the experimental results was expressed following the ISO Guide (ISO, 1995). Uncertainties in the seakeeping codes have been evaluated for the heave, pitch, and vertical wave bending moment at midship for three heading angles. The paper found that strip theory codes showed lower dispersion both compared to the average of the other codes and the experimental values.

The uncertainties in the transfer functions were assessed through the Frequency Independent Model Error (FIME) (see Eq. 1) and other more sophisticated methods.

The paper concluded that the FIME was the most promising method. Both strip theory and 3D methods gave reasonably good results for linear wave loads. More considerable uncertainties were found in the non-linear response, such as the hydro-elastic response.

The uncertainties in non-linear responses were investigated in Hirdaris et al. (2023) regarding the importance of uncertainties in hull girder loads influenced by flexible fluid-structure interactions. The paper mentioned several accidents in which hydroelasticity could have played a significant role. Nevertheless, the influence of springing and whipping effects on structural design was not taken into account in a coordinated way due to substantial uncertainties linked with the modelling of the phenomenon. The paper concluded that despite 40 years of research, a clear understanding of hydroelastic uncertainties in wave-induced loads remained elusive.

Challenges include theoretical assumptions, data processing, and limited industry-academia collaboration. Structural models offer detailed stress information, while linear frequency domain methods are mature and time-domain approaches are emerging. Computational Fluid Dynamics (CFD) methods are still evolving but highlight the importance of coupling in hull girder modelling. Uncertainty quantification methods are crucial for design but face challenges due to nonlinearities and data ambiguity.

A fully coupled CFD-FEM method to estimate ship wave loads and hydroelastic responses was presented by Huang et al. (2022f). The method was tested on a standard S175 containership, comparing results with available experimental data. Uncertainty analyses were conducted to determine the influence of fluid grid density, time step, fluid domain size, fluid viscosity, and hull structural element number. Uncertainties in the paper were studied using two methods based on Richardson Extrapolation (Correction Factor [(Stern et al., 2001)] and the Grid Convergence Index (GCI) using a factor of safety (FS)[(Celik et al., 2008)]). The main findings were that a CFD solver using the Euler Overlay Method (EOM)wave generation method can accurately and steadily produce 5th-order Stokes waves. It suggested that a shorter downstream region (1.5 times the ship length) did not significantly affect wave calculations and ship responses compared to the recommended 3L length (3 times the ship length), reducing computational workload. A smaller time step (recommended $< 1/100$ of 2-node natural vibration period) ensured accurate high-frequency whipping load reproduction. The study also highlighted significant differences in ship wave loads obtained by different methods, emphasizing the complexity of factors influencing whipping responses, including structural model variations and external factors such as wave type and steepness.

Non-linear effects in global response for collision and grounding were presented in Kim et al. (2022b). In the paper, a benchmark study comparing the structural dynamic response by explicit nonlinear FEA approaches and the semi-numerical super-element method for grounding and collision for passenger ship was presented. In the paper, four scenarios for ship-ship collision were considered, and five different scenarios for grounding. The modelling methods accounted for hydrodynamic actions associated with operational and environmental conditions. The results were similar regarding maximum response for collision and groundings, except for oblique collision and groundings involving sharp rock. Uncertainties were reduced using the same inputs to the MCOL program (an LS-DYNA® module) and the same fracture criteria. Another important source of uncertainties was represented by the extent of the FEM model (partial or full ship) and by the fracture strains, well as by the meshing size.

Regarding experimental approaches, van Essen et al. (2023) reported an analysis of the required test durations for converged short-term waves and impact extreme value statistics using experimental analysis. In part 1 of the paper, guidelines were given for the convergence of most probable maximum wave crest heights and most probable maximum green water wave impact forces on a ferry. In contrast, in part 2, similar results for wave-in-deck loads on a stationary deck box were given. The key parameters for a good estimation were the exposure duration (e.g., 3 h for offshore structures) and the number of seeds (3 h stationary periods). Convergence plots were given in the paper that could be used to find the number of seeds needed to achieve a certain accuracy. A second aim of the paper was to understand if fitting (3-parameter Weibull fit) could influence the number of required seeds for convergence, but it was found to have a negligible influence. A final remark was that a large number of seeds (significant time and cost-consuming) were required to have reasonable estimates of impact load distributions, suggesting the need to investigate different methods.

5.1.3 Mooring

In Abdelwahab & Soares (2023), the uncertainty modelling of experimental results for a physical model of a tanker moored to a terminal inside a port was presented. During the experiments, 6 DOF motions and loads on the mooring lines were measured. The uncertainty evaluation followed the ITTC guidelines (ITTC, 2011). The uncertainty analysis of the experiments taken into account is listed in Fig. 17.

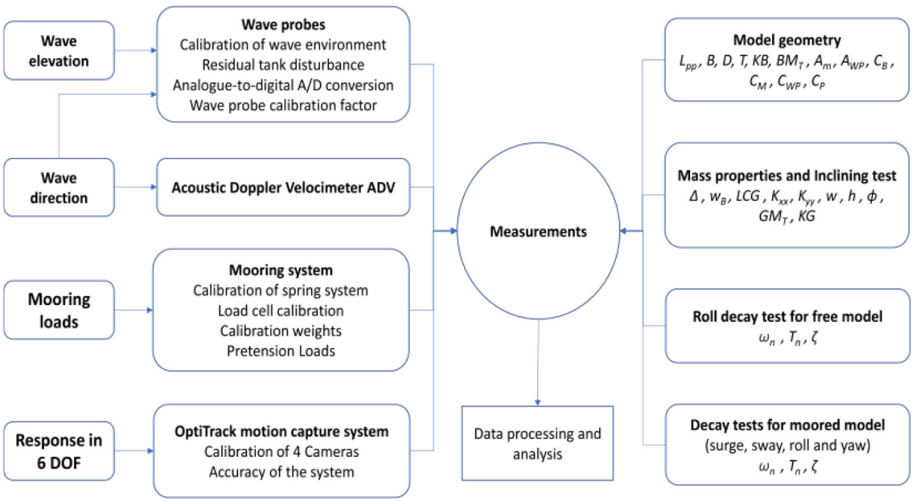

Fig. 17. Uncertainty sources for the model experiments from (Abdelwahab & Soares, 2023).

The authors found that type B uncertainties, related to wave measurements, model geometry, and mass distribution, were more significant than Type A uncertainties. Uncertainties in wave measurements in shallower waters involved non-linear effects and extremes. Non-linear influences in mooring systems, exciting forces, and ship response also impacted mooring load uncertainties. Performing systematic experimental uncertainty analysis was challenging but crucial for improving test quality despite its time and cost requirements. The results could benefit future research at the same facility by providing valuable insights into physical model uncertainties.

5.1.4 Others

In Gaidai et al. (2022), a novel structural reliability method was presented, particularly suitable for multidimensional structural responses. The method was applied to a container ship subjected to large deck panel stresses and extreme roll angles. The method was benchmarked with onboard measured time histories. The methodology presented could efficiently assess the reliability of high-dimensional dynamic systems, which is particularly useful when dealing with limited data sets. It was applied to real-time data from measured wave heights and vessel reliability during transatlantic voyages. The method produced reasonable confidence intervals and did not require restarting simulations after a system failure, making it a valuable tool for various nonlinear dynamic systems reliability studies across different engineering fields.

In Miratsu et al. (2022), the effect of ship operation on sea loads was studied using a statistical storm avoidance model of merchant ships to reconstruct the sea states encountered over 25 years in the North Atlantic. The uncertainties of the ship operation effect were investigated for different hindcasts (TodaiWW3-NK, IOWAGA, and ERA5). The sea states encountered were estimated by AIS data applying a storm avoidance model (Sasmal et al., 2021). The findings indicated that the ship operational effect averages between 0.82–0.88 with a standard deviation of 0.01–0.03, resulting in a 10–20% reduction in long-term motion and wave load predictions at a 10^-8 probability level of exceedance corresponding to a minimum of a 25-year return period. However, this estimate carried uncertainty linked to various factors such as hindcast products, ship characteristics (ship length and type), and storm avoidance model settings.

5.2 Offshore Structures

In Islam & Guedes Soares (2021), an assessment of different uncertainty analysis methods commonly used for uncertainty quantification in Computational Fluid Dynamics (CFD) was carried out and a comparison constant Courant–Friedrichs–Lewy (CFL) number-based approach for uncertainty estimation to the ITTC recommended grid and time-independent procedures was given. Four different uncertainty estimation procedures were presented. CFD-related uncertainty quantification in wave load simulation was carried out using a fixed vertical cylinder as a case study. The study directly compared the uncertainty estimation of three methods: Factor of Safety, Correction Factor, and Least-squares root approach. Comparisons were made regarding forces and moments for the three methods, both for the Courant–Friedrichs–Lewy (CFL) number-based approach for uncertainty estimation and the ITTC-recommended grid and time-independent procedures. The paper concluded that the CFL number-based simulations were more stable and provided better convergence of results in all the cases. Regarding the verification study, the paper concluded that each of the four uncertainty analysis methods had pros and cons, and all were equally applicable for uncertainty assessment in CFD studies. A summary of the results is given in Fig. 18.

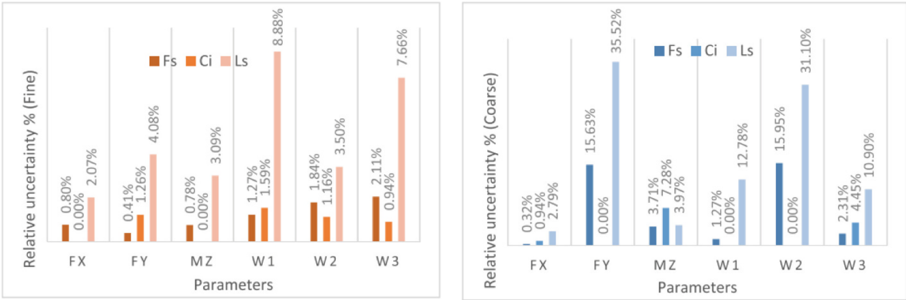

Fig. 18. Relative comparison among uncertainty at constant CFL number, using the Factor of safety, Correction factor, and Least-squares root methods by Islam & Guedes Soares (2021)

In Hallak et al. (2022), epistemic uncertainties to estimate the minimum necessary air gap for a semi-submersible accommodation unit in stormy conditions were assessed. The number of uncertainties in the air gap evaluation process of a semi-submersible platform were numerous, but the paper focused on model uncertainties. The uncertainty evaluation of the modelling was carried out by taking into account the uncertainties resulting from the binned values of scatter diagrams and from the assumption that the highest significant wave height sea state was the critical sea state. To investigate this, environmental contours were taken into account instead of a single value. Regarding the uncertainty implied in the finite set of control points, Kriging interpolation (Kleijnen, 2009) was used, allowing adaptation of the uncertainty propagation techniques to assess the variances of the estimates in points different from the control points. The requirements for operational and survival air gaps were defined in the paper as the return periods of 10 years (operational) and 100 years (survivability) plus a margin. The sea states were characterized with JONSWAP unidirectional wave spectra. For all scenarios considered, the actual critical sea states had significantly lower heights and main periods compared to the top points of the environmental contours. In the paper, it was found that FOSM methods always retained high levels of uncertainty due to the uncertainties in the estimated critical period when directly obtained from scatter diagrams. In conclusion, the paper suggested that the number of critical points had a strong effect on the uncertainties and that for long-term analysis, environmental contours had to be taken into account to reduce uncertainties.

5.3 Waves Description

In Bitner-Gregersen et al. (2022), a comparison of the uncertainty evaluation in wave data and models used for the design and laboratory testing of marine structures given by the two organizations ISSC (International Ship and Offshore Structures Congress) and ITTC (International Towing Tank Conference) was presented. In particular, the analysis focused on long-term wave descriptions. ISSC and ITTC use different definitions of uncertainties. ITTC uses the ISO definition (Type A cannot be reduced, Type B can be reduced) while ISSC uses the definitions applied by the Society for Risk Analysis community (aleatory and epistemic), and in the paper, the ISSC definition was used. One of the main sources of uncertainties was represented by the dataset, which had to be carefully selected for the specific area of interest. A finding of the paper was that many datasets were not well-calibrated for the extremes. Another important parameter to be carefully checked was the time extension of the database, which had to be not too short. The paper highlighted the importance of considering new databases such as ECMWF ERA5, Ifremer IOWAGA and Japanese TodaiWW3-NK to update the IACS scatter diagrams. In addition, frequency analysis could be carried out to find sea areas with similar statistical characteristics, improving the dataset subdivision of the scatter diagrams suggested by IACS.

In Zhang et al. (2022c), an investigation of the influence of initial uncertainties in predicting the geometrical properties of maximum waves in a short-term sea state was given. The uncertainty was investigated using Monte Carlo simulations. The Chalikov-Sheinin (CS) model was used to model the wave. Uncertainties induced by the initial conditions were evaluated by six wave profile parameters (the horizontal asymmetry parameter, the vertical asymmetry parameter, the length of maximum wave L, the maximum crest-to-trough height and the block coefficient). The maximum crest, trough, and crest-to-trough heights in a sea state were only sensitive to the amplitudes of a certain range of free waves (around the peak wavenumber). The randomness caused by the initial random-phase/amplitude model (natural uncertainty) was very large. The behaviour of the three asymmetry parameters was very high, while the maximum crest was less influenced.

Vanem et al. (2022) reviewed the latest findings regarding the Statistical modelling of the ocean environment. The review covered long-term and short-term statistics in deep and shallow water, extreme value and extreme wave statistics, multivariate analysis and joint distributions, machine learning applications and spatial and temporal statistics.

6 Conclusion

The question of determining and analysing relevant wave load scenarios that a ship might encounter in its operational lifetime and the respective consequences on ship design and operation is a topic of continuous development and research.

Within the reporting period of this committee, progress has been made in different fields related to wave loads on ships. The key insights from Sect. 2.1 are summarized below.

Potential flow theory remains a popular approach for modelling wave-induced loads on ships, offering efficient solutions for linear and weakly nonlinear problems. Recent advances in frequency-domain and time-domain methods provide approaches for improved modelling of complex boundary conditions, such as those encountered in shallow and confined waters. Recent work has focused on hybrid and fully nonlinear models to improve accuracy, particularly for added resistance and structural responses in irregular wave conditions. However, fully nonlinear approaches remain computationally demanding, prompting ongoing efforts to optimize their efficiency through parallel computation.

Field methods for wave loads on ships have been discussed, specifically in the context of roll damping and green water loading. When applied for estimating roll damping field methods compare well with model-scale experiments. Note that this does not guarantee predictive value at full scale. Field methods with advanced free surface transport formulation allow for the systematic study of green water in a range of wave steepness to obtain improved deck structure designs. Future field methods for slamming of ships in waves may include aeration compressibility due to entrained air in the water to get lower, more realistic pressure maxima during slamming.

Experimental methods continue to play a critical role in validating numerical models and improve our understanding of hydroelastic responses. Recent studies highlight the importance of segmented and fully elastic ship models, which enable detailed investigations into nonlinear phenomena such as whipping, springing, and slamming. Advances in instrumentation, such as Fiber Bragg Grating sensors, have the potential to enhance the accuracy of pressure and strain measurements. Efforts to reduce uncertainties in test setups, such as controlling wave steepness and improving model stiffness scaling, contribute to improving the reliability of experimental results.

Full-scale measurements, particularly through onboard monitoring systems, provide invaluable data for understanding operational loads and validating design criteria. Methods for indirect load estimation, using strain and motion data, have advanced significantly, allowing accurate reconstructions of unmeasured responses. These techniques enhance fatigue assessments and structural health monitoring, but challenges persist in processing and integrating large data streams into design and operational frameworks.

Data-driven approaches have the potential to significantly increase the efficiency of the prediction and analysis of wave loads and ship responses. Recent studies show that machine learning models, such as neural networks and recurrent models, offer promising tools for real-time load predictions and operational optimization. Multi-fidelity methods that combine low- and high-fidelity data have enhanced the accuracy of structural response predictions. Despite these advances, issues related to data quality, pre-processing, and integration into design workflows require further attention.

Slamming remains a critical phenomenon for structural integrity, particularly in rough seas. Recent research activities have improved the modelling and prediction of slamming loads through coupled fluid-structure interaction methods and advanced computational techniques. Experimental data from wedge-drop and segmented model tests provide valuable insights into local pressure distributions and global whipping responses. However, further work is needed to address uncertainties in asymmetric slamming and its impact on fatigue and failure modes.

For liquid cargo carriers, sloshing dynamics are critical in design and operation due to their impact on ship stability, motion behaviour and structural loads. Numerical and experimental studies have advanced understanding of global tank dynamics and local impact pressures. Innovative mitigation strategies, such as optimizing tank geometry and incorporating internal structures, appear to be promising. However, challenges remain in scaling sloshing tests and accounting for phase transitions in cryogenic fluids.

Similarly, below are the key findings from wave loads on offshore structures in Sect. 2.2.

Potential theory methods have seen refinements in linear and nonlinear formulations for efficient wave load predictions, mainly targeting wave run-up in structural elements, gap resonance, and prediction of free surface elevation in Oscillating Water Columns (OWC) type of Wave Energy Converters (WEC) resorting mainly to Boundary Element Methods, and the decomposition of the potential into first and second order problems while applying a perturbation based approach to its solution and coupling first order models with aerodynamic models for the OWC case studies.

Field methods for solving Navier-Stokes equations continue to be instrumental in understanding wave-structure interactions, addressing challenges such as highly deformed interfaces, wave breaking, and turbulence. Tools like OpenFOAM, STAR-CCM +, and REEF3D have facilitated innovative research into hydrodynamic loads, mooring dynamics, and wave-induced responses on offshore structures, complemented by hybrid and particle-based modelling approaches that enhance accuracy and efficiency in simulating complex offshore systems.

Recent studies have emphasized the critical role of wave-current interactions in determining hydrodynamic loads and structural responses in offshore structures. Key advancements include the investigation of wave-current effects on offshore wind turbines, aquaculture fish cages, tidal energy devices, submerged tunnels, floating bridges, and mooring buoys, showcasing enhanced predictive models and experimental approaches to optimize performance, reduce structural fatigue, and ensure stability under combined environmental loads.

The structural safety of offshore platforms relies heavily on accurately understanding and managing airgap and Wave-In-Deck (WID) loads, which have been the focus of extensive research in recent years. In high-fidelity numerical modelling, experimental validations and procedural improvements have enhanced the prediction of these complex, nonlinear phenomena. This leads to more efficient and robust platform designs while reducing conservatism in traditional assessment methods and better ensuring structural integrity under extreme wave conditions.

Regarding moorings, recent studies have advanced the design, analysis, and simulation of various mooring systems, including innovative solutions like shared moorings for floating wind farms, hybrid mooring materials combining synthetic fibres and steel ropes, and optimized configurations for renewable energy applications, while also addressing challenges related to fatigue resistance, corrosion effects, and dynamic responses under complex load conditions.

Advanced model testing remains a crucial activity in the study of wave loads on offshore structures, providing empirical insights that refine theoretical models and engineering practices. Recent research has explored wave impacts on offshore platforms, floating wind turbines (FOWTs), WECs, aquaculture structures, and very large floating structures (VLFS), using scale models, innovative techniques like Particle Image Velocimetry (PIV), and numerical validation to improve design, safety, and operational efficiency of the structures.

Over the past three years, the integration of data-driven methodologies and machine learning techniques into marine hydrodynamics and offshore engineering has led to significant advancements. Applications such as predicting wave-induced motions and hydrodynamic loads with models like LSTM and Wave-GAN, as well as the use of digital twins and reinforcement learning for mooring systems and coastal protection, have demonstrated notable improvements in predictive accuracy, computational efficiency, and adaptability, fostering the development of more resilient and optimized offshore structures. However, these advancements have not translated into a substantial enhancement in the fundamental understanding of wave-structure interaction. It suggests that while machine learning has proven valuable as a tool, it has not yet been instrumental in driving deeper theoretical insights in this domain.

In Sect. 3, the analysis of current and wind loads on ships and offshore structures was provided. The key findings emphasize the growing relevance of accurate load predictions, especially with modern vessels and offshore systems' increasing dimensions and operational complexity. Precise estimation of current and wind loads significantly influences and is critical to improve ship design and manoeuvrability, ensure stability of mooring systems, and increase energy generation efficiency and performance of offshore wind turbines. The integration of high-fidelity CFD simulations has proven essential for addressing the limitations of traditional experimental methods, particularly in the early phases of complex projects. Studies have shown that underestimating these aerohydrodynamic efforts can lead to premature structural fatigue and increased operational risks, among other problems. However, the combined effects of currents, wind and wave loads continue to pose a significant challenge to the design and operability of modern marine systems. In this context, future trends are related to the continuous evolution of hybrid approaches, numerical and experimental, promising enhanced accuracy in predicting and managing such environmental loads.

In Sect. 4, research on ice loads on ships and offshore structures has highlighted advancements across full-scale measurements, model-scale experiments, and modelling and simulation techniques. In Sect. 4.1, full-scale studies validated methods for estimating global and local ice loads under realistic conditions for ice loads on ships. They emphasized the importance of optimizing instrumentation setups for accurate measurements. Model-scale experiments provided cost-effective insights into ice resistance, ship performance in narrow ice channels, and impact loads, with findings showing that factors like ice thickness, channel width, and ship speed significantly affect ship-ice interactions. Simulations using advanced techniques such as coupled CFD-DEM, cohesive element methods, and machine learning algorithms enhanced the accuracy of predictions for ship resistance, ice impact loads, and manoeuvring in ice. Statistical approaches were applied to analyze extreme ice load scenarios and variability in sea ice conditions. These findings collectively contribute to improving the safety, efficiency, and design of ships operating in ice-covered waters.

Section 4.2 provided research on ice loads and their effects on offshore structures. Generally, ice-structure interactions are complex and influenced by environmental conditions, ice properties, and structural characteristics. Crushing failure is identified as a primary failure mode, with distinct ductile and brittle behaviours under varying velocities. Numerical simulations, including FEM, DEM, and coupled methods like FSI, dominate the field, offering insights into ice-induced vibrations, structural responses, and optimal designs for mitigating ice impacts. Studies on offshore wind turbines (OWTs) reveal the significance of ice thickness, drift velocity, and anti-ice cone angles in dynamic responses and fatigue resistance. Machine learning approaches have emerged as effective tools for predicting and controlling ice-induced vibration responses, enhancing accuracy and efficiency. Model-scale experiments remain crucial for exploring ice-loading mechanisms and validating numerical models, while full-scale observations, though rare, provide invaluable data for real-world applications. These efforts collectively improve the understanding of ice loads, advancing the design and safety of offshore platforms and wind turbines in polar regions.

In Sect. 5, Uncertainty quantification in the assessment of loads on ships and offshore structures was explained. Recent literature has examined slamming, global, and mooring loads on ships (Sect. 5.1), highlighting the substantial challenges posed by full-scale measurements of slamming loads. It has been demonstrated that a synergistic approach combining model-scale tests and advanced fluid-structure interaction simulations can effectively quantify slamming load uncertainties, underscoring the need for meticulous validation and favouring methods such as the CFL approach to enhance accuracy. Furthermore, an in-depth investigation of global loads on ships under various conditions has revealed that while linear wave load responses can be reliably evaluated using established numerical methods and transfer function assessments, significant uncertainties remain in non-linear dynamics. These uncertainties are influenced by hydroelasticity, fluid-structure interactions, and the complexities associated with experimental setups, indicating the necessity for improved methodologies and collaborations to refine load predictions and structural designs. Additionally, innovative reliability and statistical modelling techniques have been introduced to effectively address uncertainties in structural responses and the effects of ship operations, thereby providing valuable insights for enhancing the reliability and accuracy of marine engineering analyses.

In the context of offshore structures (Sect. 5.2), the studies underscored the critical importance of uncertainty quantification methods in CFD, highlighting the advantages of using the CFL number-based approach to achieve stability and convergence while emphasizing the necessity of incorporating environmental contours and accounting for multiple critical points to effectively manage uncertainties in assessing the air gap for semi-submersible platforms.

Moreover, in the Waves Description subsection (Sect. 5.3), the studies collectively highlighted the vital role of precise uncertainty evaluation methods in analyzing wave data and modelling marine structures, showcasing the differing definitions of uncertainties as articulated by ISSC and ITTC, the significance of dataset quality and calibration, the considerable influence of initial conditions on wave properties, and the substantial advancements in the statistical modelling of ocean environments.

This committee also performed a benchmark study (in Appendix A). Numerical simulations of flat plate impacts were conducted using CFD, SPH for rigid implications, and a two-way coupled FFSI approach with ABAQUS and STAR CCM+. A hybrid STAR CCM + method and an incompressible fluid solver in LS-DYNA were also used for hydroelastic water impacts. The simulations matched the dimensions and properties of experimental test bodies. Results showed similar peak loads between simulations and experiments, except the stiffer LS-DYNA FFSI—-simulated void fractions beneath impacting plates aligned well with experimental high-speed imaging. Differences in peak pressures, forces, and strains were due to varying assumptions and high-frequency vibration modes. Future work should focus on uncertainty modelling and prediction.

Benchmark Study

Introduction

In rough seas, ocean-going ships are subject to impact-induced loads that may induce vibrations, and noise and affect structural integrity, especially in the ship's bow and stern areas. The same problem is practically relevant to the dynamics of high-speed vessels prone to bow or bottom-slamming-induced loads (Tavakoli et al., 2024).

Objectives

This section presents comparisons between experiments and simulations for the case of flat-water plate entry (Yan et al., 2022c). The focus of the benchmark is on rigid body and hydro-elastic dynamics using the following methods:

- A two-way coupled flexible fluid-structure interaction (FFSI) model based on ABAQUS and STAR CCM + simulations presented by Yan et al. (2022c).
- A hybrid hydroelasticity method was introduced by the National Research Council of Canada (NRC) (Sitek et al., 2021). Whereas this approach is similar to Yan et al. (2022c), it combines fluid and solid solvers inherently available in STARCCM +.
- Two different methods by the National Maritime Research Institute of Japan (NMRI) using the LSDYNA explicit fluid structure interactions scheme (Livermore Software Technology Corporation, 2014) and Smoothed Particle Hydrodynamics.

The outcomes of the above methodologies are compared with the results obtained from the experiments presented by Tödter et al. (2019).

Experimental Configurations

The test setup consisted of a vertically moving platform powered by an electric motor, allowing freely adjustable platform velocities. The topologies and sensors considered are shown in Fig. 19 and Fig. 20 and described in Table 1.

Several key points for easy reference are summarized in this section.

- The platform was positioned above the test section of a circulating water channel of 6.0 m length and 1.5 m width, with the water depth set at 0.55 m. A control loop kept the velocity of the test body constant during water impacts.
- The body's walls and flanges consisted of rigid aluminium plates. The quadratic flat bottom plate of 0.09 m^2 area had a thickness of 4.7 mm and was made of poly-oxymethylene copolymers (POM-C) having an elasticity modulus of approximately 2.8 GPa.

- The rigid test body had an aluminium bottom plate of 12.0 mm thickness, which was welded to the walls of the test body. The bottom's shape and its area were the same for the elastic and the rigid test cases.
- Inside the test body, two stiffeners were fastened to the rigid bottom to minimize deformations during impact. Three pressure sensors and one accelerometer were placed inside both test bodies. Additionally, the elastic bottom was equipped with two strain gauges.
- Three absolute pressure sensors, Kulite XTM-190(M) depicted as P1, P2, and P3 in Fig. 1, were placed along the centre line of the bottom plates. Following hammer tests, the lowest natural plate frequency was estimated at 147.1 Hz in air, 53.0 Hz on the water surface, and 47.1 Hz when submerged.
- For the elastic bottom plate, small sleeves made of POM-C with a diameter of 10 mm and a total height of 10.92 mm were glued to the bottom plate at the sensor positions to allow the sensor mounting.
- The bottom plate thickness for the rigid test body was reduced to 10.92 mm over a circular area of 20 mm diameter at these sensor positions. The sensor's circular measurement area had a diameter of 3.8 mm.
- As the sensors recorded absolute pressures, the atmospheric pressure had to be subtracted from every measurement.
- A PCB 353B34 accelerometer was located a distance of 30 mm from the bodies' walls above the bottom plate to decouple accelerometer measurements from structural responses (depicted as Acc in Figure A1 and Figure A2). This accelerometer was able to measure acceleration peaks up to 50 × acceleration of gravity of 9.81 m/s^2.
- Two HBM 1-XY-93–3/350 strain gauges (depicted as S1, S2 in Fig. 19) were mounted along the center line of the elastic bottom plate at a distance of 100 and 150 mm between bottom plate edges and strain gauge centres, respectively.
- Two additional strain gauges (not shown in Fig. 19) were placed at the elastic test bodies' walls to monitor the temperature compensation of strain gauge measurements.

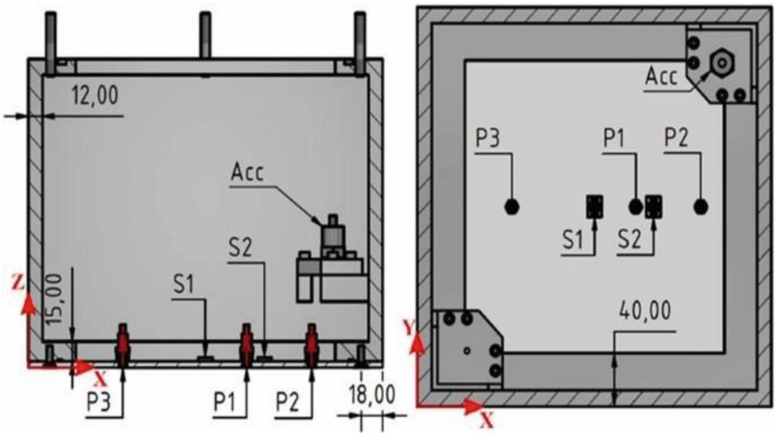

Fig. A1. Side view (left) and top view (right) of the test body with an elastic bottom and the arrangement of pressure sensors P1, P2 and P3, strain gauges S1 and S2 and accelerometer Acc (Displayed values are in mm).

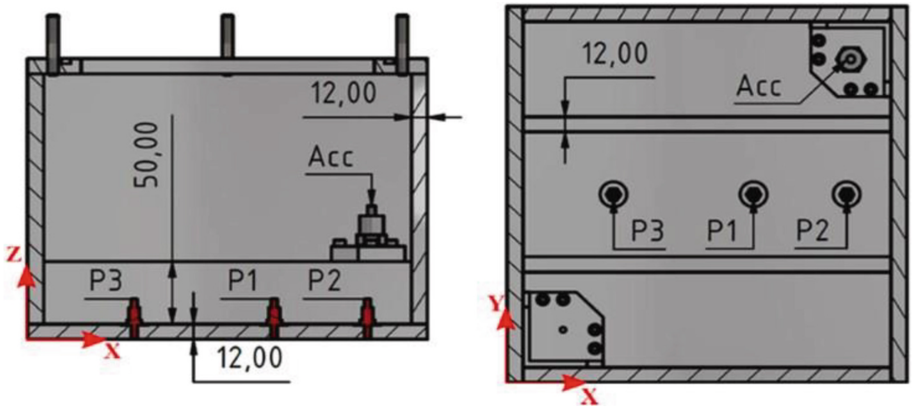

Fig. A2. Side view (left) and top view (right) of the test body with a rigid bottom and the arrangement of pressure sensors P1, P2 and P3 and accelerometer Acc (Displayed values are in mm).

Table 1. Coordinates specifying the positions of the three pressure sensors, the two strain gauges and the accelerometer ([a]Elastic, [b]Rigid).

Sensor	X [mm]	Y[mm]	Z[mm]
Pressure Sensor P1	185	150	0.0
Pressure Sensor P2	240[a]/255[b]	150	0.0
Pressure Sensor P3	80	150	0.0
Strain Gauge S1	150	150	4.7
Strain Gauge S2	200	150	4.7
Accelerometer	258	258	74[a] / 81.7[b]

The elastic and the rigid test bodies weighed 18.45 and 20.32 kg, respectively, and they were mounted underneath a load cell to measure integral forces acting on the test bodies during water entry. The HBM U3/10 load cell, which measured forces up to 10.0 kN with an uncertainty of 0.2%, was connected to the platform via an extension. A Ballupp BTL5-A11-M1000-P-32 type magnetostrictive sensor with an uncertainty of 0.02% measured the platform's motion to yield a reproducible resolution of 4.0 µm. The time derivative of the platform's motion determined its velocity. Further details on the experimental setup are explained by Tödter et al. (2019).

Benchmark Cases

The benchmark cases are summarized in Table 2 and focused on benchmarks of pressures (sensor location P1), plate entry impact forces, elastic strains (sensor locations S1, S2) and air entrapment effects in the way of the plate bottom under rigid body and elastic conditions. The modelling and simulation boundary conditions are highlighted in Table 3. A summary of the modelling assumptions in structural and fluid domains is given in Table 4. All methods except the NMRI SPH accounted for flexible dynamics by two-way coupling. The NMRI SPH method considered rigid body dynamics only. The ABAQUS FEA method presented in Yan et al. (2022c) assumed pinned (point A, Figure A3), fixed (point B, Figure A3) and restricted displacements in x- and y-directions (point C, Fig. 21), respectively. In NRC simulations, the pinned boundary conditions were unavailable due to the use of solid elements. They used fixed boundary conditions at the A and C locations.

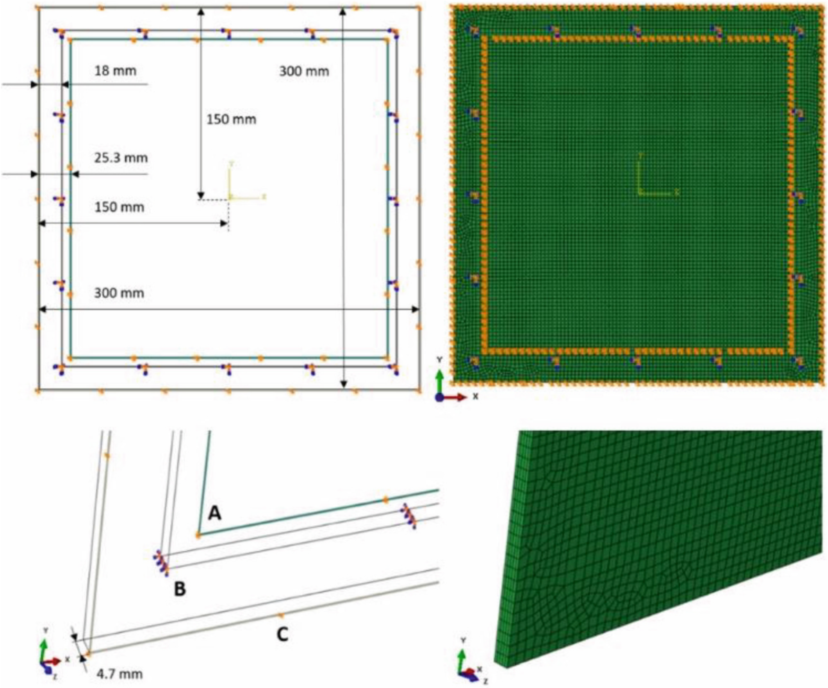

Fig. A3. Three-dimensional plate FE model assuming pinned (point A), fixed (point B) and restricted displacements in x- and y-directions (point C) (Yan et al., 2022c). In NRC simulations, the pinned boundary conditions were unavailable due to the use of solid elements. Hence, they used fixed boundary conditions at the A and C locations.

For NMRI-LSDYNA, the simulation is conducted using the ICFD function of LSDYNA, which is based on the Finite Element Method. The influence of air is not considered in the analysis. Water is treated as an incompressible fluid (Livermore Software Technology Corporation, 2014). For the FFSI analysis, implicit coupling is utilized. The boundary conditions used are precisely the same as those applied in the ABAQUS FEM method. For NMRI–SPH, the WCSPH model (Monaghan, 1994) is developed based on the open-source code DualSPHysics (Domínguez et al., 2022). In the WCSPH model, the influence of air is not considered, and water is modelled using the weakly compressible assumption governed by the equation of state. The Wendland kernel is employed for spatial interpolation. The boundary condition is implemented by directly applying the entry velocity to the rigid plate.

Table 2. Benchmark cases

Case	Benchmark			
	Focus	*Plate model*	*Location*	*Entry velocities*
1	Pressure	Rigid	P1	0.519 m/s, 0.782 m/s, 1.041 m/s
2		Elastic		
3	Impact force	Rigid	Entry point	0.782 m/s
4		Elastic		
5	Strain	Elastic	S1, S2	1.041 m/s
6	Air entrapment	Rigid	Plate bottom	1.041 m/s for impact moment 2. 5 ms 5.833ms 4.833 ms 30.83 ms
7		Elastic		

Table 3. Boundary conditions in fluid domain

Boundary surfaces	Boundary conditions			
	[1]	NRC	NMRI - LSDYNA	NMRI - SPH
Plate	wall	wall	moving body	moving body
Side (box/plate side)	wall	wall	moving body	moving body
Bottom	velocity inlet	velocity inlet	wall (free slip)	wall (free slip)
Top	pressure outlet	pressure outlet	air is not considered	air is not considered
Symmetry (or tank side)	symmetry	velocity inlet	tank side	tank side

Table 4. Summary of modelling assumptions in fluid and structural domains

Method	Material modelling	Structural modelling	Fluid Modelling	Coupling	BC
Yan et al. (2022c)	Isotropic	ABAQUS FEA using 50,660 8-node continuum shell elements (SC8R)	STAR CCM + RANS CFD see Fig. 22	Two-way coupling with morphing	see Fig. 21 and Table 3
NRC	Isotropic	STAR CCM + FEA (8-node) using 92,000 Hexahedral elements	RANS CFD	Two-way coupling with morphing	FEA used fixed boundary conditions at the A and C locations (see Fig. 21 and Table 3)
NMRI LSDYNA	Isotropic	FEA (8-node) using 7,500 Hexahedral elements	Incompressible CFD (Livermore Software Technology Corporation, 2014)	Two-way coupling with morphing	Moving boundary with the predefined boundary velocity (see Table 3)
NMRI SPH	Only Rigid	-	WCSPH (Domínguez et al., 2022)	No coupling	Moving boundary with the predefined boundary velocity (see Table 3)

Comparisons and Discussion

Figure 22 illustrates comparisons of simulations with experimental data in the way of pressure sensor P1 for test cases corresponding to three different impact velocities (0.519, 0.782, 1.041m/s). The left column graphs directly compare results from rigid body simulations, while the right column graphs demonstrate the comparisons when flexible dynamics are considered. In both rigid and flexible domains, the NMRI (LS DYNA) simulations overestimate the experimental and other simulation trends. This could be attributed to the stiffness of the structural dynamic model. Neglecting air influence and assuming incompressible water may make the NMRI (LS DYNA) simulation more sensitive to entry velocity, especially in cases where the body is regarded as rigid. However, for NMRI SPH, although air influence is also not considered, the weakly compressible water model can somewhat mitigate this sensitivity to entry velocity. The differences between simulation peaks and experiments increase with increasing entry velocity. In the rigid domain, the simulation peak values appear larger than experimental peak values at the onset of impact. Overall, the pressure results from the simulations seem to be relatively smoother than the experimental results, where small fluctuations are captured. This could be attributed to the influence of higher-order vibration modes, which were also observed in experiments and in the way of the first two crests of numerical and experimental pressure results depicted by sensor P1, differences of pressure amplitudes indicated that the plate vibrated upwards with larger amplitudes in the way of water entry. The differences between peak values become smaller when comparing hydroelastic CFD results from Yan et al. (2022c) and NRC to experimental results. Figure 23 demonstrates impact force comparisons between simulations and experiments for 0.782 m/s entry velocity when the body is rigid and hydroelastic. Forces rise and decay in the same fashion as pressures. When excluding the LSDYNA simulations, the maximum experimental impact force in the way of the band range seems higher than the STAR CCM + CFD simulations. This could be attributed to uncertainties associated with the entry velocities, e.g., the numerical records of the lowest entry velocity (0.519 m/s) deviated slightly from experimental data, where the vibration frequency was smaller than that measured in the test tank.

The larger pressure in rigid or flexible CFD simulations could be attributed to the boundary conditions, uncertainties in impact velocity and the structural rigidity of the structure. Regarding the latter, it is noted that in CFD simulations, the rigidity of the structure is considered either infinite (for rigid body simulations) or suitably adjusted for hydroelastic simulations while in experiments, the aluminium structure is not physically completely rigid, and the experimental aluminium flange on top of the plate has a broader influencing area (and, therefore, additional rigidity). For example, in the experiments, the additional rigidity from the aluminium flange on top of the plate limited the amplitude of upward vibrations. Therefore, the air trapped under the plate during experiments has been lower. When the entry velocity increases, the air trapped under the plate during pressure peak time increases. The differences observed between experimental and computational results decay as hydroelastic dynamics reach a quasi-steady state.

Air entrapment during impact was recorded by a high-speed imaging camera during experiments. To better understand the air entrapment process, experiments were compared against simulation results. Special focus was attributed to qualitative comparisons of relevance to the volume fraction of air and its distribution on the plate at different time instances. Air entrapment features idealized by experiments and simulations are directly comparable for cells where air occupies over 50%. Figure 25 and Fig. 26 show comparisons of results for the rigid and flexible cases with a water entry velocity of 1.041 m/s. In Fig. 25, experimental results are compared with numerical results from (Yan et al., 2022c) and NRC. Stage (a) represents impact at the start of the water entry when the space under the plate bottom is almost full of air. Stage (b) demonstrates an initial period when the plate enters the water, and most air is still trapped at the centre of the plate (bright white area in the experiments). Simulation results show similar features, namely: (1) the volume fraction of air near the plate central area is nearly 100%, so there is a large area of trapped air in the way of the plate centre; (2) near the plate edge, the volume fraction of air decreases to about 95% as compared to the stage (a). It may be concluded that some air is escaping from the central air pockets towards the edge of the plate. This phenomenon conveys the influence of fluctuating water near the plate edge, as shown in the experimental graph at stage (b). Stage (c) corresponds to the moment after the first pressure peak. The pressure decreases to around 20% of its peak value, and the air volume under the plate decreases. The simulated area of trapped air in the way of the plate central area decreases significantly, and the average volume fraction of air is around 93%. More air is escaping through the edges while the area of fluctuated water is getting larger. The latter is well shown in both experiments and simulations (dark, bubbly area in the experiments and the colour transition from orange to yellow in the simulations). A review of stages (d) and (e) demonstrates that in both experiments and simulations, the air underwater diminishes gradually as we move away from the centre of the plate. In simulations, the average air volume fraction near the plate centre decreases from about 80% at stage (d) to about 55% at stage (e).

Consequently, the percentages of air entrapped in central cells are lower than in stages (b) and (c). It is noted that the simulation method assumed infinite rigidity. In experiments, some local deformations in the way of the plate centre may exist, possibly leading to slightly different levels of air entrapment. However, based on overall comparisons, their influence is not significant.

In Fig. 26, columns display the volume of the fraction of air from experiments and simulations. Notably, the column Wet/Dry displays a version of structural deformations following simulations according to the methodology (Yan et al., 2022c). The structural deformation characteristics are not visible in the hybrid NRC simulation presented in the last column. Stage (a) represents impact at the start of the water entry when the space under the plate bottom is almost full of air. Stages (b) and (c) demonstrated a gradual process whereby the pressure reaches approximately 70% of its first peak. The maximum structural displacements are 3.4 mm during stage (b) and 3.9 mm during stage (c). The entrapped air is in the way of the centre area of the deformed plate (white and dark red areas in the experiment and simulations, respectively). Stage (d) demonstrates the moment the plate vibrates vertically from its crest to its neutral position. Stage (e) demonstrates the moment the plate vibrates from the neutral axis to the bottom. At stage (d), the maximum structural displacement is 2.6 mm. During deformation, air is pushed out from the central area, forming a ring-shaped distribution. The phenomenon is observed in both experiments and simulations (see the dark, bubbly ring in the experiment and the dark red ring in the simulations at stage (d)). The latter observation suggests that the air volume fraction with an average value of 0.9 is distributed partially in the centre and partially as a ring shape between the plate centre and edge. After one vibration cycle, air and water mix and lumpy air bubbles form. The simulated area is slightly wider than the observed in experiments (Fig. 24).

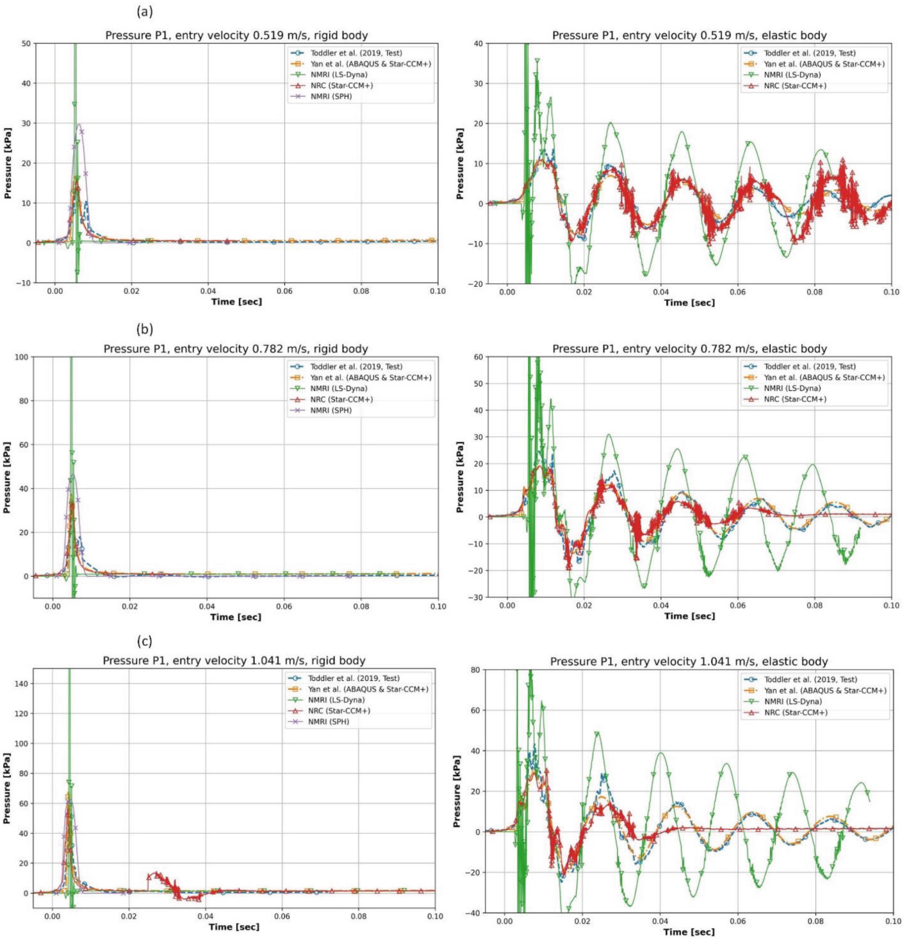

Fig. A4. Comparison of rigid versus hydroelastic responses in pressure sensor P1 at different entry velocities.

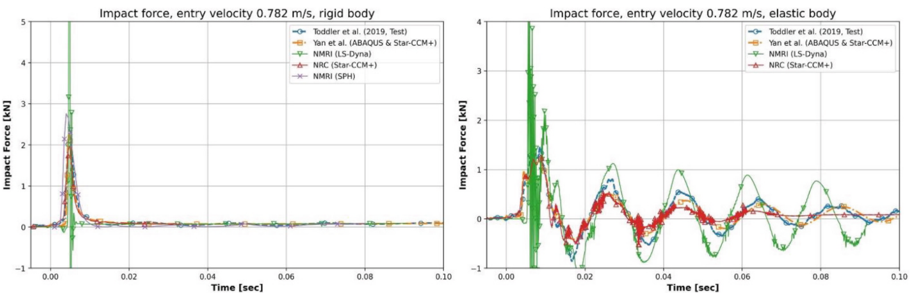

Fig. A5. Rigid versus hydroelastic impact forces at entry velocity 0.782 m/s

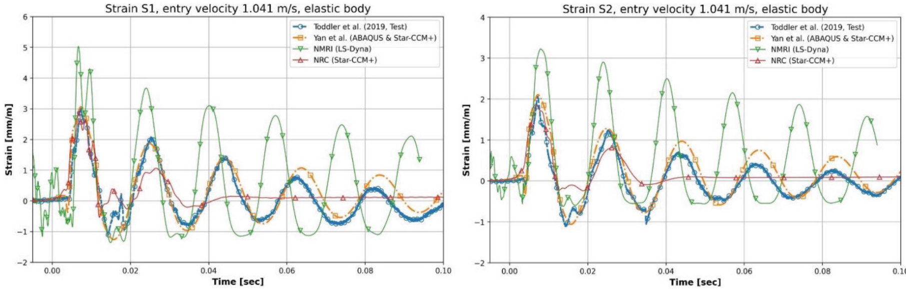

Fig. A6. Strains at sensors S1 and S2 when hydroelastic impact is considered at entry velocity 1.041 m/s.

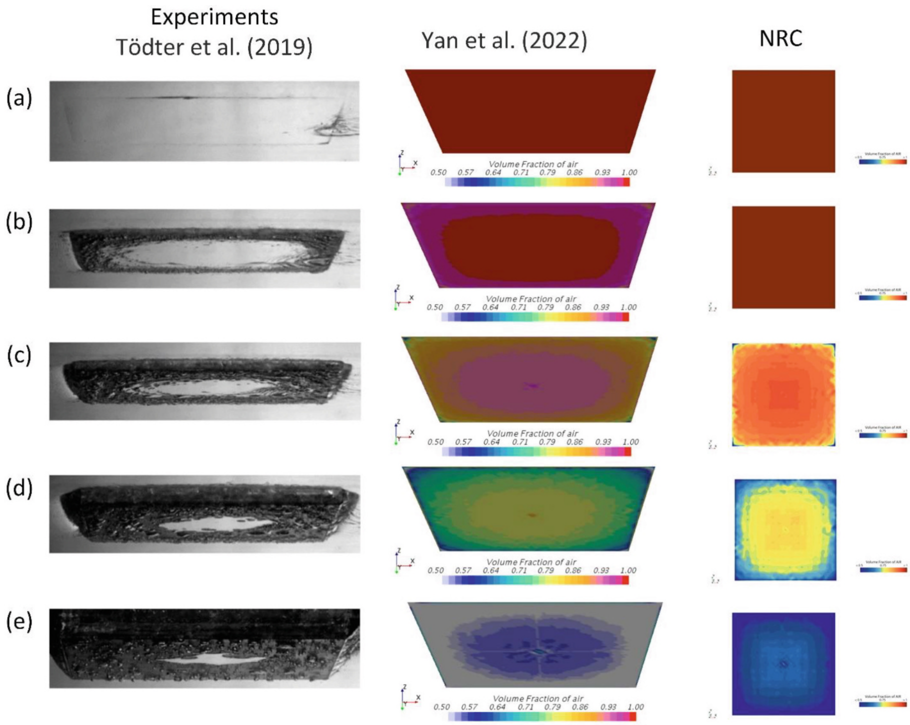

Fig. A7. Air entrapment underneath the rigid plate bottom at different time instants (t) of the water entry (1.041 m/s) for (a) impact, (b) $t = 2.500$ ms, (c) $t = 5.833$ ms, (d) $t = 10.832$ ms, (e) $t = 30.830$ ms. B: air entrapment in CFD simulation.

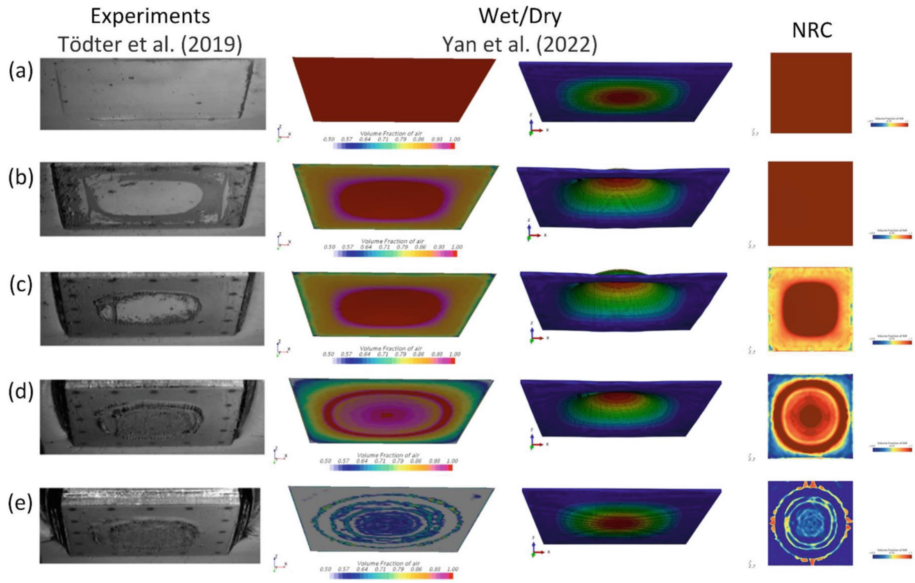

Fig. A8. Air entrapment underneath the elastic plate bottom at different time instants (t) of water entry (1.041 m/s) for (a) impact, (b) $t = 5.500$ ms, (c) $t = 5.833$ ms, (d) $t = 10.832$ ms, (e) $t = 30.830$ ms. Simulations in columns 2 and 4 display the air entrapment in FFSI simulation. The ABAQUS structural dynamic displacement depicted in column 3 assumes a deformation scale factor of 15.

Conclusions

Numerical simulations of flat plate impacts were carried out to analyze the capability of the applied methods. Computational Fluid Mechanics (CFD) and Smoothed Particle Hydrodynamics (SPH) methods were used to model rigid impacts. A two-way coupled Flexible Fluid-Structure Interaction (FFSI) approach was implemented, using ABAQUS for the structural domain and STAR CCM + for the fluid domain (Yan et al., 2022c). A hybrid STAR CCM + method for the fluid domain (Sitek et al., 2021) was employed, and an incompressible fluid solver implemented in LS DYNA (Livermore Software Technology Corporation, 2014) was applied for hydroelastic water impacts. The modelled test bodies had the exact dimensions and properties as those experimentally investigated by (Tödter et al., 2019). Time histories of simulations and experiments attained similar peak loads, excluding LS DYNA FFSI, that appeared significantly stiffer.

The simulated void fraction underneath the impacting plates compared favourably to cavities experimentally captured by high-speed imaging. The uncertainties associated with the peaks of pressures, forces and strains are considered to reflect the differences in assumptions between numerical simulations and experiments. Also, the simulated peak loads seem to be affected by high-frequency vibration modes and their interactions with boundary conditions, highlighting sensitivity to modelling details.

It is recommended that future work on uncertainty modelling prediction is assessed along the lines of the American Society of Mechanical Engineers (ASME) standard for Verification and Validation (V&V) (ASME, 2009. As part of this process, well-documented experiments and close cooperation between experimentalists and simulation engineers for validation are highly recommended.

ASME. (2009). Standard for verification and validation in computational fluid dynamics and heat transfer: ASME V&V 20, The American Society of Mechanical Engineers. Retrieved from https://www.asme.org/codes-standards/find-codes-standards

Domínguez, J. M., Fourtakas, G., Altomare, C., Canelas, R. B., Tafuni, A., García-Feal, O., et al. (2022). DualSPHysics: from fluid dynamics to multiphysics problems. Computational Particle Mechanics, 9(5), pp. 867–895. Retrieved from https://doi.org/10.1007/s40571-021-00404-2

Livermore Software Technology Corporation. (2014). ICFD theory manual: Incompressible fluid solver in LS-DYNA. Retrieved from https://ftp.lstc.com/anonymous/outgoing/inaki/docs/pdf_icfd/ICFD_theory.pdf

Monaghan, J. J. (1994). Simulating Free Surface Flows with SPH. Journal of Computational Physics, 110(2), pp. 399–406. Retrieved from https://www.sciencedirect.com/science/article/pii/S0021999184710345

Sitek, M., Bojanowski, C., Bergeron, A., Licht, J. (2021). Involute Working Group – FSI Analysis of Fuel Plates Using Finite Volume and Finite Element Methods. United States. Retrieved from https://www.osti.gov/biblio/1845461

Tavakoli, S., Zhang, M., Kondratenko, A. A., Hirdaris, S. (2024). A review on the hydrodynamics of planing hulls. Ocean Eng. 303.

Tödter, S., el Moctar, O., Neugebauer, J., Schellin, T. E. (2019). Experimentally Measured Hydroelastic Effects on Impact-Induced Loads During Flat Water Entry and Related Uncertainties. Journal of Offshore Mechanics and Arctic Engineering, 142(1). Retrieved from https://doi.org/10.1115/1.4044632

Yan, D., Mikkola, T., Lakshmynarayanana, A., Tödter, S., Schellin, T. E., Neugebauer, J., et al. (2022). A study into the FSI modelling of flat plate water entry and related uncertainties. Marine Struct. 86. Retrieved August 29, 2023

References

Abbasnia, A., Guedes Soares, C.: OpenMP parallelism in computations of three-dimensional potential numerical wave tank for fully nonlinear simulation of wave-body interaction using NURBS. Eng. Anal. Boundary Elem. **117**, 321–331 (2020)

Abbasnia, A., Karimirad, M., Friel, D., Whittaker, T.: Fully nonlinear dynamics of floating solar platform with twin hull by tubular floaters in ocean waves. Ocean Eng. **257** (2022)

Abbasnia, A., Kosleck, S., Buhr, E., Lutz, M., Adam, F.: Volumetric design for hydrodynamic response of modularized lightweight TLP structures under irregular waves (2024a)

Abbasnia, A., Rezanejad, K., Guedes Soares, C.: Adaptive fully nonlinear potential model for the free surface under compressible air pressure of oscillating water column devices. Eng. Anal. Boundary Elem. **133**, 153–164 (2021)

Abbasnia, A., Sutulo, S., Soares, C.G.: Frequency-domain 3D computer program for predicting motions and loads on a ship in regular waves. J. Mar. Sci. Appl. **23**(1), 64–73 (2024)

Abdelwahab, H.S., Soares, C.G.: Experimental uncertainty of a physical model of a tanker moored to a terminal in a port. Marine Struct. **87** (2023)

Agarwal, S., Sriram, V., Murali, K.: Three-dimensional coupling between Boussinesq (FEM) and Navier–Stokes (particle based) models for wave structure interaction. Ocean Eng. **263** (2022)

Agarwal, S., Sriram, V., Yan, S., Murali, K.: Improvements in MLPG formulation for 3D wave interaction with fixed structures. Comput. Fluids **218** (2021)

Ahani, A., Abrahamsen, B.C., Greco, M.: Experimental analysis of high and steep wave impacts and related hydroelastic effects relevant for offshore structures in steel (2022). https://ntnuopen.ntnu.no/ntnu-xmlui/handle/11250/3050174. Accessed 4 Sept 2023

Ahn, Y.: Sloshing loads estimation using a genetic programming. In: Proceedings of the Thirty-Third International Ocean and Polar Engineering Conference, Melbourne (2023)

Ahn, Y., et al.: Analyzing experimental data of 6-dof motions and sloshing impacts in lng carriers. In: Proceedings of the ASME 2024 43rd International Conference on Ocean, Offshore and Arctic Engineering, Singapore (2024)

Alexandru, I., et al.: Comparison of experimental and numerical impact loads on ship-like sections. Adv. Marine Struct. 339–349 (2007)

Aliyar, S., Ducrozet, G., Bouscasse, B., Venkatachalam, S., Ferrant, P.: Efficiency and accuracy of the domain and functional decomposition strategies for the wave-structure interaction problem. Ocean Eng. **266** (2022)

Alkhabbaz, A., et al.: The aero-hydrodynamic interference impact on the NREL 5-MW floating wind turbine experiencing surge motion. Ocean Eng. **295** (2024)

AlMashan, N., Neelamani, S., Al-Houti, D.: Experimental investigations on wave impact pressures under the deck and global wave forces and moments on offshore jacket platform for partial and full green water conditions. Ocean Eng. **234** (2021)

Amaechi, C.V., Wang, F., Ye, J.: Numerical studies on CALM buoy motion responses and the effect of buoy geometry cum skirt dimensions with its hydrodynamic waves-current interactions. Ocean Eng. **244** (2022)

Amini-Afshar, M., Bingham, H.B.: Added resistance using Salvesen–Tuck–Faltinsen strip theory and the Kochin function. Appl. Ocean Res. **106** (2021)

Amouzadrad, P., Mohapatra, S.C., Guedes Soares, C.: Hydroelastic response to the effect of current loads on floating flexible offshore platform. J. Marine Sci. Eng. **11**(2) (2023)

Ao, Y., Li, Y., Gong, J., Li, S.: An artificial intelligence-aided design (AIAD) of ship hull structures. J. Ocean Eng. Sci. **8**(1), 15–32 (2023)

API. API Recommended Practice 2A-WSD (2014)

Arya, T., Ranjan Behera, M.: Numerical Investigation Of A Spar Type Floating Offshore Wind Turbine Platform Under Extreme Waves (2023). http://asmedigitalcollection.asme.org/OMAE/proceedings-pdf/IOWTC2023/87578/V001T01A013/7234398/v001t01a013-iowtc2023-119363.pdf

Asim, T., Islam, S.Z., Hemmati, A., Khalid, M.S.U: A review of recent advancements in offshore wind turbine technology. Energies **15**(2) (2022)

ASME. Standard for verification and validation in computational fluid dynamics and heat transfer: ASME V&V 20. The American Society of Mechanical Engineers (2009). https://www.asme.org/codes-standards/find-codes-standards

Audiffren, C., Nugue, J., Marcer, R., Couty, N., Laurent, T.: Simulation of liquid hydrogen jet impacts on a corrugated membrane. In: Proceedings of the Thirty-Fourth International Ocean and Polar Engineering Conference. Rhodes (2024)

Aursand, M., Haagensen, P.J., Skallerud, B.H.: Remaining fatigue life assessment of corroded mooring chains using crack growth modelling. Marine Struct. **90** (2023)

Aydın, Ç., Ünal, U.O., Sarıöz, K.: Computation of environmental loads towards an accurate dynamic positioning capability analysis. Ocean Eng. **243**, 110201 (2022). Accessed 18 Oct 2024

Bandizadeh Sharif, M., Ghassemi, H., He, G., Karimirad, M.: A review of the flow-induced vibrations (FIV) in marine circular cylinder (MCC) fitted with various suppression devices. Ocean Eng. **289**(P1), 116261 (2023). https://doi.org/10.1016/j.oceaneng.2023.116261

Bardazzi, A., Lugni, C., Faltinsen, O.M., Durante, D., Colagrossi, A.: Different scenarios in sloshing flows near the critical filling depth. J. Fluid Mech. **984**, A73 (2024)

Barooni, M., Nezhad, S.K., Ali, N.A., Ashuri, T., Sogut, D.V.: Numerical study of ice-induced loads and dynamic response analysis for floating offshore wind turbines. Marine Struct. **86**(September), 103300 (2022). https://doi.org/10.1016/j.marstruc.2022.103300

El Beshbichi, O., Xing, Y., Ong, M.C.: Comparative dynamic analysis of two-rotor wind turbine on spar-type, semi-submersible, and tension-leg floating platforms. Ocean Eng. **266**, 112926 (2022). https://www.sciencedirect.com/science/article/pii/S0029801822022090?pes=vor. Accessed 22 Feb 2023

Bitner-Gregersen, EM., et al.: Uncertainties in long-term wave modelling. Marine Struct. **84** (2022)

Böhm, A.M., von Bock und Polach, R.U.F., Herrnring, H., Ehlers, S.: The measurement accuracy of instrumented ship structures under local ice loads using strain gauges. Marine Struct. **76** (2021)

Bonci, M., de Jong, P.: High-speed RHIB seakeeping analysis using non-linear time domain simulations and systematic hull parametrization. In: Proceedings of the 13th Symposium on High Speed Marine Vehicles (2023)

Buljac, A., Kozmar, H., Yang, W., Kareem, A.: Concurrent wind, wave and current loads on a monopile-supported offshore wind turbine. Eng. Struct. **255** (2022)

Cai, J., Ding, S., Zhang, Q., Liu, R., Zeng, D., Zhou, L.: Broken ice circumferential crack estimation via image techniques. Ocean Eng. **259** (2022)

Califano, A., Berthelsen, P.A., Magalhaes Duque Da Fonseca, N.M.: Effect of body motion on the wave loads computed with CFD on the INO-WINDMOOR floater. In: Journal of Physics: Conference Series. Institute of Physics (2023)

Caputano, E., Goodwin, P.: Sloshing and free surface correction in hydrodynamic analyses. In: Proceedings of the Thirty-third (2023) International Ocean and Polar Engineering Conference, Ottawa, pp. 2667–2673 (2023)

Carapellese, F., Pasta, E., Paduano, B., Faedo, N., Mattiazzo, G.: Intuitive LTI energy-maximising control for multi-degree of freedom wave energy converters: the PeWEC case. Ocean Eng. 256 (2022)

de Carvalho, A. van L.B., Campello, E.M.B., Franzini, G.R., Skaf, K.J.: An assessment of mooring systems' forces of ships berthed at dolphins. Ocean Eng. **253**(March), 111090 (2022). https://doi.org/10.1016/j.oceaneng.2022.111090

Celik, I.B., Ghia, U., Roache, P.J., Freitas, C.J., Coleman, H., Raad, P.E.: Procedure for estimation and reporting of uncertainty due to discretization in CFD applications. J. Fluids Eng. Trans. ASME **130**(7), 0780011–0780014 (2008)

Chen, C., Ma, Y., Fan, T.: Review of model experimental methods focusing on aerodynamic simulation of floating offshore wind turbines. Renew. Sustain. Energy Rev. **157**(May 2021), 112036 (2022a). https://doi.org/10.1016/j.rser.2021.112036

Chen, D., Feng, X., Hou, C., Chen, J.F.: A coupled frequency and time domain approach for hydroelastic analysis of very large floating structures under focused wave groups. Ocean Eng. **255**, 111393 (2022b)

Chen, H., Hall, M.: CFD simulation of floating body motion with mooring dynamics: coupling MoorDyn with OpenFOAM. Appl. Ocean Res. **124** (2022)

Chen, J., Milne, I., Taylor, P.H., Gunawan, D., Zhao, W.: Forward prediction of surface wave elevations and motions of offshore floating structures using a data-driven model. Ocean Eng. **281**, 114680 (2023a)

Chen, J.S., et al.: VHF radar observations of sea surface in the Northern Taiwan strait. J. Atmos. Oceanic Tech. **36**(2), 297–315 (2019)

Chen, J., Zhang, J., Wang, G., Zhang, Q., Guo, J., Sun, X.: Numerical simulation of the wave dissipation performance of floating box-type breakwaters under long-period waves. Ocean Eng. **266** (2022c)

Chen, P., Zhang, J.: Study on the liquefaction mechanism of shipping iron ore by adopting perspective materials. In: Proceedings of the Thirty-Fourth International Ocean and Polar Engineering Conference, Rhodes, pp. 2704–2710 (2024)

Chen, R., Huang, W., Chen, X., Kang, M.: Prediction of ice resistance of icebreaker during continuous icebreaking. Chin. J. Ship Res. **16**(5), pp. 101–108+120 (2021a)

Chen, S., et al.: Design, dynamic modeling and wave basin verification of a hybrid wave–current energy converter. Appl. Energy **321** (2022d)

Chen, S., Zou, B., Han, C., Yan, S.: Comparative study on added resistance and seakeeping performance of x-bow and wave-piercing monohull in regular head waves. J. Marine Sci. Eng. **10**(6) (2022e)

Chen, X., Xu, G., Chen, Z., Zhu, L., Cai, S.: A study of the interaction between depression internal solitary waves and submerged floating tunnels in stratified fluids. Appl. Ocean Res. **132** (2023b)

Chen, Y., Meringolo, D.D., Liu, Y.: SPH study of wave force on simplified superstructure of open-type sea access road. Ocean Eng. **249** (2022f)

Chen, Y., Liu, Y., Meringolo, D.D., Ming Hu, J.: Study on the hydrodynamics of a twin floating breakwater by using SPH method. Coast. Eng. **179** (2023c)

Chen, Y., Zhang, S., Chen, W.K., Magee, A.: Design, construction and testing of a fully elastic ship model for investigating hydro-elastic responses of container ships. Mar. Struct. **98**, 103663 (2024)

Chen, Z., He, Y., Ren, Y., Liu, Y.: Analysis and realization of the influence of sea ice flexural strength on ice resistance in numerical simulation of icebreaking by icebreaker. Ocean Eng. **273**(February), 113995 (2023d). https://doi.org/10.1016/j.oceaneng.2023.113995

Chen, Z., Zhang, C., Zhao, C., Chen, X., Liu, H.: Shipboard coherent microwave radar, pp. 1–5 (2021b)

Cheng, H., Li, L., Ong, M.C., Aarsæther, K.G., Sim, J.: Effects of mooring line breakage on dynamic responses of grid moored fish farms under pure current conditions. Ocean Eng. **237** (2021)

Cheng, Y., et al.: Experimental and numerical analysis of a hybrid WEC-breakwater system combining an oscillating water column and an oscillating buoy. Renew. Sustain. Energy Rev. **169** (2022a)

Cheng, Y., et al.: Experimental and numerical investigation of WEC-type floating breakwaters: a single-pontoon oscillating buoy and a dual-pontoon oscillating water column. Coast. Eng. **177** (2022b)

Choi, S.M., Park, C.D., Cho, S.H., Lim, B.J.: Effects of various inlet angle of wind and wave loads on floating photovoltaic system considering stress distributions. J. Clean. Prod. **387** (2023)

Chueh, C.J., Chien, C.H., Lin, C., Lin, T.Y., Chiang, M.H.: Dynamic co-simulation analysis and control of an IEA 15 MW offshore floating semi-submersible wind turbine under taiwan offshore-wind-farm conditions of wind and wave. J. Marine Sci. Eng. **11**(1) (2023)

Class, N.K.: Investigation report on structural safety of large container ships (2014)

Clément, C., Bozonnet, P., Vinay, G., Pagnier, P., Nadal, A.B., Réveillon, J.: Evaluation of Morison approach with CFD modelling on a surface-piercing cylinder towards the investigation of FOWT Hydrodynamics. Ocean Eng. **251** (2022)

Cong, P., Ning, D., Teng, B.: Enhancement of the energy capture performance of oscillating water column (OWC) devices using multi-chamber multi-turbine (MCMT) technology. Energy Convers. Manage. **322** (2024)

Cong, P., Teng, B., Bai, W.: Second-order wave run-up on a vertical cylinder adjacent to a plane wall based on the application of quadratic transfer function in bi-directional waves. Marine Struct. **76** (2021)

da Cruz, D.M., Penaquioni, A., Zangalli, L.B., Bastos, M.B., Bastos, I.N., da Silva, A.L.N.: Non-destructive testing of high-tenacity polyester sub-ropes for mooring systems. Appl. Ocean Res. **134** (2023)

Cui, H., Turan, O., Sayer, P.: Learning-based ship design optimization approach. CAD Comput. Aided Design **44**(3), 186–195 (2012)

Cui, J., Chen, X., Sun, P.N., Li, M.Y.: Numerical investigation on the hydrodynamic behavior of a floating breakwater with moon pool through a coupling SPH model. Ocean Eng. **248** (2022)

Dai, J., Abrahamsen, B.C., Viuff, T., Leira, B.J.: Effect of wave-current interaction on a long fjord-crossing floating pontoon bridge. Eng. Struct. **266**, 114549 (2022)

Dao, M.H., et al.: Wind tunnel and CFD studies of wind loadings on topsides of offshore structures. Ocean Eng. **285**(P1), 115310 (2023). https://doi.org/10.1016/j.oceaneng.2023.115310

Deng, R., Song, Z., Ren, H., Li, H., Wu, T.: Investigation on the effect of container configurations and forecastle fairings on wind resistance and aerodynamic performance of large container ships. Eng. Appl. Comput. Fluid Mech. **16**(1), 1279–1304 (2022). https://doi.org/10.1080/19942060.2022.2086177

Deng, S., Liu, Y., Ning, D.: Fully coupled aero-hydrodynamic modelling of floating offshore wind turbines in nonlinear waves using a direct time-domain approach. Renew. Energy **216** (2023a)

Deng, Y., Li, H., Wang, Z.:. A numerical study of wave impacts on a semi-submersible (2023b). http://asmedigitalcollection.asme.org/OMAE/proceedings-pdf/OMAE2023/86878/V005T06A052/7041067/v005t06a052-omae2023-106568.pdf

Depalo, F., Wang, S., Xu, S., Guedes Soares, C., Yang, S.H., Ringsberg, J.W.: Effects of dynamic axial stiffness of elastic moorings for a wave energy converter. Ocean Eng. **251** (2022)

Derbanne, Q., Storhaug, G., Shigunov, V., Xie, G., Zheng, G.: Rule formulation of vertical hull girder wave loads based on direct computation. In: PRADS 2016 - Proceedings of the 13th International Symposium on PRActical Design of Ships and Other Floating Structures (2016)

Diez, M., et al.: Experimental and computational fluid-structure interaction analysis and optimization of deep-V planing-hull grillage panels subject to slamming loads – part I: regular waves. Marine Struct. **85**, 103256 (2022). https://www.sciencedirect.com/science/article/pii/S0951833922000958

DNV. Fatigue and ultimate strength assessment of container ships including whipping and springing (2015)

DNV-GL. Fatigue Assessment of Ship Structures (DNVGL-CG-0129) (2015)

DNV-GL. Offshore Technical Guidance Prediction of air gap for column stabilised units (2019)

Dombre, E., Harris, J.C., Benoit, M., Violeau, D., Peyrard, C.: A 3D parallel boundary element method on unstructured triangular grids for fully nonlinear wave-body interactions. Ocean Eng. **171**, 505–518 (2019)

Domínguez, J.M., et al.: DualSPHysics: from fluid dynamics to multiphysics problems. Comput. Part. Mech. **9**(5), 867–895 (2022). https://doi.org/10.1007/s40571-021-00404-2

Dong, G., Yao, C., Yu, J., Sun, X., Feng, D.: A frequency domain hybrid Green function method for seakeeping and added resistance performance of ships advancing in waves. Eng. Anal. Bound. Elem. **168** (2024)

Du, Z., et al.: An experimental investigation on vortex-induced motion (VIM) of a tension leg platform in irregular waves combined with a uniform flow. Appl. Ocean Res. **123**(December 2021), 103185 (2022). https://doi.org/10.1016/j.apor.2022.103185

Duan, F., Ma, N., Gu, X.C., Zhou, Y.H., Wang, S.M.: A fast time domain method for predicting of motion and excessive acceleration of a shallow draft ship in beam waves. Ocean Eng. **262** (2022)

Duan, F., Ma, N., Gu, X., Zhou, Y.: An improved method for predicting roll damping and excessive acceleration for a ship with moonpool based on computational fluid dynamics method. J. Offshore mech. Arctic Eng.-Trans. ASME **145**(5) (2023)

Dutta, D., Bihs, H., Afzal, M.S.: Computational fluid dynamics modelling of hydrodynamic characteristics of oscillatory flow past a square cylinder using the level set method. Ocean Eng. **253** (2022)

Edwards, E.C., Holcombe, A., Brown, S., Ransley, E., Hann, M., Greaves, D.: Trends in floating offshore wind platforms: a review of early-stage devices. Renew. Sustain. Energy Rev. **193**, 114271 (2024). https://linkinghub.elsevier.com/retrieve/pii/S1364032123011292

van der Eijk, M., Wellens, P.: An efficient pressure-based multiphase finite volume method for interaction between compressible aerated water and moving bodies. J. Comput. Phys. **514**(November 2023), 113167 (2024). https://doi.org/10.1016/j.jcp.2024.113167

El-Shahat, S.A., Li, G., Fu, L.: Investigation of wave–current interaction for a tidal current turbine. Energy **227** (2021)

Engelbrecht, M., Bekker, A.: A discomfort threshold for impulsive whole-body vibration on a slamming-prone vessel. Appl. Ergon. **109** (2023)

Engström, J., Shahroozi, Z., Katsidoniotaki, E., Stavropoulou, C., Johannesson, P., Göteman, M.: Offshore measurements and numerical validation of the mooring forces on a 1:5 scale buoy. J. Marine Sci. Eng. **11**(1) (2023)

Erceg, S., Erceg, B., von Bock und Polach, F., Ehlers, S.: A simulation approach for local ice loads on ship structures in level ice. Marine Struct. **81**(February 2021), 1–15 (2022)

van Essen, S.M., Scharnke, J., Seyffert, H.C.: Required test durations for converged short-term wave and impact extreme value statistics — part 1: ferry dataset. Mar. Struct. **90**, 103410 (2023)

Ezeta, R., Kimmoun, L., Brosset, L.: Influence of ullage pressures on wave impacts induced by solitary waves in a flume tank, in: ISOPE (Ed.), Proceedings of the Thirty-Third International Ocean and Polar Engineering Conference (2023)

Faltilsen, R., Aarsnes, O.M., Zhao, J.V.: Water entry of arbitrary two dimensional sections with and without flow separation. In: Symposium on Naval Hydrodynamics, pp. 408–423 (1996)

Fan, Q., Xu, Y., Xie, Q., Zhang, M., Ren, H., Sun, T.: Investigation of the dynamic response of a floating wind-aquaculture platform under the combined actions of wind, waves and current. J. Ocean Eng. Sci. (2023)

Fan, Y.L., Jain, U., van der Meer, D.: Air-cushioning below an impacting wave-structured disk: free-surface deformation and slamming load. Phys. Rev. Fluids (2024)

Farsi, M., Ghadimi, P.: Effect of flat deck on catamaran water entry through smoothed particle hydrodynamics. Proc. Inst. Mech. Eng. Part M: J. Eng. Maritime Environ. **230**(2), 267–280 (2016). https://doi.org/10.1177/1475090214563960

Ferri, G., Marino, E., Bruschi, N., Borri, C.: Platform and mooring system optimization of a 10 MW semisubmersible offshore wind turbine. Renew. Energy **182**, 1152–1170 (2022)

Fonseca de Carvalho e Silva, D., Gouveia Telles de Menezes, F., Schmidt, D., Cardozo de Mello, P.: Slamming effects on fpso balconies: numerical and experimental analysis of alternative configurations for impact attenuation (2023). http://asmedigitalcollection.asme.org/OMAE/proceedings-pdf/OMAE2023/86878/V005T06A010/7041100/v005t06a010-omae2023-105066.pdf

Fonseca, N., Nybø, S., Rodrigues, J.M., Gallego, A., Garrido, C.: Identification of wave drift forces on a floating wind turbine sub-structure with heave plates and comparison with predictions. In: Proceedings of the International Conference on Offshore Mechanics and Arctic Engineering - OMAE, p. 8 (2022). /OMAE/proceedings-abstract/OMAE2022/85932/1147962. Accessed 19 Jan 2023

Føre, H.M., Endresen, P.C., Bjelland, H.V.: Load coefficients and dimensions of raschel knitted netting materials in fish farms. J. Offshore Mech. Arctic Eng. **144**(4) (2022)

Fujarra, A.L.C., Leal, A.P., Carnier, R.M., Gonçalves, R.T., Suzuki, H.: Validation of a low-cost IMU for flow-induced vibration tracking in offshore systems. J. Braz. Soc. Mech. Sci. Eng. **45**(7), 1–17 (2023). https://doi.org/10.1007/s40430-023-04275-x

Gadelho, J.F.M., Guedes Soares, C.: CFD study of a dual chamber floating oscillating water column device. Ocean Eng. **261** (2022)

Gaidai, O., Fu, S., Xing, Y.: Novel reliability method for multidimensional nonlinear dynamic systems. Marine Struct. **86** (2022)

Gao, S., Cong, P., Teng, B.: Effect of incident wave angle to gap resonance between two fixed barges. Ocean Eng. **257** (2022)

Gebrezgabir, S., Holloway, D.S., Ali-Lavroff, J.: Slam and wave load response reconstruction in high speed catamarans using transmissibility on full scale sea trials. Ocean Eng. **271** (2023)

Gemilang, G.M., Reed, P.A.S., Sobey, A.J.: Low-cycle fatigue assessment of offshore mooring chains under service loading. Marine Struct. **76**, 102892 (2021). https://linkinghub.elsevier.com/retrieve/pii/S0951833920301854

George, A., Cho, I.H., Kim, M.H.: Optimal design of a u-shaped oscillating water column device using an artificial neural network model. Processes **9**(8) (2021)

Ghadirian, A., Vested, M.H., Carstensen, S., Christiensen, E.D., Bredmose, H.: Wave-current interaction effects on waves and their loads on a vertical cylinder. Coastal Eng. **165** (2021)

Ghamari, I., Mahmoudi, H.R., Hajivand, A., Seif, M.S.: Ship roll analysis using CFD-derived roll damping: numerical and experimental study. J. Marine Sci. Appl. **21**(1), 67–79 (2022)

Gilbert, C., Gilber, J., Javaherian, J.: Water entry of a flexible wedge: how flexural rigidity influences spray root and pressure wave propagation. Phys. Rev. Fluids **8**(9) (2023)

Gonçalves, R.T., Malta, E.B., Simos, A.N., Hirabayashi, S., Suzuki, H.: Influence of heave plate on the flow-induced motions of a floating offshore wind turbine. J. Offshore Mech. Arctic Eng. **145**(3) (2023a). https://doi.org/10.1115/1.4056345. Accessed 18 Oct 2024

Gonçalves, R.T., Marques, M.A., Da Silva, L.S.P., Hirabayashi, S., Suzuki, H.: Experimental study of the draft on the flow-induced motions (FIM) of a semi-submersible platform with four square columns. In: Proceedings of the International Conference on Offshore Mechanics and Arctic Engineering - OMAE. American Society of Mechanical Engineers Digital Collection (2023b). https://doi.org/10.1115/OMAE2023-102704. Accessed 18 Oct 2024

Gong, J., Li, Y., Cui, M., Yan, S., Ma, Q.: Study on the surf-riding and broaching of trimaran in oblique stern waves. Ocean Eng. **266**(4) (2022)

Gong, J., Yan, S., Ma, Q., Li, Y.: Numerical simulation of fixed and moving cylinders in focusing wave by a hybrid method. Int. J. Offshore Polar Eng. **31**(1), 102–111 (2021)

Gözcü, O., Kontos, S., Bredmose, H.: Dynamics of two floating wind turbines with shared anchor and mooring lines. In: Journal of Physics: Conference Series. Institute of Physics (2022)

Grammatikopoulos, A.: A review of physical flexible ship models used for hydroelastic experiments. Marine Struct. **90**(February) (2023)

Gu, N., Liang, D., Zhou, X., Ren, H.: A CFD-FEA method for hydroelastic analysis of floating structures. J. Marine Sci. Eng. **11**(4) (2023)

Gu, Y., Zhou, L., Ding, S., Tan, X., Gao, J., Zhang, M.: Numerical simulation of ship maneuverability in level ice considering ice crushing failure. Ocean Eng. **251**(March), 111110 (2022). https://doi.org/10.1016/j.oceaneng.2022.111110

Gubesch, E., Abdussamie, N., Penesis, I., Chin, C.: Maximising the hydrodynamic performance of offshore oscillating water column wave energy converters. Appl. Energy **308**, 118304 (2022a). Accessed 4 Sept 2023

Gubesch, E., Abdussamie, N., Penesis, I., Chin, C.: Effects of mooring configurations on the hydrodynamic performance of a floating offshore oscillating water column wave energy converter. Renew. Sustain. Energy Rev. **166** (2022b)

Guo, C., Zhang, C., Wang, C., Wang, C.: Experimental Study On IRV ramming artificial model ice. J. Marine Sci. Eng. **11**(10) (2023)

Guo, W., Zou, J., He, M., Mao, H., Liu, Y.: Comparison of hydrodynamic performance of floating breakwater with taut, slack, and hybrid mooring systems: an SPH-based preliminary investigation. Ocean Eng. **258** (2022)

Guo, X., Zhang, X., Tian, X., Li, X., Lu, W.: Predicting heave and surge motions of a semi-submersible with neural networks. Appl. Ocean Res. **112** (2021a)

Guo, Y., Xiao, L., Wei, H., Li, X., Li, L., Deng, Y.: Classification and comparison of wave impact modes on semi-submersibles. China Ocean Eng. **35**(2), 161–175 (2021b)

Ha, Y.J., Nam, B.W., Kim, K.H., Hong, S.Y.: Numerical study for slamming loads on the bow of a ship-type FPSO model under breaking waves. Ocean Eng. **299** (2024)
Hallak, T.S., Teixeira, Â.P., Guedes Soares, C.: Epistemic uncertainties on the estimation of minimum air gap for semi-submersible platforms. Marine Struct. **85** (2022)
Han, D., Paik, K.-J., Jeong, S.-Y., Choung, J.: Prediction of the ice resistance of icebreakers using explicit finite element analyses with a real-time load control technique. Ocean Eng. **240** (2021)
Han, X., Dong, S.: Interaction between regular waves and floating breakwater with protruding plates: Laboratory experiments and SPH simulations. Ocean Eng. **287** (2023)
Han, Y., Zhu, X., Zhou, L.: Numerical simulation of multi-tug towing of a gravity-based structure in broken sea ice. Ocean Eng. **261** (2022)
Hao, L., Pan, Z.: Translating and pulsating Green function with an ice cover. J. Eng. Math. **134**(1) (2022)
He, M., Liang, D., Ren, B., Li, J., Shao, S.: Wave interactions with multi-float structures: SPH model, experimental validation, and parametric study. Coast. Eng. **184** (2023)
Van He, N., Van Hien, N., Bui, N.T.: Analyis of aerodynamic performance of passenger ship with different frontal accommodations using CFD. Ocean Eng. **270**(January), 113622 (2023). https://doi.org/10.1016/j.oceaneng.2023.113622
He, S., Chen, X., Kong, S., Ji, S.: Measurement and identification of ice loads on hull structures in far field based on dynamic effects. Chin. J. Ship Res. **16**(5), 54–63 (2021)
He, W., Xie, L., Wang, S., Hu, Z., Xie, D., Wang, C.: Preliminary assessment of the mooring fatigue performance of a semi-submersible platform in time-domain utilizing fracture mechanics-based approach. Appl. Ocean Res. **129** (2022)
Hernández-Fontes, J.V., Mendoza, E., Hernández, I.D., Silva, R.: A detailed description of flow-deck interaction in consecutive green water events. J. Offshore Mech. Arctic Eng. **143**(4) (2021)
Herrnring, H., Kubiczek, J.M., Ehlers, S.: The ice extrusion test: a novel test setup for the investigation of ice-structure interaction–results and validation. Ships Offshore Struct. **15**(S1), S1–S9 (2021). https://doi.org/10.1080/17445302.2020.1713437
Hirdaris, S.E., et al.: Loads for use in the design of ships and offshore structures. Ocean Eng. **78**, pp. 131–174 (2014). https://linkinghub.elsevier.com/retrieve/pii/S0029801813003557
Hirdaris, S., et al.: Review of the uncertainties associated to hull girder hydroelastic response and wave load predictions. Marine Struct. **89**, 103383 (2023). Accessed 22 Feb 2023,
Hmedi, M., et al.: Experimental analysis of CENTEC-TLP self-stable platform with a 10 MW turbine. J. Marine Sci. Eng. **10**(12) (2022)
Honey, L., Judge, C.Q., Gilbert, C.M.: Slamming events of a planing hull and wedge water entry experiment: comparisons and insights on fluid-structure interaction. In: SNAME International Conference on Fast Sea Transportation, p. D021S003R003 (2021). https://doi.org/10.5957/FAST-2021-003
Hosseinzadeh, S., Tabri, K., Topa, A., Hirdaris, S.: Slamming loads and responses on a non-prismatic stiffened aluminium wedge: Part II. Numerical simulations. Ocean Eng. **279**, 114309 (2023a)
Hosseinzadeh, S., et al.: Slamming loads and responses on a non-prismatic stiffened aluminium wedge: part I. Experimental study. SSRN Electron. J. **279**, 114309 (2023b)
Hou, H.M., Liu, Y., Dong, G.H., Xu, T.J.: Reliability assessment of mooring system for fish cage considering one damaged mooring line. Ocean Eng. **257** (2022)
Hsiao, Y., Hsiao, S.C.: Experimental study on the interaction of solitary wave with elastic submerged plate. Ocean Eng. **261** (2022)
Hu, B., Liu, L., Wang, D.: Prediction of performance of a non-icebreaking ship in marginal ice zone. J. Hydrodynam. **34**(2), pp. 315–328 (2022a)
Hu, S., Zhang, S., Liu, M., Dong, S., Zheng, R.: Hydrodynamic response research of a cage system under waves and currents based on modal analysis. Ocean Eng. **243** (2022b)

Hu, T., et al.: Experimental investigation on hydrodynamic forces of semi-submerged cylinders in combined steady flow and oscillatory flow. Ocean Eng. **268** (2023)

Huang, B., et al.: The effects of heave motion on the performance of a floating counter-rotating type tidal turbine under wave-current interaction. Energy Convers. Manage. **252** (2022a)

Huang, H.C., Yang, Y.F., Zhu, R.H., Wang, C.Z.: Nonlinear wave resonance due to oscillations of twin cylinders in a uniform current. Appl. Ocean Res. **121** (2022b)

Huang, H., Gu, H., Chen, H.C.: A new method to couple FEM mooring program with CFD to simulate Six-DoF responses of a moored body. Ocean Eng. **250** (2022c)

Huang, H., Liu, Q., Yue, M., Miao, W., Wang, P., Li, C.: Fully coupled aero-hydrodynamic analysis of a biomimetic fractal semi-submersible floating offshore wind turbine under wind-wave excitation conditions. Renew. Energy **203**, 280–300 (2023a)

Huang, J., Teng, B.: The second-order interaction of monochromatic waves with three-dimensional bodies in a channel. Ocean Eng. **217** (2020)

Huang, J., Teng, B., Cong, P.W.: Second-order sum- and difference-frequency bichromatic wave forces on three-dimensional bodies in a channel. Ocean Eng. **224** (2021)

Huang, L., Li, F., Li, M., Khojasteh, D., Luo, Z., Kujala, P.: An investigation on the speed dependence of ice resistance using an advanced CFD+DEM approach based on pre-sawn ice tests. Ocean Eng. **264** (2022d)

Huang, L., Pena, B., Liu, Y., Anderlini, E.: Machine learning in sustainable ship design and operation: a review. Ocean Eng. **266** (2022e)

Huang, S., Jiao, J., Guedes Soares, C.: Uncertainty analyses on the CFD–FEA co-simulations of ship wave loads and whipping responses. Marine Struct. **82** (2022f)

Huang, W.H., Yang, R.Y.: Water depth variation influence on the mooring line design for fowt within shallow water region. J. Marine Sci. Eng. **9**(4) (2021)

Huang, Y., Wang, P., Zhao, M., Zhang, C., Du, X.: Dynamic response of sea-crossing bridge under combined seismic and wave-current action. Structures **40**, 317–327 (2022g)

Huang, Y., Zhao, W., Wan, D.: Wake interaction between two spar-type floating offshore wind turbines under different layouts. Phys. Fluids **35**(9) (2023b)

Huo, F., Yang, H., Yao, Z., An, K., Xu, S.: Study on slamming pressure characteristics of platform under freak wave. J. Marine Sci. Eng. **9**(11) (2021)

Huynh, L.E., Chu, C.R., Wu, T.R.: Hydrodynamic loads of the bridge decks in wave-current combined flows. Ocean Eng. **270** (2023)

IACS. The international association of classification Societies longitudinal strength standard S11 (2015)

Ibarra, M.A.C., Simão, M.L., Videiro, P.M., Sagrilo, L.V.S.: Long-term fatigue analysis of mooring lines considering wind-sea and swell waves using the univariate dimension-reduction method. Appl. Ocean Res. **118** (2022)

Ibrahim, A.M., Morabito, M.G., Beaver, W.: Development of a segmented model for a medium-sized semi-displacement vessel. In: SNAME Maritime Convention. SNAME, Houston (2022)

International Maritime Organization (IMO). Revised GHG reduction strategy for global shipping adopted, p. 1 (2023). https://www.imo.org/en/MediaCentre/PressBriefings/pages/Revised-GHG-reduction-strategy-for-global-shipping-adopted-.aspx, https://www.imo.org/en/MediaCentre/PressBriefings/pages/Revised-GHG-reduction-strategy-for-global-shipping-adopted-.aspx. Accessed 18 Oct 2024

Islam, H., Guedes Soares, C.: Assessment of uncertainty in the CFD simulation of the wave-induced loads on a vertical cylinder. Marine Struct. **80** (2021). Accessed 29 Aug 2023

Islam, H., Soares, C.G.: Head wave simulation of a KRISO container ship model using openFOAM for the assessment of sea margin. J. Offshore Mech. Arctic Eng.-Trans. ASME **144**(3) (2022)

Islam, H., Sutulo, S., Guedes Soares, C.: Aerodynamic load prediction on a patrol vessel using computational fluid dynamics. J. Marine Sci. Eng. **10**(7) (2022)

ISO.x ISO/IEC Guide 98-3:2008 - Uncertainty of measurement—Part 3: Guide to the expression of uncertainty in measurement (GUM:1995) (2023)

ISSC. ISSC Report. Proceedings of the 20th international ship and offshore structures congress, 1 (2018)

ITTC. ITTC – Recommended Procedures and Guidelines - Verification and validation of linear and weakly nonlinear seakeeping computer codes. 7.5-02-07-02.5 (Revision 01). International Towing Tank Conference. Lyngby, Denmark, p. 17 (2011)

ITTC. ITTC Report. Proceedings of the 21st international towing tank symposium (2021)

Jabary, W., et al.: Development of machine learning approaches to enhance ship operational performance evaluation based on an integrated data model. In: 33rd International Ocean and Polar Engineering Conference, Ottawa (2023)

JAIC (Joint Accident Investigation Commission). Final report on the capsizing on 28 September 1994 in the Baltic Sea of the Ro-ro passenger vessel MV Estonia. Edita Books, Helsinki (1997)

Jain, U., Vega-Martinez, P., van der Meer, D.: Air entrapment and its effect on pressure impulses in the slamming of a flat disc on water (2021)

Jalani, M.A., et al.: Experimental study on a bottom corner of the floating WEC. Ocean Eng. **243** (2022)

Jeon, W., Park, S., Cho, S.: Moored motion prediction of a semi-submersible offshore platform in waves using an OpenFOAM and MoorDyn coupled solver. Int. J. Naval Archit. Ocean Eng. **15** (2023)

Jeon, W., Park, S., Jeon, G.-M., Park, J.-C.: Computational study on rogue wave and its application to a floating body. Appl. Sci.-Basel **12**(6) (2022)

Jeong, K., Min, S., Jang, M., Won, D., Kim, S.: Feasibility study of submerged floating tunnels with vertical and inclined combined tethers. Ocean Eng. **265** (2022)

Ji, S., Yang, D.: Ice loads and ice-induced vibrations of offshore wind turbine based on coupled DEM-FEM simulations. Ocean Eng. **243**(July 2021), 110197 (2022). https://doi.org/10.1016/j.oceaneng.2021.110197

Jiang, C., et al.: A multi-fidelity prediction model for vertical bending moment and total longitudinal stress of a ship based on composite neural network. J. Hydrodyn. **35**(1), 27–35 (2023a)

Jiang, F., Yin, D., Califano, A., Berthelsen, P.A.: Application of CFD on VIM of semi-submersible FOWT: a case study. J. Phys. Conf. Ser. **2626**(1), 1–11 (2023)

Jiang, Z., Li, F., Suominen, M., Tavakoli, S., Kujala, P., Hirdaris, S.: An investigation of the influence of added mass on the ICE loads in various sea states. In: Proceedings of the International Conference on Offshore Mechanics and Arctic Engineering - OMAE, 6(August) (2023c)

Jiang, Z., Li, F., Tavakoli, S., Kujala, P., Suominen, M., Hirdaris, S.: A viscous investigation on the hydrodynamic coefficients and wave loads under the interaction of side-by-side cylinders in regular waves. Ocean Eng. **297** (2024)

Jiao, J., Zhao, M., Jia, G., Ding, S.: SPH simulation of two side-by-side LNG ships' motions coupled with tank sloshing in regular waves. Ocean Eng. **297** (2024)

Jin, J., Zhou, L., Ding, S., Gu, Y.: Numerical simulation of the ice breaking process for hovercraft. J. Marine Sci. Eng. **9**(9) (2021)

Kapsemberg, G., Brizzolara, S.: Hydro-elastic effects of bow flare slamming on a fast monohull. In: International Fast Ship Conference FAST 1999 (1999)

Kapsenberg, G., Carette, N.: A consistent method to design and evaluate the performance of anti-roll tanks for ships. Ship Technol. Res. **70**(2), 117–145 (2023)

Kapsenberg, G.K.: Slamming of ships: where are we now? Philos. Trans. Roy. Soc. A: Math. Phys. Eng. Sci. **369**(1947), 2892–2919 (2011)

Kardakaris, K., Konispoliatis, D.N., Soukissian, T.H.: Theoretical evaluation of the power efficiency of a moored hybrid floating platform for wind and wave energy production in the Greek seas. AIMS Geosci. **9**(1), 153–183 (2023) von Karman, T.H.: The impact on seaplane floats during landing. NACA Technical Note, NACA-TN-32 (1929)

Katsidoniotaki, E., Psarommatis, F., Göteman, M.: Digital twin for the prediction of extreme loads on a wave energy conversion system. Energies **15**(15), 5464 (2022). https://www.mdpi.com/1996-1073/15/15/5464/htm. Accessed 4 Sept 2023

Katsidoniotaki, E., Shahroozi, Z., Eskilsson, C., Palm, J., Engström, J., Göteman, M. : Validation of a CFD model for wave energy system dynamics in extreme waves. Ocean Eng. **268** (2023)

Khan, L.J., Macklin, J.J.R., Peck, B.C.D., Morton, O., Souppez, J.-B.R.G.: A review of wind-assisted ship propulsion for sustainable commercial shipping. In: Wind Propulsion Conference, 15th–16th September 2021, London, UK (2021)

Kharazmi, R., Ketabdari, M.J.: Numerical modeling to develop strake design of Spar platform for Vortex-Induced motions suppression. Ocean Eng. **250**(March), 111060 (2022). https://doi.org/10.1016/j.oceaneng.2022.111060

Kim, D., Tezdogan, T., Incecik, A.: A high-fidelity CFD-based model for the prediction of ship manoeuvrability in currents. Ocean Eng. **256**, 111492 (2022a). Accessed 18 Oct 2024

Kim, M., Pipiras, V., Reed, A. M., Weems, K.: Calibration of low-fidelity ship motion programs through regressions of high-fidelity forces. Ocean Eng. **290** (2023a)

Kim, S., Bouscasse, B., Ducrozet, G., Delacroix, S., De Hauteclocque, G., Ferrant, P.: Experimental investigation on wave-induced bending moments of a 6,750-TEU containership in oblique waves. Ocean Eng. **284** (2023b)

Kim, S., de Hauteclocque, G., Bouscasse, B., Lasbleis, M., Ducrozet, G.: Experimental analysis of extreme wave loads on a containership. Ocean Eng. **306** (2024)

Kim, S.J., Kim, M.H., Koo, W.: Nonlinear hydrodynamics of freely floating symmetric bodies in waves by three-dimensional fully nonlinear potential-flow numerical wave tank. Appl. Ocean Res. **113** (2021)

Kim, S.J., et al.: Comparison of numerical approaches for structural response analysis of passenger ships in collisions and groundings. Marine Struct. **81** (2022b)

Kim, Y., Kim, J.-H.: Benchmark study on motions and loads of a 6750-TEU containership (2016). https://doi.org/10.1016/j.oceaneng.2016.04.015

Kleijnen, J.P.C.: Kriging metamodeling in simulation: a review. Eur. J. Oper. Res. **192**(3), 707–716 (2009)

Kobayashi, H., et al.: CFD assessment of the wind forces and moments of superstructures through RANS. Appl. Ocean Res. **129**(September), 103364 (2022). https://doi.org/10.1016/j.apor.2022.103364

Komoriyama, Y., Iijima, K., Tatsumi, A., Fujikubo, M.: Identification of wave profiles encountered by a ship with no forward speed using Kalman filter technique and validation by tank tests - long-crested irregular wave case -. Ocean Eng. **271** (2023)

Konispoliatis, D.N., Chatjigeorgiou, I.K., Mavrakos, S.A.: Hydrodynamics of a moored permeable vertical cylindrical body. J. Marine Sci. Eng. **10**(3) (2022a)

Konispoliatis, D.N., et al.: Refos: a renewable energy multi-purpose floating offshore system. Energies **14**(11) (2021)

Konispoliatis, D.N., Manolas, D.I., Voutsinas, S.G., Mavrakos, S.A.: Coupled dynamic response of an offshore multi-purpose floating structure suitable for wind and wave energy exploitation. Front. Energy Res. **10** (2022b)

Kume, K., Hamada, T., Kobayashi, H., Yamanaka, S.: Evaluation of aerodynamic characteristics of a ship with flettner rotors by wind tunnel tests and RANS-based CFD. Ocean Eng. **254**(March), 111345 (2022). https://doi.org/10.1016/j.oceaneng.2022.111345

Lakshmynarayanana, P.A.K., Hirdaris, S.: Comparison of nonlinear one- and two-way FFSI methods for the prediction of the symmetric response of a containership in waves. Ocean Eng. **203**, 107179 (2020). Accessed 30 Aug 2023

Leal, A.P., Condino Fujarra, A.L., Carnier, R.M., Gonçalves, R.T., Suzuki, H.: Flow-induced vibration analysis using a low-cost inertial measurement unit. In: Proceedings of the International Conference on Offshore Mechanics and Arctic Engineering - OMAE. American Society of Mechanical Engineers Digital Collection (2023). https://doi.org/10.1115/OMAE2023-105138. Accessed 18 Oct 2024

Lee, J., Ahn, Y., Kim, Y.: Experimental study on effect of density ratio and phase transition during sloshing impact in rectangular tank. Ocean Eng. **242**, 110105 (2021a)

Lee, J.H., Kim, Y., Kim, B.S., Gerhardt, F.: Comparative study on analysis methods for added resistance of four ships in head and oblique waves. Ocean Eng. **236** (2021b)

Lee, J.-H., Lee, J., Kim, Y., Ahn, Y.: Prediction of wave-induced ship motions based on integrated neural network system and spatiotemporal wave-field data. Phys. Fluids **35**(9) (2023)

Lemström, I., Polojärvi, A., Tuhkuri, J.: Model-scale tests on ice-structure interaction in shallow water, Part I: global ice loads and the ice loading process. Marine Struct. **81**(October 2021), 103106 (2022). https://doi.org/10.1016/j.marstruc.2021.103106

Leroy, V., Delacroix, S., Merrien, A., Bachynski-Polić, E.E., Gilloteaux, J.C.: Experimental investigation of the hydro-elastic response of a spar-type floating offshore wind turbine. Ocean Eng. **255** (2022)

Li, F., Huang, L.: A review of computational simulation methods for a ship advancing in broken ice. J. Marine Sci. Eng. **10**(2) (2022)

Li, F., Suominen, M., Kujala, P.: Ship performance in ice channels narrower than ship beam: model test and numerical investigation. Ocean Eng. **240** (2021)

Li, H., Zou, J., Deng, B., Liu, R., Sun, S.: Experimental study of stern slamming and global response of a large cruise ship in regular waves. Marine Struct. **86**(April), 103294 (2022a). https://doi.org/10.1016/j.marstruc.2022.103294

Li, H., Zou, J., Peng, Y., Zhou, X., Lu, L., Sun, S.: Numerical study of slamming and whipping loads in moderate and large regular waves for different forward speeds. Marine Struct. **94**, 103563 (2024a). https://www.sciencedirect.com/science/article/pii/S095183392300196X

Li, L., Han, G., Ji, S.: Statistical analysis of ice load on icebreaker ship based on stochastic ice fields. J. Marine Sci. Eng. **12**(3) (2024b)

Li, X., Xiao, Q., Wang, E., Peyrard, C., Gonçalves, R.T.: The dynamic response of floating offshore wind turbine platform in wave-current condition. Phys. Fluids **35**(8) (2023)

Li, Y., Peng, T., Xiao, L., Wei, H., Li, X.: Wave runup prediction for a semi-submersible based on temporal convolutional neural network. J. Ocean Eng. Sci. (2022b). Accessed 4 Sept 2023

Lian, Y., et al.: An upper and lower bound method for evaluating residual strengths of polyester mooring ropes with artificial damage. Ocean Eng. **262** (2022)

Liang, H., Zhao, E., Qin, H., Mu, L., Su, H.: A model coupling CFD and DRL: investigation on wave dissipation by actively controlled flat plate. IEEE Access **10**, pp. 98290–98308 (2022a). Accessed 4 Sept 2023

Liang, J., Liu, Y., Chen, Y., Li, A.: Experimental study on hydrodynamic characteristics of the box-type floating breakwater with different mooring configurations. Ocean Eng. **254** (2022b)

Lihin, Z.H., Khan, R., Ishak, M.I.M., Rahman, A.A., Kar, S., Abdul Rahman, A.R.: Revised methodology for assessing fixed offshore structures with wave in deck loading. In: Offshore Technology Conference Asia, OTCA 2022. Offshore Technology Conference (2022)

Lin, J., kun Guo, Y.: Numerical investigation of non-cohesive seabed response around a mono-pile by crossing wave-current. Water Sci. Eng. **15**(1), 57–68 (2022)

Liu, H., Zhao, C., Ma, G., He, L., Sun, L., Li, H.: Reliability assessment of a floating offshore wind turbine mooring system based on the TLBO algorithm. Appl. Ocean Res. **124** (2022a)

Liu, J., Liu, M., Xiao, L., Wei, H., Li, X.: Experimental study on the effect of flare barriers on wave run-up and motion response of a semi-submersible platform. Ocean Eng. **281** (2023a)

Liu, J., Xiao, L., Yang, L., Liu, M.: Experimental study on the effect of flare barriers on wave run-up and wave loads of a rounded-square column. Ocean Eng. **260** (2022b)

Liu, L., Ji, S.: Dilated-polyhedron-based DEM analysis of the ice resistance on ship hulls in escort operations in level ice. Marine Struct. **80** (2021)
Liu, L., et al.: Study on numerical simulation and mitigation of parametric rolling in a container ship under head waves. BRODOGRADNJA **75**(3) (2024)
Liu, R., Xue, Y., Lu, X.: Coupling of finite element method and peridynamics to simulate ship-ice interaction. J. Marine Sci. Eng. **11**(3), **481** (2023b)
Liu, X., Liu, F., Ren, H., Chen, X., Xie, H.: Experimental investigation on the slamming loads of a truncated 3D stern model entering into water. Ocean Eng. **252**, 110873 (2022c). https://doi.org/10.1016/j.oceaneng.2022.110873
Liu, Y., Ge, D., Bai, X., Li, L.: A CFD study of vortex-induced motions of a semi-submersible floating offshore wind turbine. Energies **16**(2) (2023c)
Liu, Y., Shi, W., Wang, W., Li, X., Qi, S., Wang, B.: Dynamic analysis of monopile-type offshore wind turbine under sea ice coupling with fluid-structure interaction. Front. Marine Sci. **9** (2022d)
Liu, Z., Guedes Soares, C.: Sensitivity analysis of the cage volume and mooring forces for a gravity cage subjected to current and waves. Ocean Eng. **287** (2023)
Liu, Z., Xu, H., Guedes Soares, C.: Experimental study on the mooring forces and motions of a fish cage under regular waves. Ocean Eng. **280** (2023d)
Livermore Software Technology Corporation. ICFD theory manual: Incompressible fluid solver in LS-DYNA (2014). https://ftp.lstc.com/anonymous/outgoing/inaki/docs/pdf_icfd/ICFD_theory.pdf
Lloyd, C., et al.: Validation of the dynamic load characteristics on a tidal stream turbine when subjected to wave and current interaction. Ocean Eng. **222**, 108360 (2021). Accessed 18 Oct 2024
Lone, E.N., Mainçon, P., Gabrielsen, Ø., Sauder, T., Larsen, K., Leira, B.J.: Analysis of S-N data for new and corroded mooring chains at varying mean load levels using a hierarchical linear model. Mar. Struct. **91**, 103466 (2023)
Lone, E.N., Sauder, T., Larsen, K., Leira, B.J.: Probabilistic fatigue model for design and life extension of mooring chains, including mean load and corrosion effects. Ocean Eng. **245** (2022a)
Lone, E.N., Sauder, T., Larsen, K., Leira, B.J.: Fatigue reliability of mooring chains, including mean load and corrosion effects. Ocean Eng. **266** (2022b)
Lozon, E., Hall, M.: Coupled loads analysis of a novel shared-mooring floating wind farm. Appl. Energy **332** (2023)
Lu, L., Ren, H., Li, H., Zou, J., Chen, S., Liu, R.: Numerical method for whipping response of ultra large container ships under asymmetric slamming in regular waves. Ocean Eng. **287**(P2), 115830 (2023). https://doi.org/10.1016/j.oceaneng.2023.115830
Luo, G., Zhang, Y., Pan, S., Ren, Y.: Dynamic response analysis of submerged floating tunnels to coupled wave-seismic action. J. Eng. Mech. **38**(2), 211–220 (2021)
Luo, M., Rubinato, M., Wang, X., Zhao, X.: Experimental investigation of freak wave actions on a floating platform and effects of the air gap. Ocean Eng. **253**, 111192 (2022)
Ma, C., Bi, C.W., Xu, Z., Zhao, Y.P.: Dynamic behaviors of a hinged multi-body floating aquaculture platform under regular waves. Ocean Eng. **243** (2022a)
Ma, C., Zhao, Y.P., Bi, C.W.: Numerical study on hydrodynamic responses of a single-point moored vessel-shaped floating aquaculture platform in waves. Aquacult. Eng. **96** (2022b)
Ma, C., Zhao, Y.-P., Bi, C.-W., Xie, S.: Numerical study on dynamic analysis of a nine-module floating aquaculture platform under irregular waves. Ocean Eng. **285**, 115253 (2023). https://linkinghub.elsevier.com/retrieve/pii/S0029801823016372
Ma, L., Swan, C.: The effective prediction of wave-in-deck loads. J. Fluids Struct. **95** (2020)
Ma, L., Swan, C.: An experimental study of wave-in-deck loading and its dependence on the properties of the topside structure. Marine Struct. **88** (2023a)

Ma, L., Swan, C.: Wave-in-deck loads: an assessment of present design practice given recent improvements in the description of extreme waves and the nature of the applied loads. Ocean Eng. **285** (2023b)

Ma, Y., Sclavounos, P.D.: Support vector machines model of the nonlinear hydrodynamics of fixed cylinders. J. Offshore Mechan. Arctic Eng. **143**(5) (2021)

MAIB. Report on the investigation of the structural failure of MSC Napoli, marine accident investigation Branch - MAIB. Carlton House Carlton Place, Southampton (2008)

Makarov, O., Bekker, A., Li, L.: Comparative analysis of numerical methods for the modeling of ice–structure interaction problems. Continuum Mech. Thermodyn. **34**(6), 1621–1639 (2022)

Malenica, S., Seng, S., Diebold, L., Scolan, Y.-M., Korobkin, A.A., Khabakhpasheva, T.: On three dimensional hydroelastic impact. In: 9th International Conference on HYDROELASTICITY IN MARINE TECHNOLOGY. Roma (2022)

Mandru, A., Rusu, L., Bekhit, A., Pacuraru, F.: Numerical study of a model and full-scale container ship sailing in regular head waves. INVENTIONS **9**(1) (2024)

Mao, Y., Wang, T., Duan, M.: A DNN-based approach to predict dynamic mooring tensions for semi-submersible platform under a mooring line failure condition. Ocean Eng. **266** (2022)

Marty, A., Schoefs, F., Damblans, G., Facq, J. V., Gaurier, B., Germain, G.: Experimental study of two kinds of hard marine growth effects on the hydrodynamic behavior of a cylinder submitted to wave and current loading. Ocean Eng. **263** (2022)

Mauro, F., Valentina, E. Della, Ferrari, V., Begovic, E. A method for early-stage design current loads determination on drill-ships. Ocean Eng. **287**(September) (2023)

van der Meer, D.: Linear stability analysis of a time-divergent slamming flow. J. Fluid Mech. **934** (2022). https://doi.org/10.1017/jfm.2021.1064

Men, J., Yan, F., Wang, Y., Wang, L., Zheng, X., Wang, W.: An evaluation of mooring system in a wind-wave hybrid system under intact and accident states. Ocean Eng. **283** (2023)

Mendoza, J., Haagensen, P. J., Köhler, J.: Analysis of fatigue test data of retrieved mooring chain links subject to pitting corrosion. Marine Struct. **81** (2022)

Meyer, J., Windt, C., Sinn, P., Hildebrandt, A: On the mooring methodology of heaving point absorber arrays. Ocean Eng. **281** (2023)

Miao, Y., Chen, X., Ye, Y., Ding, J., Huang, H.: Numerical modeling and dynamic analysis of a floating bridge subjected to wave, current and moving loads. Ocean Eng. **225** (2021)

Miratsu, R., Sasmal, K., Kodaira, T., Fukui, T., Zhu, T., Waseda, T.: Evaluation of ship operational effect based on long-term encountered sea states using wave hindcast combined with storm avoidance model. Marine Struct. **86** (2022)

Miškov, V., Dragić, M., Tomin, V., Hofman, M.: Sea trials of Sigma wave energy converter – slacking and snapping of TLP mooring lines. Marine Struct. **89** (2023)

MJB. Maritime Bureau of Japan's Ministry of Land, Infrastructure, Transport and Tourism Final report of committee on large container ship safety (2015)

El Moctar, O., Lantermann, U., Shigunov, V., Schellin, T.E.: Experimental and numerical investigations of effects of ship superstructures on wind-induced loads for benchmarking. Phys. Fluids **35**(4) (2023)

Mohajernasab, S., Drobyshevski, Y., Abdussamie, N., Ojeda, R.: Experimental investigation into the effects of air pockets on wave-in-deck loads of offshore structures. Marine Struct. **90** (2023)

Mohapatra, S.C., Islam, H., Hallak, T.S., Soares, C.G.: Solitary wave interaction with a floating pontoon based on boussinesq model and CFD-based simulations. J. Marine Sci. Eng. **10**(9) (2022)

Mohseni, M., Guedes Soares, C.: Numerical investigation of inline wave force on a truncated vertical cylinder with different cross-sections in regular head waves. Ocean Eng. **251** (2022a)

Mohseni, M., Guedes Soares, C.: Numerical simulation of wave interaction with a pair of fixed large tandem cylinders subjected to regular, non-breaking waves. J. Offshore Mech. and Arctic Eng. **144**(3) (2022b)

Mohseni, M., Guedes Soares, C.: CFD analysis of wave loading on a 10 MW TLP-type offshore floating wind turbine in regular waves. Ocean Eng. **301** (2022)

Monaghan, J.J.: Simulating free surface flows with SPH. J. Comput. Phys. **110**(2), 399–406 (1994). https://www.sciencedirect.com/science/article/pii/S0021999184710345

Monteiro, L.F.G.: High-fidelity analysis of flettner rotors aerospace engineering examination committee (2024)

Müller, F., Böhm, A., Herrnring, H., von Bock und Polach, F., Ehlers, S.: Influence of the ice shape on ice-structure impact loads. Cold Regions Sci. Technol. **221**(January) (2024)

Munir, H., Lee, C.F., Ong, M.C.: Global analysis of floating offshore wind turbines with shared mooring system. IOP Conf. Ser.: Mater. Sci. Eng. **1201**(1), 12024 (2021)

Nam, B.W., Hong, S.Y., Kim, H.J.: An experimental study on characteristics of relative wave elevations around a tension leg platform in irregular waves. Appl. Ocean Res. **122** (2022)

Nan, M.Y., Hu, J.J., Wang, X.L., Vladimir, Y.: Study on Ice load inversion based on LSTM networks. Chuan Bo Li Xue/J. Ship Mech. **25**(12), 1675–1684 (2021)

Neisi, A., Ghassemi, H., Iranmanesh, M., He, G.: Effect of the multi-segment mooring system by buoy and clump weights on the dynamic motions of the floating platform. Ocean Eng. **260** (2022)

Neugebauer, J., et al.: Sloshing-Induced Impact Loads and Free Surface Elevation in a Pool in Waves. In: Proceedings of the Thirty-Third International Ocean and Polar Engineering Conference, Ottawa, pp. 2623–2630 (2023)

Nguyen, N., Thiagarajan, K: Nonlinear viscoelastic modeling of synthetic mooring lines. Marine Struct. **85** (2022)

Ni, B., Wang, Y., Xu, Y., Chen, W.: Numerical simulation of ship collision with rafted ice based on cohesive element method. J. Mar. Sci. Appl. **23**(1), 127–136 (2024)

Ni, B., Xu, Y., Huang, Q., You, J., Xue, Y.: Application of improved cohesive zone length formula in ice mode I crack propagation. Chin. J. Ship Res. **17**(3), 58–66 (2022)

Nielsen, U.D., Mounet, R.E.G., Brodtkorb, A.H.: Tuning of transfer functions for analysis of wave–ship interactions. Marine Struct. **79** (2021)

Ning, D., Xu, J., Chen, L., Cong, P., Zhao, M., Jiang, C.: Boussinesq modelling of near-trapping in a four-cylinder array. Ocean Eng. **248** (2022)

Nizamani, M., Nizamani, Z., Nakayama, A., Osman, M.: Analysis of loads caused by waves on the deck near the free surface of the offshore platform using computational fluid dynamics. Ships Offshore Struct. **17**(9), 1964–1974 (2022)

de Oliveira Costa, D., Araújo Perim, J., Guedes Camargo, B., Sena Sales Junior, J., Carlos Fernandes, A.: Wave impact loads on the bottom of flat decks (2021). http://asmedigitalcollection.asme.org/OMAE/proceedings-pdf/OMAE2021/85161/V006T06A012/6780540/v006t06a012-omae2021-62990.pdf

Otori, H., Kikuchi, Y., Rivera-Arreba, I., Viré, A.: Numerical study of hydrodynamic forces and dynamic response for barge type floating platform by computational fluid dynamics and engineering model. Ocean Eng. **284** (2023)

Otter, A., Murphy, J., Pakrashi, V., Robertson, A., Desmond, C.: A review of modelling techniques for floating offshore wind turbines. Wind Energy **25**(5), 831–857 (2022)

Panciroli, R., Porfiri, M.: Analysis of hydroelastic slamming through particle image velocimetry. J. Sound Vib. **347**, 63–78 (2015)

Papini, G., Paduano, B., Pasta, E., Carapellese, F., Mattiazzo, G., Faedo, N.: On the influence of mooring systems in optimal predictive control for wave energy converters. Renew. Energy 119242 (2023). https://linkinghub.elsevier.com/retrieve/pii/S0960148123011576

Park, C.-J., Lee, J.-K., Kim, Y.: Study on hydroelastic responses of membrane-type LNG cargo containment structure under impulsive sloshing loads of different media. J. Marine Sci. Eng. (2024)

Parunov, J., et al.: Benchmark on the prediction of whipping response of a warship model in regular waves. Marine Struct. **94**, 103549 (2024). https://www.sciencedirect.com/science/article/pii/S095183392300182X

Parunov, J., et al.: Benchmark study of global linear wave loads on a container ship with forward speed. Marine Struct. **84** (2022)

Pena, B., Huang, L.: Wave-GAN: A deep learning approach for the prediction of nonlinear regular wave loads and run-up on a fixed cylinder. Coast. Eng. **167**, 103902 (2021). Accessed 4 Sept 2023

Pena-Sanchez, Y., Windt, C., Davidson, J., Ringwood, J.V.: A critical comparison of excitation force estimators for wave-energy devices. IEEE Trans. Control Syst. Technol. **28**(6), 2263–2275 (2020)

Petranović, T., Mikulić, A., Katalinić, M., Ćorak, M., Parunov, J.: Method for prediction of extreme wave loads based on ship operability analysis using hindcast wave database. J. Marine Sci. Eng. **9**(9) (2021)

Pillai, A.C., et al.: Anchor loads for shallow water mooring of a 15 MW floating wind turbine — Part I: chain catenary moorings for single and shared anchor scenarios. Ocean Eng. **266** (2022)

Pilloton, C., Colagrossi, A., Marrone, S., Bardazzi, A.: Three hours real–time SPH simulation of sloshing flows inside a LNG ship with realistic severe sea-state forcing. In: SPHERIC 2022, Xi'an (2022)

Pinguet, R., Benoit, M., Molin, B., Rezende, F.: CFD analysis of added mass, damping and induced flow of isolated and cylinder-mounted heave plates at various submergence depths using an overset mesh method. J. Fluids Struct. **109** (2022)

Pitchforth, D.J., Mills, R.S., Rogers, T.J., Tygesen, U.T., Cross, E.J.: Physics-informed gaussian processes for wave loading prediction. In: Structural Health Monitoring 2023: Designing SHM for Sustainability, Maintainability, and Reliability - Proceedings of the 14th International Workshop on Structural Health Monitoring, pp. 2205–2214 (2023). https://www.scopus.com/inward/record.uri?eid=2-s2.0-85182281713&partnerID=40&md5=c8871a735c8f6aeb8ab6d664947396af

Qi, Y., Söring, H., El Moctar, O., Neugebauer, J.: An efficient numerical approach to predict waves in swimming pools on ships. In: Proceedings of the Thirty-Third International Ocean and Polar Engineering Conference, Ottawa, pp. 2603–2608 (2023)

Qvale, P., Nordhagen, H.O., Ås, S.K., Skallerud, B.H.: Effect of long periods of corrosion on the fatigue lifetime of offshore mooring chain steel. Marine Struct. **85** (2022)

Qvale, P., Zarandi, E. P., Ås, S.K., Skallerud, B.H.: Digital image correlation for continuous mapping of fatigue crack initiation sites on corroded surface from offshore mooring chain. Int. J. Fatigue **151** (2021)

Ramzanpoor, I., Nuernberg, M., Tao, L.: Coupled aero-hydro-servo-elastic analysis of 10MW TLB floating offshore wind turbine. J. Ocean Eng. Sci. (2023)

Ren, D., Park, J.C.: Particle-based numerical simulation of continuous ice-breaking process by an icebreaker. Ocean Eng. **270**(January), 113478 (2023). https://doi.org/10.1016/j.oceaneng.2022.113478

Ren, X., Tao, L., Liang, Y., Han, D.: Nonlinear wave surface elevation around a multi-column offshore structure. Ocean Eng. **238** (2021)

Robaux, F., Benoit, M.: Assessment of one-way coupling methods from a potential to a viscous flow solver based on domain- and functional-decomposition for fixed submerged bodies in nonlinear waves. Eur. J. Mech. B/Fluids **95**, 315–334 (2022)

Rodrigues, J.M., Viuff, T., Økland, O.D.: Model tests of a hydroelastic truncated floating bridge. Appl. Ocean Res. **125** (2022)

Rogers, F., Haddara, M., Molyneux, D.: Dynamic bending moment identification using neural networks. In: 25th American Towing Tank Conference. SNAME (1998)

Rueda-Bayona, J.G., Guzmán, A., Eras, J.J.C.: Vortex-induced vibration effect of extreme sea states over the structural dynamics of a scaled monopile offshore wind turbine. J. Ocean Eng. Marine Energy **9**(2), 359–376 (2023). https://doi.org/10.1007/s40722-022-00272-9

Ryan, C., Huang, L., Li, Z., Ringsberg, J.W., Thomas, G.: An Arctic ship performance model for sea routes in ice-infested waters. Appl. Ocean Res. **117** (2021)

Saincher, S., Sriram, V.: A three dimensional hybrid fully nonlinear potential flow and Navier Stokes model for wave structure interactions. Ocean Eng. **266**, 112770 (2022)

Sasikala, N., Sannasiraj, S. A., Manasseh, R.: 3D simulation of wave slamming on a horizontal deck using WCSPH. In: Lecture Notes in Civil Engineering (2021)

Sasmal, K., Miratsu, R., Kodaira, T., Fukui, T., Zhu, T., Waseda, T.: Statistical model representing storm avoidance by merchant ships in the North Atlantic Ocean. Ocean Eng. **235**, 109163 (2021)

Sauder, T., Alterskjær, S.A.: Hydrodynamic testing of wind-assisted cargo ships using a cyber–physical method. Ocean Eng. **243**(June 2021), 110206 (2022). https://doi.org/10.1016/j.oceaneng.2021.110206

Sazidy, M.: Development of velocity dependent ice flexural failure model and application to safe speed (2015)

Sazonov, K., Dobrodeev, A.: Ice Resistance assessment for a large size vessel running in a narrow ice channel behind an icebreaker. J. Mar. Sci. Appl. **20**(3), 446–455 (2021)

Scharnke, J., van Essen, S.M., Seyffert, H.C.: Required test durations for converged short-term wave and impact extreme value statistics–Part 2: deck box dataset. Marine Struct. **90** (2023). Accessed 29 Aug 2023

Schirmann, M.L., Collette, M.D., Gose, J.W.: Data-driven models for vessel motion prediction and the benefits of physics-based information. Appl. Ocean Res. **120** (2022)

Sclavounos, P.D., Ma, Y.: Artificial intelligence machine learning in marine hydrodynamics. In: Proceedings of the International Conference on Offshore Mechanics and Arctic Engineering - OMAE (2018)

Sergiienko, N.Y., da Silva, L.S.P., Bachynski-Polić, E.E., Cazzolato, B.S., Arjomandi, M., Ding, B.: Review of scaling laws applied to floating offshore wind turbines. Renew. Sustain. Energy Rev. **162**(March), 112477 (2022). https://doi.org/10.1016/j.rser.2022.112477

Shabani, B., Lavroff, J., Davis, M.R., Holloway, D.S., Thomas, G.A.: Slam loads and kinematics of wave-piercing catamarans during bow entry events in head seas. J. Ship Res. **62**(03), 134–155 (2018). https://doi.org/10.5957/JOSR.180001

Shao, X., Ringsberg, J.W., Yao, H.-D., Li, Z., Johnson, E., Fredriksson, G.: A comparison of two wave energy converters' power performance and mooring fatigue characteristics – one WEC vs many WECs in a wave park with interaction effects. J. Ocean Eng. Sci. (2023). https://linkinghub.elsevier.com/retrieve/pii/S2468013323000384

Shen, L., Wei, Z., Ji, S., Ivanov, D.: Experimental investigation of the flip-through impact: The generation mechanism and statistical characteristics. Ocean Eng. **294**, 116690 (2024)

Shen, Y., Firoozkoohi, R., Greco, M., Faltinsen, O.M.: Comparative investigation: closed versus semi-closed vertical cylinder-shaped fish cage in waves. Ocean Eng. **245** (2022)

Si, H., et al.: Effects of design and fabrication of segmented ship models on test results of wave-induced loads. Ocean Eng. **305** (2024)

Silva, L.S.P., Cazzolato, B., Sergiienko, N.Y., Ding, B.: Nonlinear dynamics of a floating offshore wind turbine platform via statistical quadratization—mooring, wave and current interaction. Ocean Eng. **236** (2021)

Sinsabvarodom, C., Leira, B.J., Chai, W., Næss, A.: Short-term extreme mooring loads prediction and fatigue damage evaluation for station-keeping trials in ice. Ocean Eng. **242**, 109930 (2021) (2021). https://linkinghub.elsevier.com/retrieve/pii/S0029801821012750

Sitek, M., Bojanowski, C., Bergeron, A., Licht, J.: Involute working group – FSI analysis of fuel plates using finite volume and finite element methods. United States (2021). https://www.osti.gov/biblio/1845461
Sivaprasad, H., et al.: Fatigue damage prediction of top tensioned riser subjected to vortex-induced vibrations using artificial neural networks. Ocean Eng. **268**(December 2022), 113393 (2023). https://doi.org/10.1016/j.oceaneng.2022.113393
Slagstad, M., Yu, Z., Amdahl, J.:A simplified approach for fatigue life prediction of aquaculture nets under waves and currents. Ocean Eng. **272** (2023)
Song, S., Jung, J.H., Jung, S.J., Jung, D.: Numerical investigation of current loads of side-by-side moored vessel. In: Proceedings of the International Offshore and Polar Engineering Conference, OnePetro, pp. 3677–3681 (2023). https://dx.doi.org/. Accessed 18 Oct 2024
Sørum, S.H., Fonseca, N., Kent, M., Faria, R.P.: Modelling of synthetic fibre rope mooring for floating offshore wind turbines. J. Marine Sci. Eng. **11**(1) (2023a)
Sørum, S.H., Fonseca, N., Kent, M., Faria, R.P.: Assessment of nylon versus polyester ropes for mooring of floating wind turbines. Ocean Eng. **278** (2023b)
Southall, N., Choi, S., Lee, Y., Hong, C., Hirdaris, S., White, N.: Impact analysis using CFD - a comparative study. In: Proceedings of the International Offshore and Polar Engineering Conference (2015). http://www.scopus.com/inward/record.url?eid=2-s2.0-84944675448&partnerID=MN8TOARS
Southall, N., Lee, Y., Johnson, M., Hirdaris, S., White, N.: Towards a pragmatic method for prediction of whipping: wedge impact simulations using OpenFOAM. In: Proceedings of the International Offshore and Polar Engineering Conference (2014)
Srinu, D., Venkateswarlu, V., Vijay, K.G., Atmanand, M.A.: Hydrodynamic analysis of oscillating water column in the presence of seabed undulations. J. Marine Sci. Technol. (Jpn.) **29**(2), 404–417 (2024)
Stansby, P., et al.: Experimental study of mooring forces on the multi-float WEC M4 in large waves with buoy and elastic cables. Ocean Eng. **266** (2022)
Stenius, I., Rosén, A., Kuttenkeuler, J.: Explicit FE-modelling of hydroelasticity in panel-water impacts. Int. Shipbuild. Prog. **54**, 111–127 (2007)
Stenius, I., Rosén, A., Kuttenkeuler, J.: Hydroelastic interaction in panel-water impacts of high-speed craft. Ocean Eng. **38**(2–3), 371–381 (2011)
Stern, F., Wilson, R.V., Coleman, H.W., Paterson, E.G.: Comprehensive approach to verification and validation of CFD simulations—part 1: methodology and procedures. J. Fluids Eng. Trans. ASME **123**(4), 793–802 (2001)
Subbulakshmi, A., Verma, M.: Transient response reduction of floating offshore wind turbine subjected to sudden mooring line failure. Ocean Eng. **271** (2023)
Sumislawski, P., Abdel-Maksoud, M.: Advances on numerical and experimental investigation of ship roll damping. J. Hydrodyn. **35**(3), 431–448 (2023)
Sun, B., Zhao, B., Xu, Y., Ma, S., Duan, W.: Numerical study of green water on a tumblehome vessel in strong nonlinear regular waves. J. Marine Sci. Appl. **22**(1, SI), 102–114 (2023a)
Sun, J., Gaidai, O., et al.: Extreme riser experimental loads caused by sea currents in the Gulf of Eilat. Probab. Eng. Mech. **68**(November 2021) (2022a)
Sun, J., Huang, Y.: Investigations on the ship-ice impact: Part 2. Spatial and temporal variations of ice load. Ocean Eng. **240**(February), 109686 (2021). https://doi.org/10.1016/j.oceaneng.2021.109686
Sun, K., et al.: Dynamic response analysis of floating wind turbine platform in local fatigue of mooring. Renew. Energy **204**, 733–749 (2023b)
Sun, Q., Zhang, M., Zhou, L., Garme, K., Burman, M.: A machine learning-based method for prediction of ship performance in ice: Part I. ICE resistance. Marine Struct. **83** (2022b)

Sun, S.L., Wang, J.L., Li, H., Chen, R.Q., Zhang, C.J.: Investigation on responses and wave climbing of a ship in large waves using a fully nonlinear boundary element method. Eng. Anal. Bound. Elem. **125**, 250–263 (2021)

Tagliafierro, B., et al.: Numerical validations and investigation of a semi-submersible floating offshore wind turbine platform interacting with ocean waves using an SPH framework. Appl. Ocean Res. **141** (2023)

Takami, T., Dam Nielsen, U., Juncher Jensen, J., Maki, A., Matsui, S., Komoriyama, Y.: Onboard identification of stability parameters including nonlinear roll damping via phase-resolved wave estimation using measured ship responses. Mech. Syst. Signal Process. **210**(December 2023) (2024)

Tan, Z., Sun, P.N., Liu, N.N., Li, Z., Lyu, H.G., Zhu, R.H.: SPH simulation and experimental validation of the dynamic response of floating offshore wind turbines in waves. Renew. Energy **205**, 393–409 (2023)

Tang, H.J., Yao, H.C., Yang, R.Y.: Experimental and numerical studies on successive failures of two mooring lines of a net cage subjected to currents. Ocean Eng. **266** (2022a)

Tang, H.J., Yao, H.C., Yang, R.Y.: Experimental and numerical study of a barge-type floating offshore wind turbine under a mooring line failure. Ocean Eng. **278** (2023a)

Tang, X., Zou, M., Zou, Z., Li, Z., Zou, L.: A parametric study on the ice resistance of a ship sailing in pack ice based on CFD-DEM method. Ocean Eng. **265** (2022b)

Tang, Y., Sun, S.L., Abbasnia, A., Guedes Soares, C., Ren, H.L.: A fully nonlinear BEM-beam coupled solver for fluid–structure interactions of flexible ships in waves. J. Fluids Struct. **121** (2023b)

Tang, Y., Sun, S.L., Ren, H.L.: Numerical investigation on a container ship navigating in irregular waves by a fully nonlinear time domain method. Ocean Eng. **223** (2021)

Tang, Y., Sun, S.L., Yang, R.S., Ren, H.L., Zhao, X., Jiao, J.L.: Nonlinear bending moments of an ultra large container ship in extreme waves based on a segmented model test. Ocean Eng. **243** (2022c)

Tavakoli, S., Hirdaris, S.: the hydroelastic slamming in oblique seas. In: Proceedings of the ASME 2023 42nd International Conference on Ocean, Offshore and Arctic Engineering. Ocean Engineering, p. 5 (2023)

Tavakoli, S., Mikkola, T., Hirdaris, S.: A fluid–solid momentum exchange method for the prediction of hydroelastic responses of flexible water entry problems. J. Fluid Mech. **965**, A19 (2023)

Tavakoli, S., Zhang, M., Kondratenko, A.A., Hirdaris, S.: A review on the hydrodynamics of planing hulls. Ocean Eng. **303** (2024)

Thome, M., el Moctar, O., Schellin, T.E.: Assessment of hydrodynamic loads on an offshore monopile structure considering hydroelasticity effects. J. Marine Sci. Eng. **11**(2) (2023)

Tian, J., Zhu, P.Q., Ding, J., Sun, S.L.: Fully nonlinear interaction between a ship-type floater and waves. Ocean Eng. **309** (2024)

Tian, Y., Yu, C., Gang, X., Kong, S., Ji, S., Wang, Y.: Experimental investigation on ice loading mechanism of typical offshore structures under the action of level ICE (2022). www.isope.org

Tödter, S., el Moctar, O., Neugebauer, J., Schellin, T.: Experimentallymeasured hydroelastic effects on impact-induced loads during flat waterentry and related uncertainties. J Offshore Mech Arct Eng. **142**, 011604 (2020)

Tödter, S., el Moctar, O., Neugebauer, J., Schellin, T.E.: Experimentally measured hydroelastic effects on impact-induced loads during flat water entry and related uncertainties. J. Offshore Mech. Arctic Eng. **142**(1) (2019). https://doi.org/10.1115/1.4044632

Torre, S., Burlando, M., Ruscelli, D., Repetto, M.P., Camauli, G.: Wind tunnel experimental investigation of the aerodynamic coefficients reduction due to sheltering surroundings on a cruise ship moored in port. J. Wind Eng. Industr. Aerodyn. **218**(June), 104731 (2021). https://doi.org/10.1016/j.jweia.2021.104731

Truong, D.D., Jang, B.S.: Estimation of ice loads on offshore structures using simulations of level ice-structure collisions with an influence coefficient method. Appl. Ocean Res. **125**(December 2021), 103235 (2022). https://doi.org/10.1016/j.apor.2022.103235

Truong, D.D., et al.: Benchmark study on slamming response of flat-stiffened plates considering fluid-structure interaction. Marine Struct. **79** (2021)

Uto, S., Matsuzawa, T., Shimoda, H., Wako, D., Toyota, T.: Formulation and validation of resistance prediction scheme for ships in ice regime described in WMO egg code. Cold Regions Sci. Technol. 221(February), 104159 (2024). https://doi.org/10.1016/j.coldregions.2024.104159

Vanem, E., Zhu, T., Babanin, A.:Statistical modelling of the ocean environment – A review of recent developments in theory and applications. Marine Struct. **86** (2022).

Veen, D., Gourlay, T.: A combined strip theory and smoothed particle hydrodynamics approach for estimating slamming loads on a ship in head seas. Ocean Eng. **43**, 64–71 (2012)

Verde, S., Lages, E N.: A comparison of anchor loads, planar displacement, and rotation for nylon and polyester moored systems for a 15 MW floating wind turbine in shallow water. Ocean Eng. **280** (2023)

Vineesh, P., Sriram, V.: Numerical investigation of wave interaction with two closely spaced floating boxes using particle method. Ocean Eng. **268** (2023)

Viuff, T., Ravinthrakumar, S., Økland, O.D., Grytå, O.A., Xiang, X.: Experimental study of floating bridge global response when subjected to waves and current. Appl. Ocean Res. **138** (2023)

Wagner, H.: Uber stoss und Gleitvorgange an der Oberache von Flussigkeiten. Z. Angew. Math. Mech. **12**, 192–215 (1932)

Wan, Z., Yuan, Y., Tang, W.: Experimental investigation on ice resistance of an arctic LNG carrier under multiple ice breaking conditions. Ocean Eng. **267** (2023)

Wang, B., Liu, Y., Zhang, J., Shi, W., Li, X., Li, Y.: Dynamic analysis of offshore wind turbines subjected to the combined wind and ice loads based on the cohesive element method. Front. Marine Sci. **9** (2022a)

Wang, G., Martin, T., Huang, L., Bihs, H.: An improved screen force model based on CFD simulations of the hydrodynamic loads on knotless net panels. Appl. Ocean Res. **118** (2022b)

Wang, G., Martin, T., Huang, L., Bihs, H.: Numerical investigation of the hydrodynamics of a submersible steel-frame offshore fish farm in regular waves using CFD. Ocean Eng. **256** (2022c)

Wang, H., Duan, W., Chen, J., Tian, C.: Numerical predictions of motions and coupled bending and torsional vibrations of containerships in regular head and oblique waves. Eng. Anal. Bound. Elem. **166** (2024a)

Wang, J., Chen, X., Sun, K., Ji, S.: Far-field identification of ice loads on ship structures by radial basis function neural network. Ocean Eng. **282**(April), 115072 (2023a). https://doi.org/10.1016/j.oceaneng.2023.115072

Wang, K., Chu, Y., Huang, S., Liu, Y.: Preliminary design and dynamic analysis of constant tension mooring system on a 15 MW semi-submersible wind turbine for extreme conditions in shallow water. Ocean Eng. **283** (2023b)

Wang, L., Robertson, A., Jonkman, J., Yu, Y. H.: Uncertainty assessment of CFD investigation of the nonlinear difference-frequency wave loads on a semisubmersible FOWT platform. Sustain. (Switz.) **13**(1), 1–25 (2021a). https://www.scopus.com/record/display.uri?eid=2-s2.0-85099183562&origin=resultslist&sort=plf-t&src=s&st1=%22+Uncertainty+assessment+of+CFD+investigation+of+the+nonlinear+difference-+frequency+wave+loads+on+a+semisubmersible+FOWT+platform%22&sid=7d230c92a7

Wang, L., et al.: Validation of CFD simulations of the moored DeepCwind offshore wind semisubmersible in irregular waves. Ocean Eng. **260** (2022d)

Wang, Q., Liaot, K. P., Fan, N., Duan, W.Y., Ma, Q.W.: Numerical analysis of flow kinematics in green water on deck. Int. J. Offshore Polar Eng. **32**(1), pp. 58–65 (2022e)

Wang, Q., et al.: Real-time prediction of wave-induced hull girder loads for a large container ship based on the recurrent neural network model and error correction strategy. Int. J. Naval Archit. Ocean Eng. **16** (2024b)

Wang, S.D., Wei, G., Du, H., Wang, X.L., Xu, J N.: Experimental investigation on the three-dimensional oblique interaction of an internal solitary wave with a horizontal finite-length cylinder. J. Fluids Struct. **111** (2022f)

Wang, S., Guedes Soares, C.: Numerical study on the water impact of 3D bodies by explicit finite element method. Ocean Eng. (2014)

Wang, S., Islam, H., Guedes Soares, C.: Uncertainty due to discretization on the ALE algorithm for predicting water slamming loads. Marine Struct. **80**, 103086 (2021b)

Wang, S., Li, C., Zhang, Y., Jing, F., Chen, L.: Influence of pitching motion on the hydrodynamic performance of a horizontal axis tidal turbine considering the surface wave. Renew. Energy **189**, 1020–1032 (2022g)

Wang, S., Soares, C.G.: Article in The International Journal of Maritime Engineering (2012). https://www.researchgate.net/publication/260869000

Wang, S., Zhang, Y., Xie, Y., Xu, G., Liu, K., Zheng, Y.: The effects of surge motion on hydrodynamics characteristics of horizontal-axis tidal current turbine under free surface condition. Renew. Energy **170**, pp. 773–784 (2021c)

Wang, W. hua, Zhao, Z. han, Wang, L. jian, Huang, Y.: Improved analysis method on extreme upwell of irregular waves for the airgap of floating platforms based on OTG-13. Ocean Eng. **274** (2023c)

Wang, X., et al.: A review of aerodynamic and wake characteristics of floating offshore wind turbines. Renew. Sustain. Energy Rev. **175**(October 2022), p. 113144 (2023d). https://doi.org/10.1016/j.rser.2022.113144

Wang, Y., Chen, H.C., Koop, A., Vaz, G.: Hydrodynamic response of a FOWT semi-submersible under regular waves using CFD: verification and validation. Ocean Eng. **258** (2022h)

Wang, Y., Jiang, S., Zhou, T.: Experimental investigation on response of ship rolling motion coupled with liquid sloshing. In: Proceedings of the ASME 2023 42nd International Conference on Ocean, Offshore and Arctic Engineering, Melbourne (2023e)

Wang, Y., Jiang, S., Zhou, T.: Experimental and numerical investigation on ship rolling motion response coupled with liquid sloshing. In: Proceedings of the ASME 2024 43rd International Conference on Ocean, Offshore and Arctic Engineering OM, Singapore (2024c)

Warren, M.F., et al.: Fatigue estimation on a high-speed wave piercing catamaran during normal operations. Trans. Roy. Inst. Naval Archit. Part A: Int. J. Maritime Eng. **164**(1 A), A55–A67 (2022)

Waskito, K. T., Sasa, K., Chen, C., Kitagawa, Y., Lee, S. W.: Comparative study of realistic ship motion simulation for optimal ship routing of a bulk carrier in rough seas. Ocean Eng. **260** (2022)

Watanabe, S., Hu, C., Aoki, T.: Coupled lattice boltzmann and discrete element simulations of ship-ice interactions. IOP Conf. Ser.: Mater. Sci. Eng. **1288**(1), 012015 (2023)

Wei, K., Yin, X.: Numerical study into configuration of horizontal flanges on hydrodynamic performance of moored box-type floating breakwater. Ocean Eng. **266** (2022)

Wei, S., Liang, Z., Cui, L., Zhai, H., Jeng, D.: Numerical study of seabed response and liquefaction around a jacket support offshore wind turbine foundation under combined wave and current loading. Water Sci. Eng. **15**(1), 78–88 (2022)

Wei, W., Ling, A., Liang, Y.: Applicable analysis of the environment condition for the air gap of the semi-submersible platform (2023). www.isope.org

Wen, B., Jiang, Z., Li, Z., Peng, Z., Dong, X., Tian, X.: On the aerodynamic loading effect of a model Spar-type floating wind turbine: an experimental study. Renew. Energy **184**, 306–319 (2022)

Wilson, S., Hall, M., Housner, S., Sirnivas, S.: Linearized modeling and optimization of shared mooring systems. Ocean Eng. **241** (2021)

Windt, C., Faedo, N., Penalba, M., Dias, F., Ringwood, J.V.: Reactive control of wave energy devices – the modelling paradox. Appl. Ocean Res. **109** (2021)

Won, D., Seo, J., Kim, S. Dynamic response of submerged floating tunnels with dual sections under irregular waves. Ocean Eng. **241** (2021)

Wu, J., et al.: Analysis of full-scale riser responses in field conditions based on Gaussian mixture model. J. Fluids Struct. **116**, 103793 (2023a). https://doi.org/10.1016/j.jfluidstructs.2022.103793

Wu, J., Yu, Y., Cheng, S., Li, Z., Yu, J.: Probabilistic multilevel robustness assessment framework for a TLP under mooring failure considering uncertainties. Reliab. Eng. Syst. Saf. **223** (2022)

Wu, S., Huang, Y., Ding, Y., Wang, G., Li, J., Guo, Y.: Study on the influence of swimming pool shape of large cruise ship on its sloshing performance, in: Proceedings of the Thirty-Third International Ocean and Polar Engineering Conference, Ottawa, pp. 2609–2615 (2023b)

Wu, Z., Wang, D., Ke, W., Qin, Y., Lu, F., Jiang, M.: Experimental investigation for the dynamic behavior of submerged floating tunnel subjected to the combined action of earthquake, wave and current. Ocean Eng. **239** (2021)

Xiang, S., Cheng, B., Li, D., Tang, M., Zeng, Z.: Structural dynamic performance of floating continuous beam bridge under wave and current loadings: an experimental study. Appl. Ocean Res. **137** (2023)

Xie, C., Zhou, L., Ding, S., Liu, R., Zheng, S.: Experimental and numerical investigation on self-propulsion performance of polar merchant ship in brash ice channel. Ocean Eng. **269**(January), 113424 (2023a). https://doi.org/10.1016/j.oceaneng.2022.113424

Xie, H., Dai, X., Liu, F., Liu, X.: Experimental study on the slamming pressure distribution of a 3D stern model entering water with pitch angles. Ocean Eng. **291** (2024)

Xie, W., Liang, Z., Jiang, Z., Tu, S., Chen, W., Zhang, H.: Hydrodynamic behaviors of a spring-mounted fishing net in wave-current combined flows. Ocean Eng. **287** (2023b)

Xin, Z., Li, X., Li, Y.: Coupled effects of wave and depth-dependent current interaction on loads on a bottom-fixed vertical slender cylinder. Coastal Eng. **183** (2023)

Xiong, Z., Wu, X., Li, Y.: Research on ice resistance of ships sailing in floating ice floes. J. Marine Sci. Technol. (Taiwan) **31**(4), 460–470 (2023)

Xu, G., Chen, X., Xue, S., Townsend, J. F., Chen, X., Tang, M.: Numerical assessment of non-uniform terrain and inhomogeneous wave–current loading effects on the dynamic response of a submerged floating tunnel. Ocean Eng. **288** (2023)

Xu, G., He, B., Li, H., Gui, X., Li, Z.: FBG pressure sensor in pressure distribution monitoring of ship. Opt. Express **30**(12), 21396–21409 (2022)

Xu, K., Larsen, K., Shao, Y., Zhang, M., Gao, Z., Moan, T.: Design and comparative analysis of alternative mooring systems for floating wind turbines in shallow water with emphasis on ultimate limit state design. Ocean Eng. **219** (2021a)

Xu, S., Guedes Soares, C.:. Parametric study on the short-term extreme mooring tension of nylon rope for a point absorber. Ocean Eng. **267** (2023)

Xu, S., Wang, S., Guedes Soares, C.: Experimental study of the influence of the rope material on mooring fatigue damage and point absorber response. Ocean Eng. **232** (2021b)

Xu, S., Wang, S., Guedes Soares, C.: Experimental investigation on the influence of hybrid mooring system configuration and mooring material on the hydrodynamic performance of a point absorber. Ocean Eng. **233** (2021c)

Xuan, S., Zhan, C., Liu, Z., Feng, B., Chang, H., Wei, X.: Numerical investigation of global ice loads of maneuvering captive motion in ice floe fields. J. Marine Sci. Eng. **11**(9) (2023)

Xuan, S., Zhan, C., Liu, Z., Zhao, Q., Guo, W.: Numerical research on global ice loads of maneuvering captive motion in level ice. J. Marine Sci. Eng. **9**(12) (2021)

Xue, Y., et al.: A combined experimental and numerical approach to predict ship resistance and power demand in broken ice. Ocean Eng. **292**(August 2023) (2024)

Yamamoto, Y., Iida, K., Fukasawa, T., Murakami, T., Arai, M., Ando, A.: Structural damage analysis of a fast ship due to bow flare slamming. Int. Shipbuild. Prog. **32**, 124–136 (1985)

Yan, D., Garbatov, Y., Guedes Soares, C.: Review on uncertainties in fatigue loads and fatigue life of ships and offshore structures. Ocean Eng. **264** (2022a)

Yan, D., Mikkola, T., Kujala, P., Hirdaris, S.: Hydroelastic analysis of slamming induced impact on stiff and flexible structures by two-way CFD-FEA coupling. Ships Offshore Struct. 1–13 (2022b)

Yan, D., et al.: A study into the FSI modelling of flat plate water entry and related uncertainties. Marine Struct. **86** (2022c). Accessed 29 Aug 2023,

Yan, X., Chen, C., Yin, G., Ong, M.C., Ma, Y., Fan, T.: Numerical investigations on nonlinear effects of catenary mooring systems for a 10-MW FOWT in shallow water. Ocean Eng. **276** (2023)

Yang, B., Zhang, G., Rao, H., Wang, S., Yang, B., Sun, Z.: Numerical simulation of the maneuvering performance of ships in broken ice area. Ocean Eng. **294**(December 2023), 116783 (2024). https://doi.org/10.1016/j.oceaneng.2024.116783

Yang, Y., Li, Y., Wang, J., He, Z., Dong, X., Yuan, X.: Time-varying dynamic performance of a floating platform-mooring system based on the mechanical experimental data derivation method for corroded wire ropes. Ocean Eng. **280** (2023a)

Yang, Y., Peng, T., Liao, S.: Predicting future mooring line tension of floating structure by machine learning. Ocean Eng. **269**, 113470 (2023b). Accessed 31 Mar 2024

Yang, Y., Peng, T., Liao, S.: Predicting 3-DoF motions of a moored barge by machine learning. J. Ocean Eng. Sci. **8**(4), 336–343 (2023c). Accessed 31 Mar 2024

Yang, Y., Stansby, P.K., Rogers, B.D., Buldakov, E., Stagonas, D., Draycott, S.: The loading on a vertical cylinder in steep and breaking waves on sheared currents using smoothed particle hydrodynamics. Phys. Fluids **35**(8) (2023d)

Yang, Z., et al.: Experimental study on the solitary wave-current interaction and the combined forces on a vertical cylinder. Ocean Eng. **236** (2021)

Yang, Z., et al.: Experimental study on the wave-induced dynamic response and hydrodynamic characteristics of a submerged floating tunnel with elastically truncated boundary condition. Marine Struct. **88** (2023e)

Yao, C., Dong, G., Sun, X.S., Zheng, Y., Feng, D.: Numerical study on motion and added resistance of a trimaran advancing in waves based on hybrid Green function method. Appl. Ocean Res. **130** (2023a)

Yao, Z., Huo, F., Zhu, Y., Tang, C., Jia, K., Li, D., Ma, Y.: Experimental and numerical investigation on slamming mechanism of a mooring column-stabilised semi-submersible. Processes **11**(3) (2023b)

Yeter, B., Garbatov, Y.: Structural integrity assessment of fixed support structures for offshore wind turbines: a review. Ocean Eng. **244**(October 2021), 110271 (2022). https://doi.org/10.1016/j.oceaneng.2021.110271

Yin, D., et al.: State-of-the-art review of vortex-induced motions of floating offshore wind turbine structures. J. Marine Sci. Eng. **10**(8) (2022)

Yoo, J.H., Schrijvers, P., Koop, A., Park, J.C.: CFD prediction of wind loads on fpso and shuttle tankers during side-by-side offloading. J. Mar. Sci. Eng. **10**(5) (2022). https://www.scopus.com/inward/record.uri?eid=2-s2.0-85132836359&doi=10.3390%2Fjmse10050654&partnerID=40&md5=b152aee4d606ad575407fdc6d5b62a99

Yu, J., Cheng, X., Fan, Y., Ni, X., Chen, Y., Ye, Y.: Mooring design of offshore aquaculture platform and its dynamic performance. Ocean Eng. **275** (2023a)

Yu, T., Liu, K., Wang, G., Liu, J., Wang, Z.: A tri-axial ice model for simulating ice-stiffened panel impact: experiments and numerical modeling. Marine Struct. **88**(November 2021), 103358 (2023b). https://doi.org/10.1016/j.marstruc.2022.103358

Yu, Z., Ma, Q., Zheng, X., Liao, K., Sun, H., Khayyer, A.: A hybrid numerical model for simulating aero-elastic-hydro-mooring-wake dynamic responses of floating offshore wind turbine. Ocean Eng. **268** (2023c)

Zago, V., Dalrymple, R. A., Almashan, N., Bilotta, G., Al-Houti, D., Neelamani, S.: Characterization and modeling of greenwater overtopping of a sea-level deck. Ocean Eng. **275** (2023)

Zeng, X., Shi, W., Feng, X., Shao, Y., Li, X.: Investigation of higher-harmonic wave loads and low-frequency resonance response of floating offshore wind turbine under extreme wave groups. Marine Struct. **89** (2023)

Zhang, A., Chuang, Z., Liu, S., Zhou, L., Qu, Y., Lu, Y.: Dynamic performance optimization of an arctic semi-submersible production system. Ocean Eng. **244**(July 2021) (2022a)

Zhang, C., Wang, S., Xie, S., He, J., Gao, J., Tian, C.: Effects of mooring line failure on the dynamic responses of a semisubmersible floating offshore wind turbine including gearbox dynamics analysis. Ocean Eng. **245** (2022b)

Zhang, D., Chu, X., Wu, W., He, Z., Wang, Z., Liu, C.: Model identification of ship turning maneuver and extreme short-term trajectory prediction under the influence of sea currents. Ocean Eng. **278**, 114367 (2023a). Accessed 18 Oct 2024

Zhang, H., Liao, X., Shi, H., Babanin, A., Soares, C.G.: Effect of initial condition uncertainty on the profile of maximum wave. Marine Struct. **82** (2022)

Zhang, H., Zeng, J., Tong, S., Jin, B., Chou, C., Li, H., Dong, H.: Dynamic stiffness of polyester fiber mooring ropes: experimental investigation based on radial basis function neural networks. Ocean Eng. **280** (2023b)

Zhang, J., Gaidai, O., Ji, H., Xing, Y.: Operational reliability study of ice loads acting on oil tanker bow. Heliyon **9**(4), e15189 (2023c). https://doi.org/10.1016/j.heliyon.2023.e15189

Zhang, J., Zhang, Y., Shang, Y., Jin, Q., Zhang, L.: CFD-DEM based full-scale ship-ice interaction research under FSICR ice condition in restricted brash ice channel. Cold Regions Sci. Technol. **194**(September 2021), 103454 (2022d). https://doi.org/10.1016/j.coldregions.2021.103454

Zhang, L., Shi, W., Zeng, Y., Michailides, C., Zheng, S., Li, Y.: Experimental investigation on the hydrodynamic effects of heave plates used in floating offshore wind turbines. Ocean Eng. **267** (2023d)

Zhang, N., Xiao, L., Guo, Y., Yang, L., Chen, G.: Parametric study of wave impact pressure impulse and characteristic pressure on a square column with overhanging deck. Ocean Eng. **258** (2022e)

Zhang, R.-R., et al.: Experimental investigation and prediction model of the loads exerted by oblique internal solitary waves on FPSO (2022). https://doi.org/10.1007/s13344-022-

Zhang, X., Li, B., Hu, Z., Deng, J., Xiao, P., Chen, M.: Research on size optimization of wave energy converters based on a floating wind-wave combined power generation platform. Energies **15**(22) (2022f)

Zhang, X., Ni, W., Sun, L.: Fatigue analysis of the oil offloading lines in FPSO system under wave and current loads. J. Marine Sci. Eng. **10**(2) (2022g)

Zhang, X., Wu, W., Fu, H., Li, J.: The effect of corrosion evolution on the stress corrosion cracking behavior of mooring chain steel. Corros. Sci. **203** (2022h)

Zhang, Y., Liu, H.: Coupled dynamic analysis on floating wind farms with shared mooring under complex conditions. Ocean Eng. **267** (2023)

Zhang, Y., et al.: Quantifying the surge-induced response of a floating tidal stream turbine under wave-current flows. Energy **283** (2023e)

Zhang, Y., Xu, H., Law, Y., Santo, H., Magee, A.: Hydrodynamic analysis and validation of the floating DeepCwind semi-submersible under 3-h irregular wave with the HOS and CFD coupling method. Ocean Eng. **287** (2023f)

Zhang, Z., Ma, N., Lin, Y., Gu, X., Shi, Q.: Experimental study on non-linear wave loads of a ship model with variable cross-section backbone in irregular waves. In: 32nd International Ocean and Polar Engineering Conference, pp. 2315–2322. International Society of Offshore and Polar Engineers (2022i)

Zhao, C., Stansby, P., Johanning, L.: OrcaFlex predictions for a multi-float hinged WEC with nonlinear mooring systems: Elastic mooring force and dynamic motion. Ocean Eng. **286** (2023)

Zhao, R.-X., Faltinsen, O.M.: Water entry of two-dimensional bodies. J.. Fluid Mech **246**, 593–612 (1993). https://api.semanticscholar.org/CorpusID:121224301

Zhao, W., Wei, Z., Wan, D.: Numerical investigation on the effects of current headings on vortex induced motions of a semi-submersible. J. Hydrodyn. **34**(3), 382–394 (2022)

Zheng, Z., et al.: Motion response and energy harvesting of multi-module floating photovoltaics in seas. Ocean Eng. **310** (2024)

Zhong, K., et al.: Direct measurements and CFD simulations on ice-induced hull pressure of a ship in floe ice fields. Ocean Eng. **272** (2023)

Zhou, J., Liu, J., Guo, A.: Investigation of the dynamic behavior of the flow–structure system of submerged floating tunnels under wave and current actions. Coast. Eng. **183** (2023a)

Zhou, L., Gu, Y., Ding, S., Liu, R.: Prediction of ice-resistance distribution for R/V xuelong using measured sea-ice parameters. Water (Switzerland) **14**(4) (2022)

Zhou, Y., Ning, D., Chen, L., Mayon, R., Zhang, C.: Experimental investigation on an OWC wave energy converter integrated into a floating offshore wind turbine. Energy Convers. Manage. **276** (2023b)

Zhu, D., Dong, Y., Frangopol, D.M.: Experimental and numerical investigation on wave impacts on box-girder bridges. Struct. Infrastruct. Eng. **18**(10–11), 1379–1397 (2022)

Zhu, H., Ji, S.: Discrete element simulations of ice load and mooring force on moored structure in level ice. CMES – Comput. Model. Eng. Sci. **132**(1), 5–21 (2022)

Zilic de Arcos, F., Vogel, C.R., Willden, R.H.J.: A numerical study on the hydrodynamics of a floating tidal rotor under the combined effects of currents and waves. Ocean Eng. **286** (2023)

Zong, S., Liu, K., Zhang, Y., Yan, X., Wang, Y.: The dynamic response of a floating wind turbine under collision load considering the coupling of wind-wave-mooring loads. J. Marine Sci. Eng. **11**(9), 1741 (2023). https://www.mdpi.com/2077-1312/11/9/1741

Zou, J., Li, H., Sun, Z., Han, B., Wang, Z.: Experimental analysis of bow flare slamming and whipping responses in a ship at different sailing speeds. Ocean Eng. **305** (2024)

Zou, Q., Lu, Z., Shen, Y.: Short-term prediction of hydrodynamic response of a novel semi-submersible FOWT platform under wind, current and wave loads. Ocean Eng. **278** (2023)

ISO/IEC Guide 98-3:2008 - Uncertainty of measurement — Part 3: Guide to the expression of uncertainty in measurement (GUM:1995). https://www.iso.org/standard/50461.html. Accessed 20 Mar 2024